UCRL-ID-103735
PATC-IR 90-01

INVESTIGATION OF THE CRASH ENVIRONMENT AND IMPACT CONDITIONS OF THE PSA FLIGHT 1771 AIRCRAFT CRASH ON DECEMBER 7, 1987

February 28, 1990

C. E. Walter

Prepared for
U.S. Nuclear Regulatory Commission

DISCLAIMER

This work was supported by the United States Nuclear Regulatory Commission under a Memorandum of Understanding with the United States Department of Energy.

PATC-IR 90-01

INVESTIGATION OF THE CRASH ENVIRONMENT AND IMPACT CONDITIONS OF THE PSA FLIGHT 1771 AIRCRAFT CRASH ON DECEMBER 7, 1987

February 28, 1990

C. E. Walter

Prepared for
U.S. Nuclear Regulatory Commission

ABSTRACT

A study of the PSA Flight 1771 crash on December 7, 1987, has been conducted to ascertain the general crash environment and impact conditions. This information was needed to determine the criteria for a possible aircraft crash test that would produce conditions at least as severe as those produced in the PSA Flight 1771 crash, which has been specified by the Nuclear Regulatory Commission as representing the worst-case aircraft accident. Information from various sources was developed and analyzed, and additional studies and supporting exploratory tests were conducted. These activities were necessary because a detailed investigative report of the crash had not been prepared by the National Transportation Safety Board (the crash was not technically an "accident" but instead was the result of a criminal act). The study includes determination of the geotechnical properties of the crash site, a topological survey, analyses of in-route radar data, estimates of the aircraft's final trajectory, examination of the distribution of aircraft debris from photographs of the crash site, laboratory impact tests of a scale model of the aircraft fuselage, review of witnesses' observations on the fire that followed the crash, analysis of the effect of moist dust in a stoichiometric fuel-air mixture, flight simulations of the BAe 146-200 aircraft involved in the crash, review of the aircraft's integrity while operating outside its structural design envelope, reduction and analysis of terminal flight data from the badly damaged flight data recorder, analysis of the cockpit voice recorder tape, and searching (successfully) for a recorded seismic signal from the crash impact. The study concludes that the aircraft impacted at 00:14:35 UTC on December 8, 1987, at a speed of 282 m/s and a trajectory angle to the hill surface of 60°. The maximum Mach number did not exceed 0.86 in the time before the crash and was 0.83 at impact. The ground at the impact point consisted of intensely weathered and fractured shale and sandstone. The aircraft was intact until impact. An airborne fuel-air fire of short duration occurred on impact, but contributed only negligibly to the crash damage. Conditions of the crash make it unlikely that a significant fuel-air explosion occurred.

TABLE OF CONTENTS

TABLE OF CONTENTS
(continued)

ACKNOWLEDGMENTS

Many persons contributed to our understanding of what happened at the crash of PSA Flight 1771. Without their assistance, we would not be confident that our conclusions are correct. Dennis Grossi, NTSB, made key contributions despite his full schedule. He also loaned us the 8-cm-long piece of tape from the badly damaged flight data recorder which had the last 7 s of multiplexed data for the ill-fated flight. Garth Hess and Dick Nance at Lockheed Aircraft Service Company successfully reduced the data, in some cases manually, which allowed us to specify impact conditions. We also profited from discussions with Paul Baker, Jim Cash, Mike O'Rourke, and Terry Weaver-Berry at NTSB. Paul Burns of Textron Lycoming kindly provided us with a video tape made during the search at the crash site for engine components. Several members of Sheriff Edward Williams' staff at San Luis Obispo County provided us with photographs and a video tape of the crash scene together with first hand accounts of the crash scene. Woody Savage of PG&E located the recording made fortuitously a year and a half earlier of the crash impact signal sensed at a conveniently close seismic station.

Several persons including Gary Taylor, Taylor Pruitt, David Kaiser, and Keith Moore at the FAA Oakland ARTCC and Robert Webb and Veryl Rogge at the Los Angeles ARTCC took time from their busy day to provide us with PSA Flight 1771 radar data and additional data for other flights.

Five people from the aircraft manufacturer, British Aerospace Commercial Aircraft, represented their company in a most "proper manner": Brian Brasier, Executive Director-146 Design; Henry Geering, Chief Stressman; Roy Wells, Assistant Chief Aerodynamist; Lee Burgess, Aerodynamist; and Peter Sedgwick, Chief Test Pilot.

Keith Graham used his persuasive legal background to finally obtain the cockpit voice recorder tape from Jim Moody of the FBI. Brad Burdick listened over and over again to the CVR tape and produced clear annotated charts of sound amplitude versus time during the last 100 s of the flight. Billy Davis and Bob Sherwood provided their enthusiastic expertise in laboratory impact tests and photographic image enhancement.

Dave Carpenter, Garry Holman, and J. C. Chen ably conducted the geotechnical investigation of the crash site. Jim VanSant provided technical advice on various occasions in various areas.

C. K. Chou provided expert program leadership which allowed us to proceed with this investigation in depth. Thanks to Lisa Hensel who made each draft better, we present this effort with professional satisfaction to our supportive NRC sponsors Robert Burnett, Charles MacDonald, John Cook, and John Jankovich.

GLOSSARY

ARTCC—Air Route Traffic Control Center.
BAe—British Aerospace (the "e" is added to distinguish it from British Airways).
BLV—The designation for a specific PG&E seismic station.
CAM—Cockpit area microphone.
CAS—Calibrated airspeed.
C.G.—Center-of-gravity.
CVR—Cockpit voice recorder.
EAS—Equivalent airspeed.
FAA—Federal Aviation Administration.
FBI—Federal Bureau of Investigation.
FDR—Flight data recorder.
FI—Flight idle.
JAR—Joint Airworthiness Requirements (European).
LLNL—Lawrence Livermore National Laboratory.
m.s.l.—(above) mean sea level.
NIST—National Institute of Standards and Technology.
NRC—Nuclear Regulatory Commission.
NTSB—National Transportation Safety Board.
PAT—Plutonium air transport.
PFLF—Power for level flight.
PG&E—Pacific Gas and Electric Company (utility serving much of California).
PNC—Power Reactor and Nuclear Fuel Development Corporation.
PSA—Pacific Southwest Airlines.
PST—Pacific standard time.
smc—Standard mean chord.
TAS—True airspeed.
UTC—Universal time, coordinated.
VHS—Video Home Systems.

1. INTRODUCTION

1.1 Motivation for Investigation

The Power Reactor and Nuclear Fuel Development Corporation (PNC) of Japan initiated negotiations in 1988 with NRC for certification of a PAT package of PNC design. PNC's tentative application for certification of a PAT package is governed by U.S. legislation enacted in December 1987 which imposes new requirements for certification. As a result of these negotiations NRC agreed (Ref. 1) to develop draft criteria for tests of PAT packages as required by the legislation, Section 5062 of Public Law 100-203 (see Appendix 1). This section of the law establishes the manner in which the NRC may approve and certify the safety of packages intended for transport of plutonium through the airspace of the United States while in route from a foreign country to a foreign country. One of the provisions of the law requires, as an option, that an aircraft crash test be conducted. The law also specifies that all costs associated with the application for certification shall be reimbursed to the NRC by the applicant.

Section 5062 of Public Law 100-203 requires that the "worst-case" aircraft accident be considered to the maximum extent practicable as the basis for the aircraft crash test. Based on general information available, the NRC specified (Ref. 2) that the crash of PSA Flight 1771 on December 7, 1987, represented the worst-case accident and was suitable for use as the basis accident. A considerable technical effort, reported here, became necessary to quantify the pertinent parameters of the accident so that comparable test conditions could be specified on a sound basis.

1.2 Information Sources

Shortly after the crash of PSA Flight 1771, it was established that the crash resulted from a criminal act and not a safety deficiency in flight equipment or operations. At that time, the National Transportation Safety Board, which had already deployed its investigation teams to the crash site, discontinued their involvement without completing their investigation. Consequently, NTSB did not prepare a final report of the accident and the separate reports of their individual investigating groups* did not include the scope and detail that is customary. NTSB assigned Accident Identification Number DCA-88-M-A008 to the crash of PSA Flight 1771.

Because of the criminal aspect of the accident there is no official, thorough report that assesses the technical aspects of the crash. As a result, the more or less public information available on the accident was obtained and promulgated by local law enforcement agencies and the FBI as a result of their emergency search and rescue functions and criminal investigations. We believe that this report of our

---

* We obtained three factual reports prepared by the chairman of the Operations, Power Plant (Ref. 14), and Systems groups established by NTSB.

investigation of the PSA Flight 1771 crash is the most complete and technically correct account that is currently available.

We obtained information for the accident investigation from various sources, including:

- Discussions with NTSB personnel.
- A report prepared by the Sheriff's Office of San Luis Obispo County.
- A number of photographs taken at the time of the crash by sheriff and BAe personnel.
- Performance simulation studies and structural review of the BAe 146-200 aircraft.
- Discussions with FAA ARTCC personnel on their radar data.
- Geotechnical and topological studies we conducted of the impact area.
- Conversations with area residents who were eyewitnesses of the crash.
- Flight data recorder tape analysis.
- Cockpit voice recorder tape analysis.
- Seismic recording of the impact.
- Copies of excised FBI file papers.

1.3 Accuracy of Analysis

In our analysis of the information available, we attempted to arrive at the best estimate of parameter values that characterize the impact conditions of PSA Flight 1771. On the basis of physical principles and comparative studies, we are quite confident that: 1) the true impact velocity is not higher than 2% above our estimate and probably no lower; and 2) the true aircraft trajectory impact angle with the surface is not higher than 10° above our estimate or lower than 6°.

2. GENERAL ACCIDENT DESCRIPTION

2.1 Accident Conditions

On December 7, 1987, PSA Flight 1771 departed from Los Angeles at 15:30 PST with a scheduled arrival in San Francisco at 16:43 PST (00:43:00 UTC, December 8). Half an hour before scheduled arrival, at 00:13:03* UTC, the FAA's Oakland ARTCC recorded radio messages from the crew indicating that a gun had been fired on board and that an emergency was being declared by means of their transponder code. The last radar return was recorded at 00:14:36 UTC, at latitude and longitude coordinates 512 m northeast of the impact location. The altitudes corresponding to the last two radar returns were not recorded.

The BAe 146-200 aircraft used on PSA Flight 1771 remained intact until it crashed, nose first, on a hillside of the Santa Rita Range in San Luis Obispo County. None of the 43 persons on board survived. Only minor ground fires resulted from the approximately 3200 kg** (1000 gallons) of fuel estimated to be on board (Ref. 3) at the time of the crash. A dense black smoke cloud was observed at the time of the crash, indicating that some of the fuel apparently burned in the air above the impact point. The aircraft and its contents fragmented into many small pieces, mostly dispersed south of the impact point within a radius of about 100 m (see Fig. 2.1-1). The most distant aircraft piece was found 265 m from the impact point, and some paper debris was found as far away as 2 km.

The crash produced an irregularly shaped depression about 3.5 m deep by 6 m wide by 12 m long. These dimensions are estimated from eyewitness reports, photographs, and geophysical surveys. The volume of soil displaced is estimated to have been about 74 m^3, with a corresponding mass of about 175 Mg.

We studied available radar-tracking data and data from the aircraft flight data recorder in considerable detail to establish the impact angle and velocity of the aircraft. Also, British Aerospace performed simulation studies based on the specific aircraft configuration that crashed. We believe that the flight data recorder provides the best estimates of impact conditions. The FDR data is consistent with the studies by BAe. Data from the flight recorder and additional information are summarized in Table 2.1-1.

---

* Some times reported by FAA are approximately 4 s fast, as discussed in Section 9.

** Units of Measurement—We have used SI units in most of our original work reported here. In some cases we have converted values from some of the references to SI units. In other cases we have the hybrid systems of units used by the British and the flying industry. In some cases, e.g. Fig. 6.1-1, we used British units in our analysis for ease of comparison. We apologize for these inconsistencies.

Fig. 2.1-1. Photo of PSA Flight 1771 crash site.

Table 2.1-1. Summary of approximate impact conditions for the basis accident.

Flight	PSA 1771
Date	December 7, 1987
Aircraft type	BAe 146-200
Flight altitude (initial)	6.7 km (22,000 ft)
Elevation of crash site	402 m (1320 ft)
Surface inclination:	
Maximum slope	24°
In vertical plane containing trajectory*	16°
Surface material*	Intensely weathered and fractured shale and sandstone
Aircraft status at impact:	
Velocity (true airspeed)*	282 m/s (925 ft/s)
Mach number	0.83
Surface impact angles (see Fig. 2.3-1b)*:	
Fuselage	57° (sum of pitch and surface inclination angles)
Trajectory	60° (sum of trajectory and surface inclination angles)
Direction (heading)	210° true
Pitch angle	41° down
Trajectory angle	44° down
Mass	29,300 kg

* Important parameters for crash test.

2.2 Aircraft Description

The BAe 146-200 is a high-wing, four-engine, jet-powered aircraft designed for short-range (2000-km) intercity flights. As configured, it could carry 83 passengers and a crew of four. The series 200, shown in Fig. 2.2-1, has an overall length of 28.6 m and a wing span of 26.3 m. Fuselage diameter is 3.6 m. Maximum takeoff weight is 42,200 kg. The design cruise Mach number is 0.7. At the time of the PSA Flight 1771 crash, the estimated total weight was 29,300 kg. The aircraft was flying at 6.7 km (22,000 ft) altitude where the design true airspeed is 218 m/s (425 kt). The true airspeed and Mach number of PSA Flight 1771 just prior to the shooting as determined from analysis of radar data were 178 m/s (349 kt) and 0.56, respectively.

Fig. 2.2-1. BAe 146-200 aircraft.

2.3 Crash Site Geotechnical Properties

Figure 2.3-1 shows a topographic sketch of the crash site and a depiction of the attitude of the aircraft at impact as determined by our studies.

The characteristics and geotechnical properties of the PSA Flight 1771 crash site were studied on the basis of data from extensive field investigations and measurements as well as laboratory tests. Field investigations consisted of topography surveys, exploratory borings, seismic refraction measurements, and dynamic penetration tests. Laboratory tests measured the basic engineering properties, compressibility characteristics, and stress-strain behavior of the soil/rock samples.

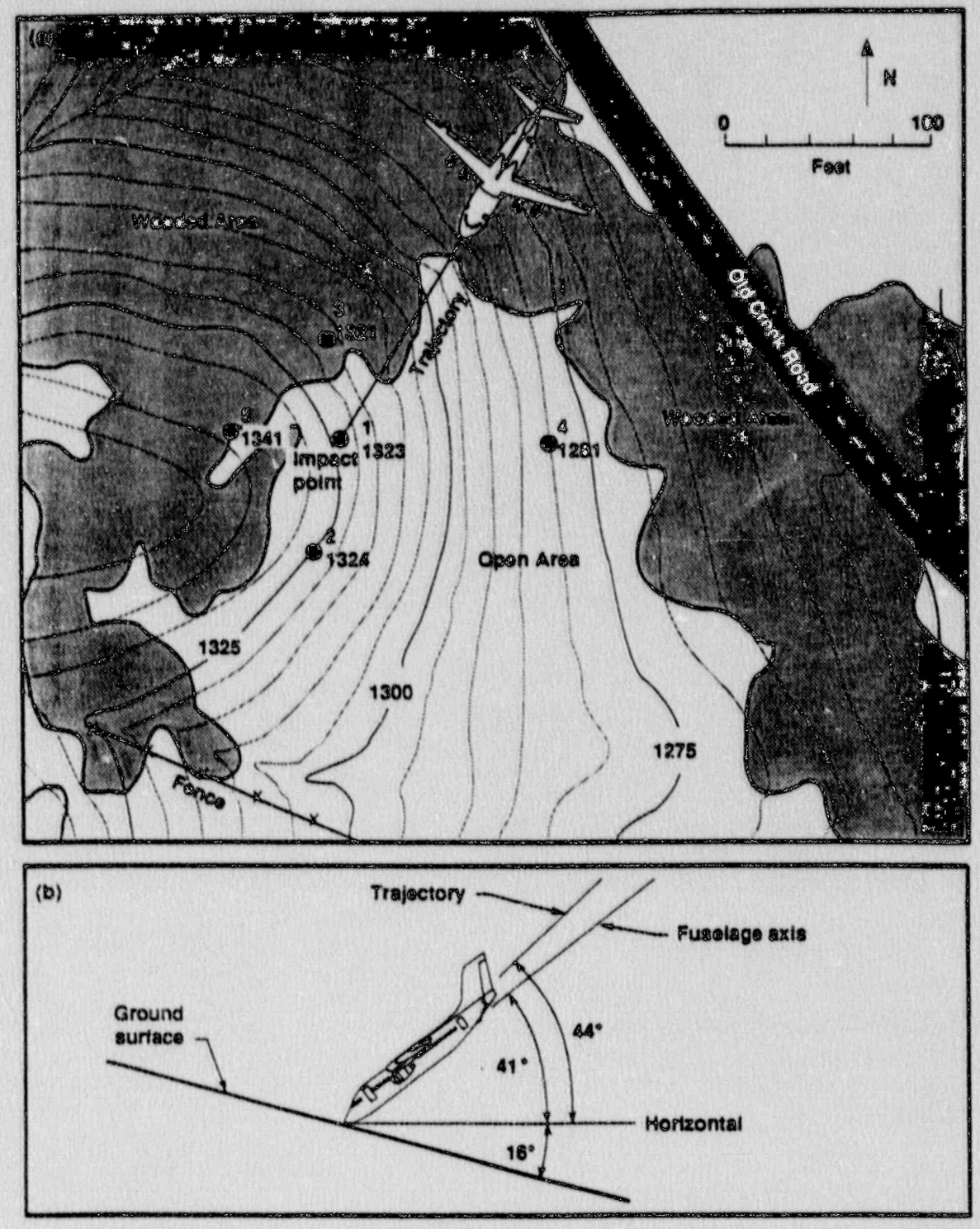

Fig. 2.3-1. (a) Topographic map of the PSA Flight 1771 crash site showing five drill hole locations and elevations (in feet). (b) Side view of final trajectory, showing pertinent angles.

A detailed geological engineering evaluation of the crash site is given in Ref. 4. The impact point is located near the top of a hill at an approximate elevation of 402 m m.s.l. The slope gradients of the hill vary from 20 to 40% (11.3 to 21.8°) in the vicinity of the impact point. We estimated the slope in the plane of the aircraft trajectory to be 16°. The crash site is covered with dark-brown, root-bearing, clayey silt colluvial soil that contains a variable amount of sand and weathered rock fragments. The thickness of the soil layer varies from approximately 0.15 m, in the vicinity of the impact point, to 2 m downslope to the southeast at the foot of the hill. The site is underlain by marine sedimentary rocks of the late Mesozoic Toro Formation. The rock near ground surface of the impact point consists mainly of intensely weathered and fractured sandstones interbedded by shales or siltstones. The average shear wave velocity we measured in the field is 610 ± 150 m/s. The measured compression wave velocity is 1220 ± 300 m/s.

The mechanical properties of the ground material at the crash site were measured in the laboratory. Rock property measurements are summarized in Ref. 5. Soil engineering properties, including compressibility characteristics and stress-strain behavior, are described in Ref. 6.

Geotechnical properties of the rocks at the site were determined from a variety of laboratory tests and measurements on drill core and outcrop samples. Pressure-volume tests to determine bulk modulus were conducted on cylindrical specimens 2.5 and 5.1 cm in diameter at pressures up to 480 MPa. The uniaxial compressive strengths for both sizes of specimens were also measured. Triaxial compression tests were conducted at pressures between 25 and 500 MPa to investigate the effect of confining pressure on stress-strain behavior. At higher confining pressure, strength increases and material response changes from brittle fracture to ductile, strain-hardening behavior. Strain-rate effect was investigated at confining pressures of 25 and 50 MPa for strain rates between 10^{-4} and 20/s. We observed an increase in ultimate strength and Young's modulus with increasing strain rate. Dry density and porosity of some specimens were also measured. Table 2.3-1 summarizes the measured properties.

The engineering properties of the soil were determined from laboratory tests of relatively undisturbed samples obtained from exploratory borings. The testing program consisted of measurements of general properties and tests of volumetric compressibility as well as stress-strain characteristics. These data are also summarized in Table 2.3-1.

Dynamic penetration tests were conducted at the site to determine the penetrability of the soil/rock at the crash site. The average penetrability constant (S-number) is about 2.5 ± 0.5 for rock and about 3.4 ± 0.3 for the top-soil layer. Details of the penetration tests are included in Ref. 4.

Table 2.3-1. Geotechnical properties of the PSA Flight 1771 crash site.

	Best Estimate or Average
Penetrability constant (S-number):	
Intensely weathered rock	2.5 ± 0.5
Soil	3.4 ± 0.3
Rock quality designation:	
Intensely weathered rock	15
Unconfined compressive strength (MPa):	
Weathered rock	22
Unweathered rock	102
Weathered and unweathered rock	53
Unconsolidated undrained strength (MPa):	
Soil	0.76 ± 0.35
Seismic wave velocities in upper 5 m (m/s):	
Shear wave velocity	610
Compression wave velocity	1220
Bulk density (kg/m^3):	
Rock	2370
Soil	2090
Water content, soil (%)	16.2
Porosity (%):	
Rock	8
Soil	32
Poisson ratio	
Rock	0.28
Soil	0.45
Unloading bulk modulus (MPa)	
Rock (average up to 4 cycles)	
First cycle (0 to 8 MPa)	2180
Up to four cycles (8 to 250 MPa)	5100
Soil (varies with mean effective stress)	130
Shear modulus (MPa)	
Rock (defined at 50% stress level)	
Unconfined	1307
Confined (25 to 250 MPa)	3394
Soil (defined at 50% stress level)	11.6

3. RADAR DATA

3.1 PSA Flight 1771 Radar Data

Reference 3 provides a listing of the radar data recorded at the FAA's Oakland ARTCC. The radar data together with recorded radio communications from the aircraft are shown in Table 3.1-1. We grouped these data into three approximately descriptive time periods representing 3.0 min of *pre-upset* operation, 1.2 min of *trouble-awareness* operation, and an overlapping period of 0.8 min of *dive* operation. Only overall average aircraft velocities calculated from these radar data for the first two time periods are considered to be meaningful.

It is possible to calculate an average aircraft velocity over a 12-s time interval (the characteristic sweep time of the radar) from the latitude, longitude, and altitude coordinates recorded at the beginning and end of each interval. We found, however, that there must be considerable error in these 12-s average velocity estimates since they vary unrealistically from one interval to the next. High accelerations and decelerations, of the order of 0.2 gee, would be present if the calculated velocities were accurate. This is not what an airline passenger normally experiences. We verified that this same situation existed on other flights for which we obtained radar data as discussed in Section 3.2.

Thus, the behavior noted in the *pre-upset* period of PSA Flight 1771 was not anomalous. Several consecutive 12-s-average velocity values can be averaged to provide a reasonable estimate of average aircraft velocity in steady level flight. These velocity calculations are illustrated in Fig. 3.1-1, which shows the 12-s-average velocities calculated from radar data recorded during the *pre-upset* period (preceding the announcement of gunfire), i. e., from 00:10:00 to 00:13:00 UTC on December 8, 1987. The overall average aircraft velocity (inertial speed) calculated for the *pre-upset* period is 178 m/s (349 kt) with a standard deviation of 11 m/s (22 kt).

During the *trouble-awareness* period, from 00:13:00 to 00:14:12 UTC, the average aircraft velocity calculated is 173 m/s (340 kt) with a standard deviation of 15 m/s (30 kt). The 12-s-average velocity values for this period are shown in Fig. 3.1-2. During the *trouble-awareness* period, the aircraft altitude changed, during the last 24 s, first to 21,900 ft then to 21,000 ft.

No radar altitude data was recorded after 00:14:12 UTC because the radar data acquisition system rejects "unrealistic" data that implies that allowable climb and dive rates are being greatly exceeded, as was the case in this instance. The average rate of altitude change during the *dive* period was in excess of 250 m/s, compared with the radar altitude data rejection limit set at a dive rate of 25 m/s.

Table 3.1-1. Radar data and pertinent radio communications recorded by FAA's Oakland ARTCC for PSA Flight 1771.

Time (UTC)		Latitude deg min sec	Longitude deg min sec	Altitude ft
00:09:48		35 : 12 : 22	120 : 32 : 04	22,000
00:10:00		35 : 13 : 15	120 : 32 : 58	22,000
00:10:12		35 : 14 : 08	120 : 33 : 52	22,000
00:10:24		35 : 15 : 01	120 : 34 : 47	22,000
00:10:36		35 : 15 : 53	120 : 35 : 42	22,000
00:10:48		35 : 16 : 40	120 : 36 : 46	22,000
00:11:00	*pre-*	35 : 17 : 32	120 : 37 : 31	22,000
00:11:12	*upset*	35 : 18 : 24	120 : 38 : 36	22,000
00:11:24		35 : 19 : 10	120 : 39 : 30	22,000
00:11:36		35 : 20 : 02	120 : 40 : 25	22,000
00:11:48		35 : 20 : 48	120 : 41 : 19	22,000
00:12:00		35 : 21 : 41	120 : 42 : 14	22,000
00:12:12		35 : 22 : 33	120 : 43 : 28	22,000
00:12:24		35 : 23 : 19	120 : 44 : 14	22,000
00:12:36		35 : 24 : 11	120 : 45 : 08	22,000
00:12:48		35 : 25 : 03	120 : 46 : 03	22,000
00:13:00		35 : 25 : 56	120 : 46 : 58	22,000
00:13:03		radio communication to Oakland ARTCC "... we've got a problem ... gun fired aboard ..."		
00:13:11		radio communication repeated "... gun fired aboard ... squawking 7700 ..." (no further radio communications)		
00:13:12	*trouble-awareness*	35 : 26 : 42	120 : 47 : 43	22,000
00:13:24		35 : 27 : 34	120 : 48 : 38	22,000
00:13:36		35 : 28 : 20	120 : 49 : 33	22,000
00:13:48		35 : 29 : 13	120 : 50 : 38	22,000
00:14:00		35 : 29 : 58	120 : 51 : 23	21,900
00:14:12	*dive*	35 : 31 : 06	120 : 51 : 42	21,000
00:14:24		35 : 31 : 43	120 : 51 : 42	---
00:14:36		35 : 31 : 36	120 : 51 : 14	---

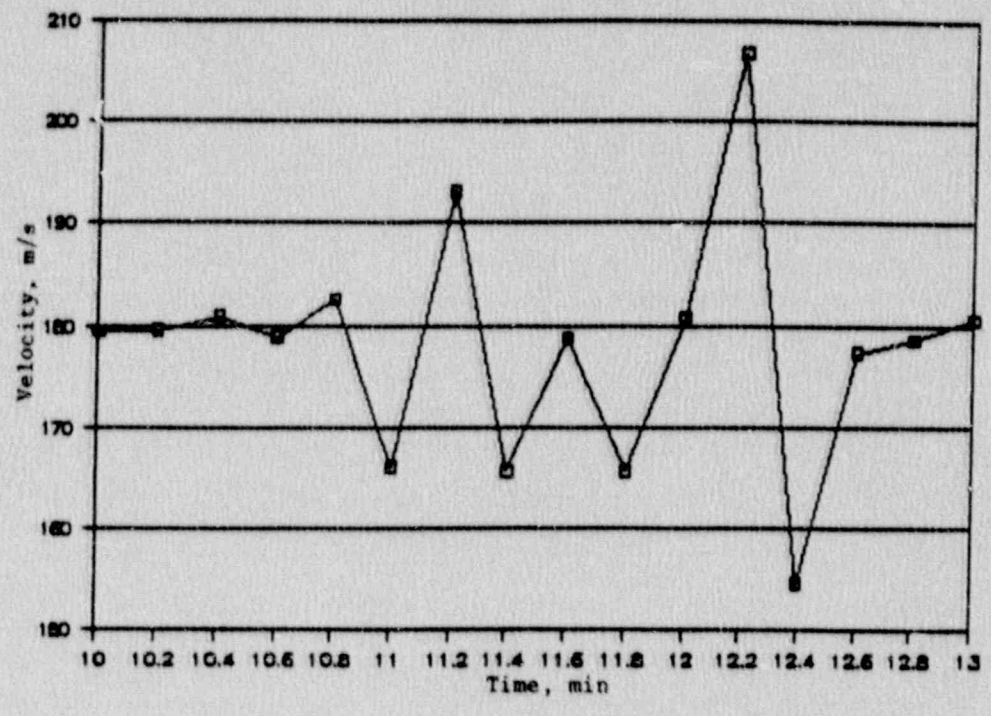

Fig. 3.1-1. Aircraft velocity during *pre-upset* operation period.

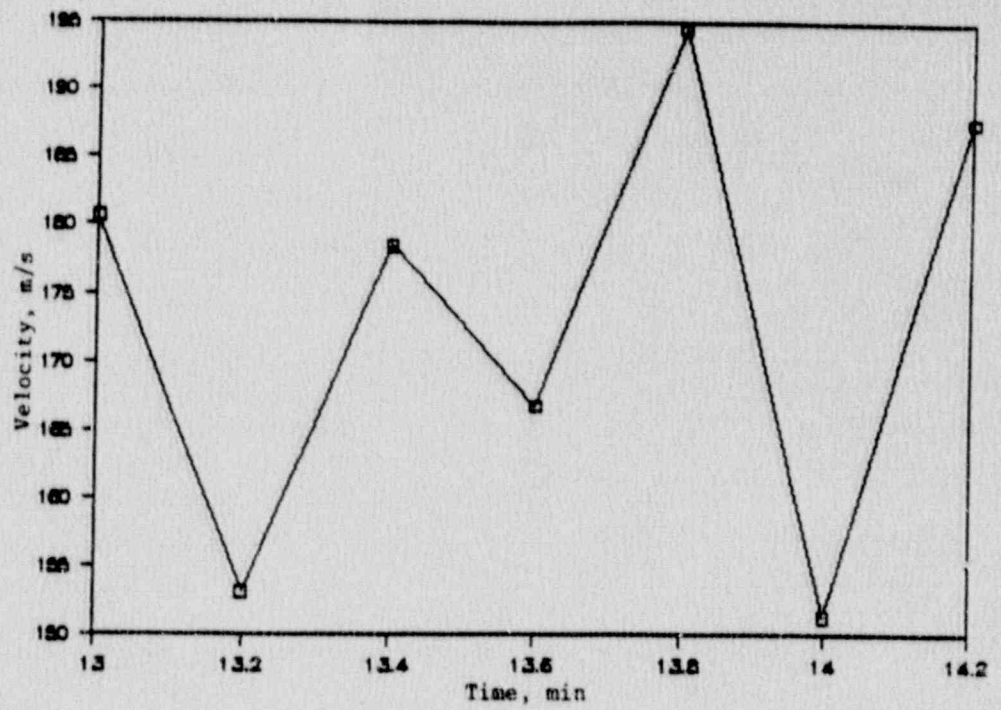

Fig. 3.2-2. Aircraft velocity during *trouble-awareness* operation period.

An accurate estimate of aircraft velocity at impact could not be obtained from analysis of the radar data during the *dive* period. The difficulty results, not only from the characteristics of the normal radar data (see Section 3.2) but also from the lack of altitude information for at least one of the radar coordinates (at 00:14:24 UTC) and the time of impact. This is illustrated in Fig. 3.1-3 (a, b, and c). In Fig. 3.1-3, the time of impact is assumed to coincide with time of the last radar data. With this assumption and an estimate of the elevation at the crash site, a remaining assumption that must be made is the altitude of the radar latitude and longitude coordinates at the next to last radar hit at 00:14:24 UTC. We made three arbitrary altitude assumptions for that time characterized as fast-slow, linear, and slow-fast as shown in Fig. 3.1-3a. The calculated aircraft velocity was then calculated for each set of assumptions. As can be seen in Fig. 3.1-3b, a wide variation of aircraft velocity at impact is obtained. The corresponding Mach number could have exceeded one (sonic) before impact or been sonic at impact under these assumptions as shown in Fig. 3.1-3c. We later determined that the aircraft did not become supersonic at any time.

Additional calculations were made, in the manner discussed above, assuming that impact occurred 12 s later since, in principle, this would be possible. This assumption allows more time before impact and consequently results in lower impact velocities. In this case we had to further assume two unspecified altitudes corresponding to the last two radar coordinates. As before we specified these altitudes in three arbitrary ways, fast-slow, linear, and slow-fast as shown in Fig. 3.1-4. None of these assumptions resulted in defensible close estimates of impact velocity.

3.2 Comparison of Radar Data

The erratic characteristic of aircraft velocity that we calculate from the radar data for PSA Flight 1771, even in the *pre-upset* period as seen in Fig. 3.1-1, does not seem plausible. Accordingly, we examined additional radar data and calculated the aircraft velocity in the same manner for other flights to observe the aircraft velocity of a "normal" flight. The additional data were provided to us by the FAA Oakland ARTCC, Ref. 7.

Since the BAe 146-200 is extensively used for flights between southern California and the San Francisco Bay Area, we requested data for three flights having the same general characteristics of PSA Flight 1771 and which used the BAe 146. The general characteristics of the three flights are listed in Table 3.2-1.

Table 3.2-1. Characteristics of flights used for radar derived velocity comparison.

ID	Time UTC	Altitude ft	Approx. Latitude deg:min	Approx. Longitude deg:min
X	1900	22,000	35:25	120:35
Y	0330	22,000	35:23	120:45
Z	0514	22,000	35:23	120:45

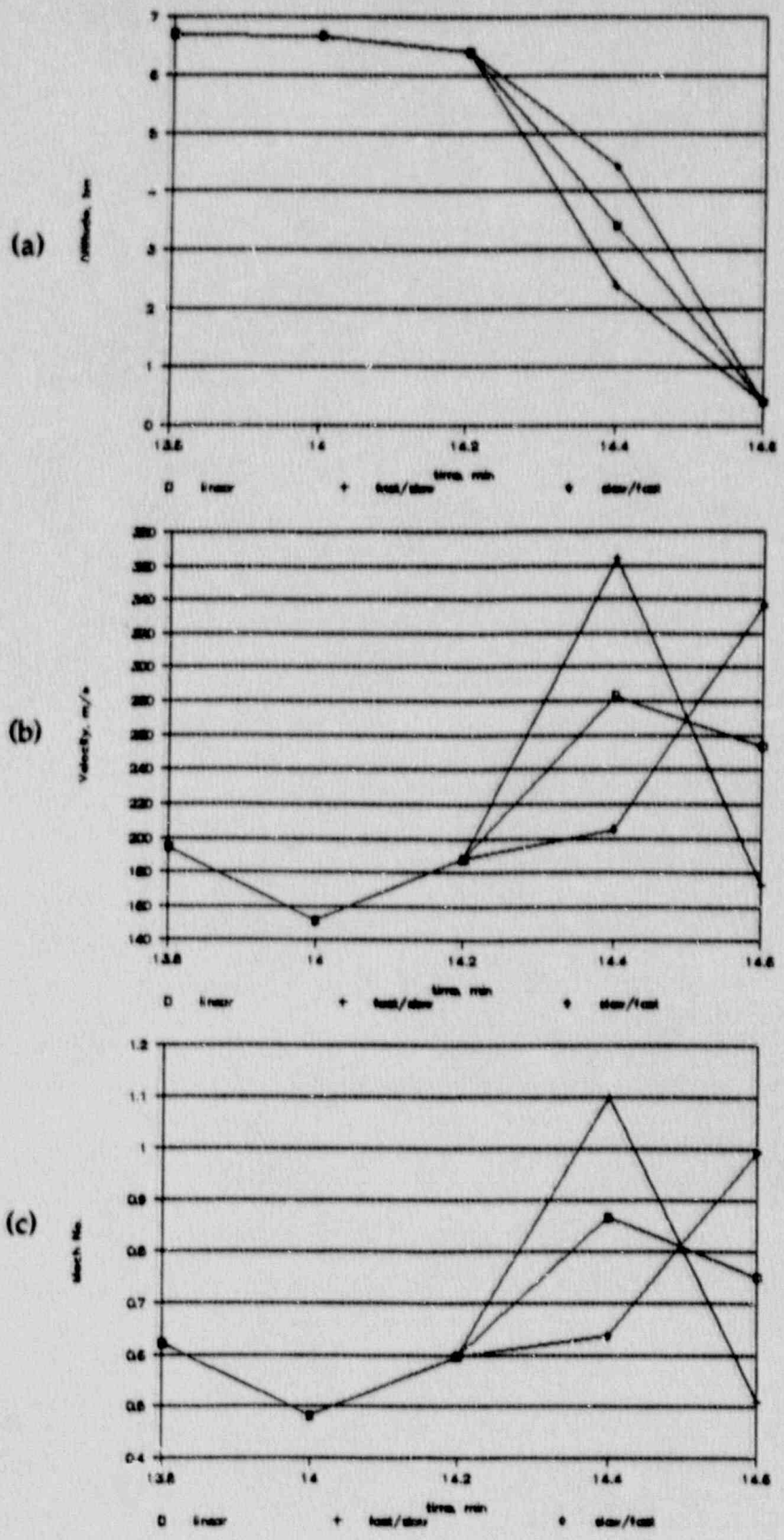

Fig. 3.1-3. Aircraft altitude (a), velocity (b), and Mach number (c) for assumed altitudes at 14.4 and 14.6 min during the *dive* period.

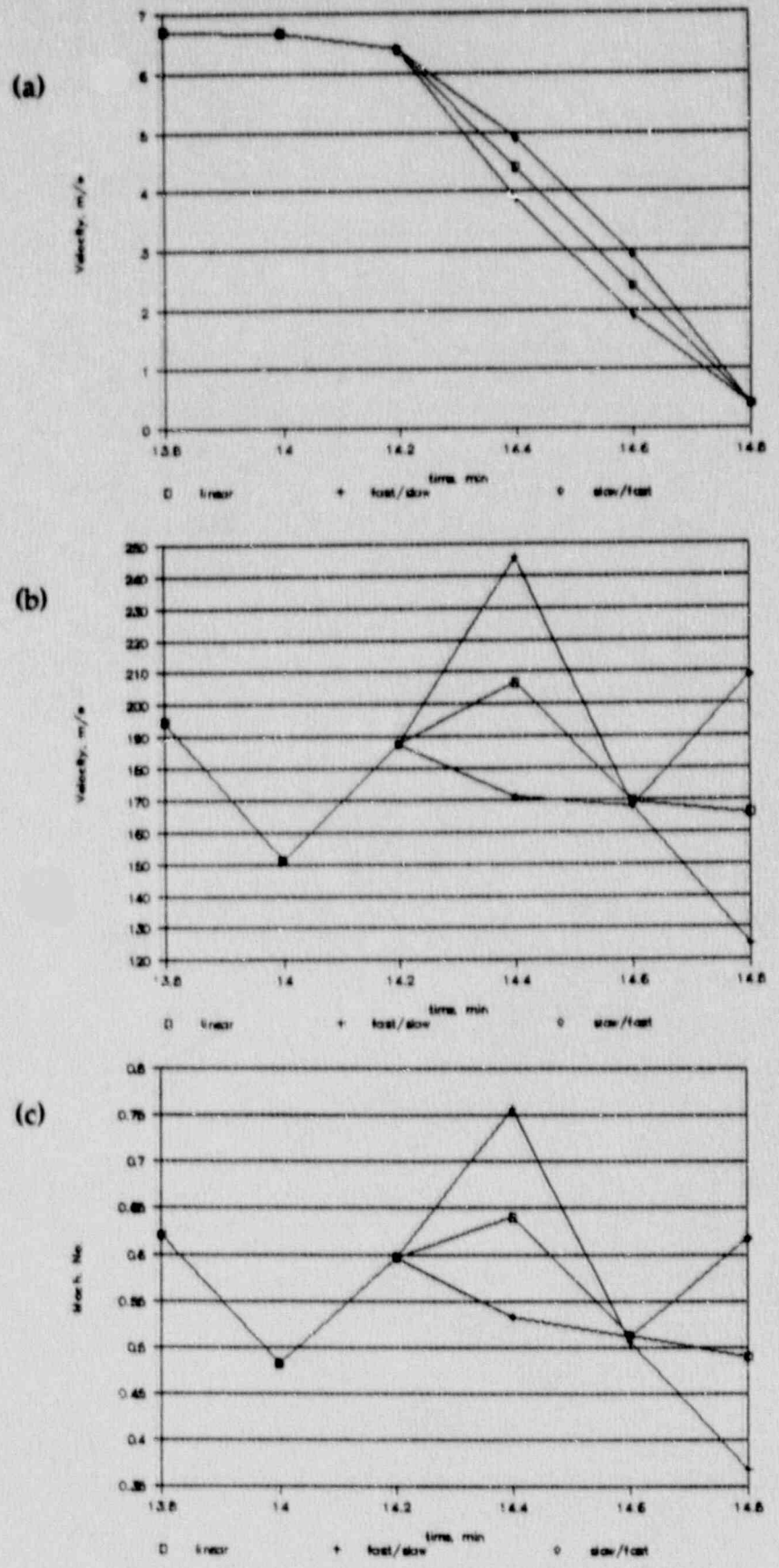

Fig. 3.1-4. Aircraft altitude (a), velocity (b), and Mach number (c) for assumed altitudes at 14.4, 14.6, and 14.8 min during the *dive* period.

The velocities we calculated for these flights from the radar data are shown in Fig. 3.2-1. Similar erratic behavior is observed for these "normal" flights as for PSA Flight 1771. Examination of Fig. 3.2-1 reveals a tendency for discrete values of velocity as opposed to a continuum of values. Although we did not investigate it further, this observation is consistent with our understanding that the radar data is treated in "bins" of five miles in length. This bin concept acts as a warning tolerance to the air traffic controller if more than one aircraft are in the same bin.

The average velocities and their standard deviations for the flights plotted in Fig. 3.2-1 are listed in Table 3.2-2 together with the values for PSA Flight 1771 during the *pre-upset* period. The average velocities of the comparison flights are somewhat higher and their standard deviations somewhat lower, but these differences are not believed to be significant.

Table 3.2-2. Calculated velocity from radar data comparisons.

Flight	Average velocity m/s	Standard deviation m/s
X	196	9
Y	190	11
Z	187	10
PSA 1771	176	13

We also compared the calculated velocity of PSA Flight 1771 from radar data recorded by the Oakland ARTCC with that recorded by the Los Angeles ARTCC, Ref. 8. The input to both centers is from the FAA's Paso Robles radar station located at Black Mountain, a 48-km line-of-sight* distance from the crash site. Just prior to the crash, at 00:11:17 UTC, responsibility for in-route control was handed over from Los Angeles to Oakland, but both centers continued to record the flight. The calculated velocities are plotted together in Fig. 3.2-2. Velocity differences of 15 m/s (about 10%) can be seen. The oscillations in the velocity calculated from the Los Angeles data appear to be less pronounced.

We did not pursue velocity calculations based on radar information further. We conclude that while average velocity over a period of time may be determined with some confidence, instantaneous values of velocity can not be estimated accurately. We also wish to make clear that we were trying to use the radar data in a manner for which it was not intended. It should not be inferred from our discussion of radar data that they are in any way deficient for their designated purpose, i.e. aircraft in-route safety.

* Because the intervening terrain is at much lower elevations, a clear line-of-sight probably exists between the radar station and the crash site.

Flight X

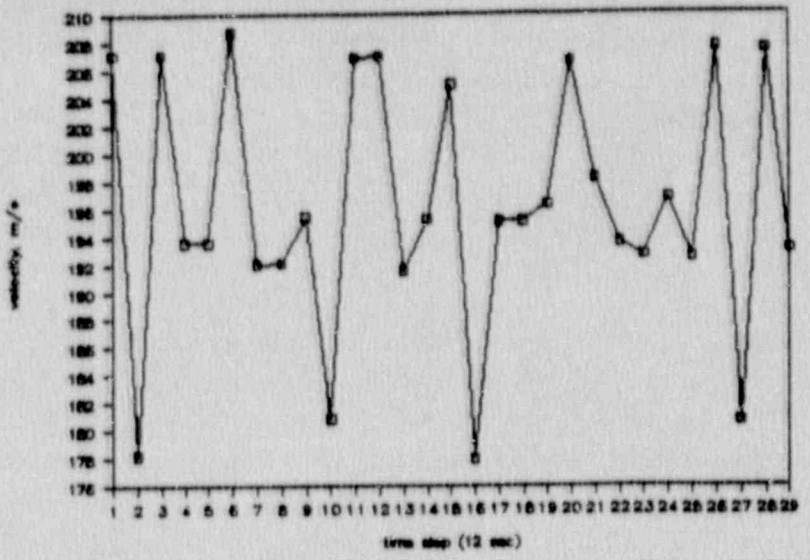

Flight Y

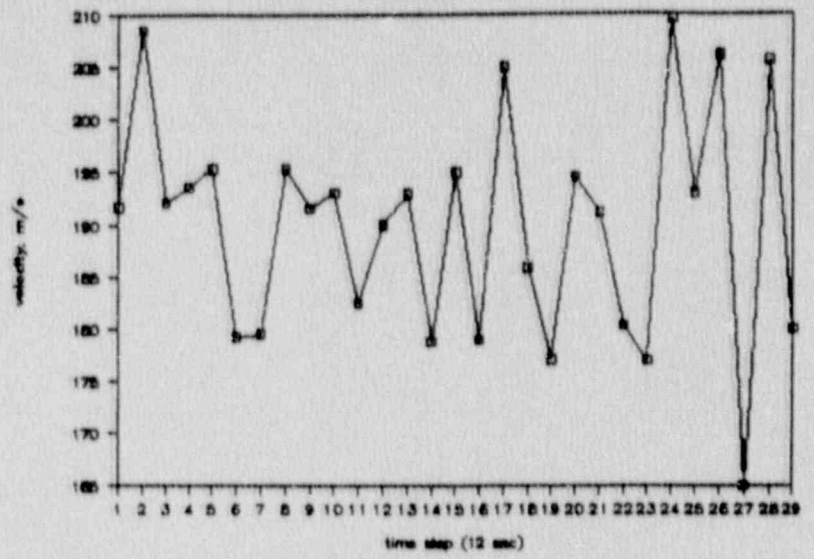

Flight Z

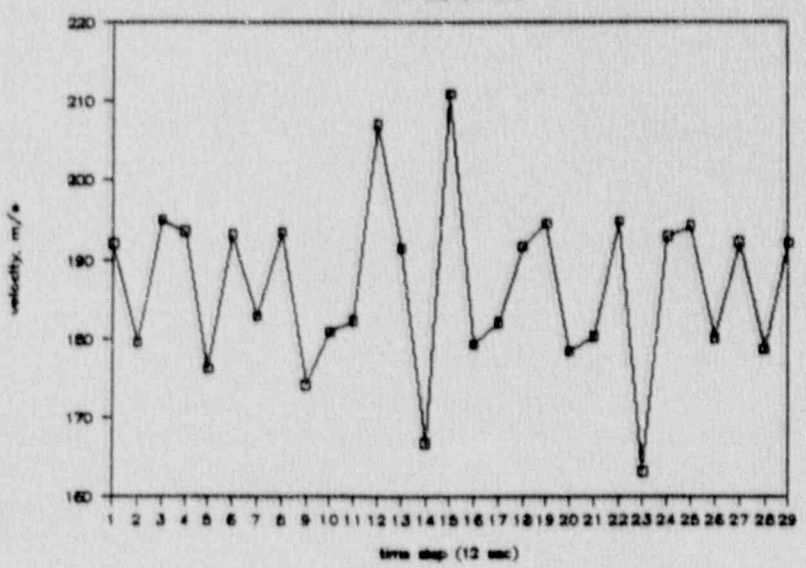

Fig. 3.2-1. Calculated aircraft velocity from radar data for three flights in the same general airspace as PSA Flight 1771 occupied during *pre-upset* operation.

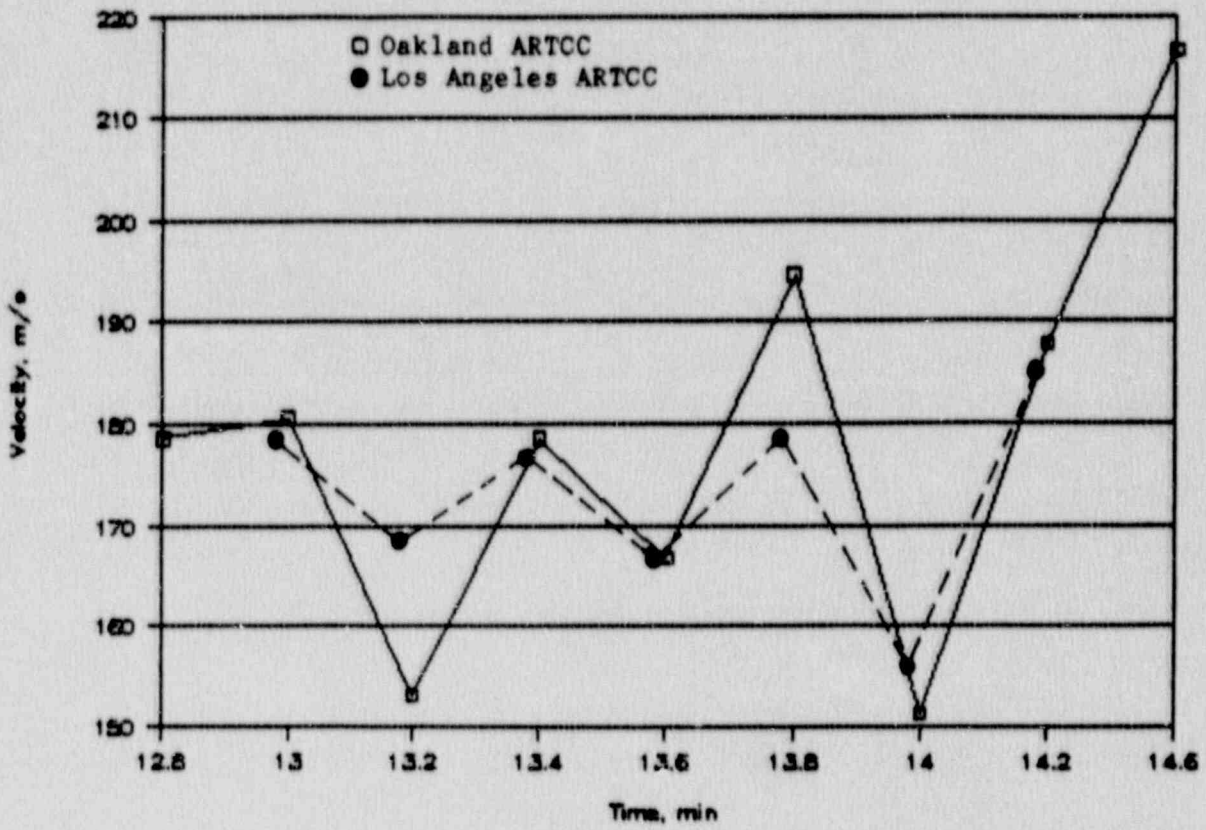

Fig. 3.2-2. Comparison of calculated velocities from radar data recorded by the Oakland and Los Angeles ARTCCs.

3.3. Early Aircraft Trajectory Estimates

Early in this study we tried a 3-D curve-fitting approach to establish the final trajectory of PSA Flight 1771. We combined the precise latitude, longitude, and elevation of the impact point with the radar data to allow a new visualization of the final aircraft trajectory in three dimensions. The altitudes for the last two radar points were then estimated after fitting a smooth curve through the known latitude-longitude coordinates for all the points.

These efforts provided reasonable but not unique trajectories. One of our early trajectories (Ref. 9), developed with a computer-aided-design program, is shown in Fig. 3.3-1. By using the altitude and speed information obtained subsequently from the FDR (see Section 7) and a timing correction from the seismic recording (see Section 9) we could (but did not) construct a fairly precise terminal trajectory of the type shown in Fig. 3.3-1.

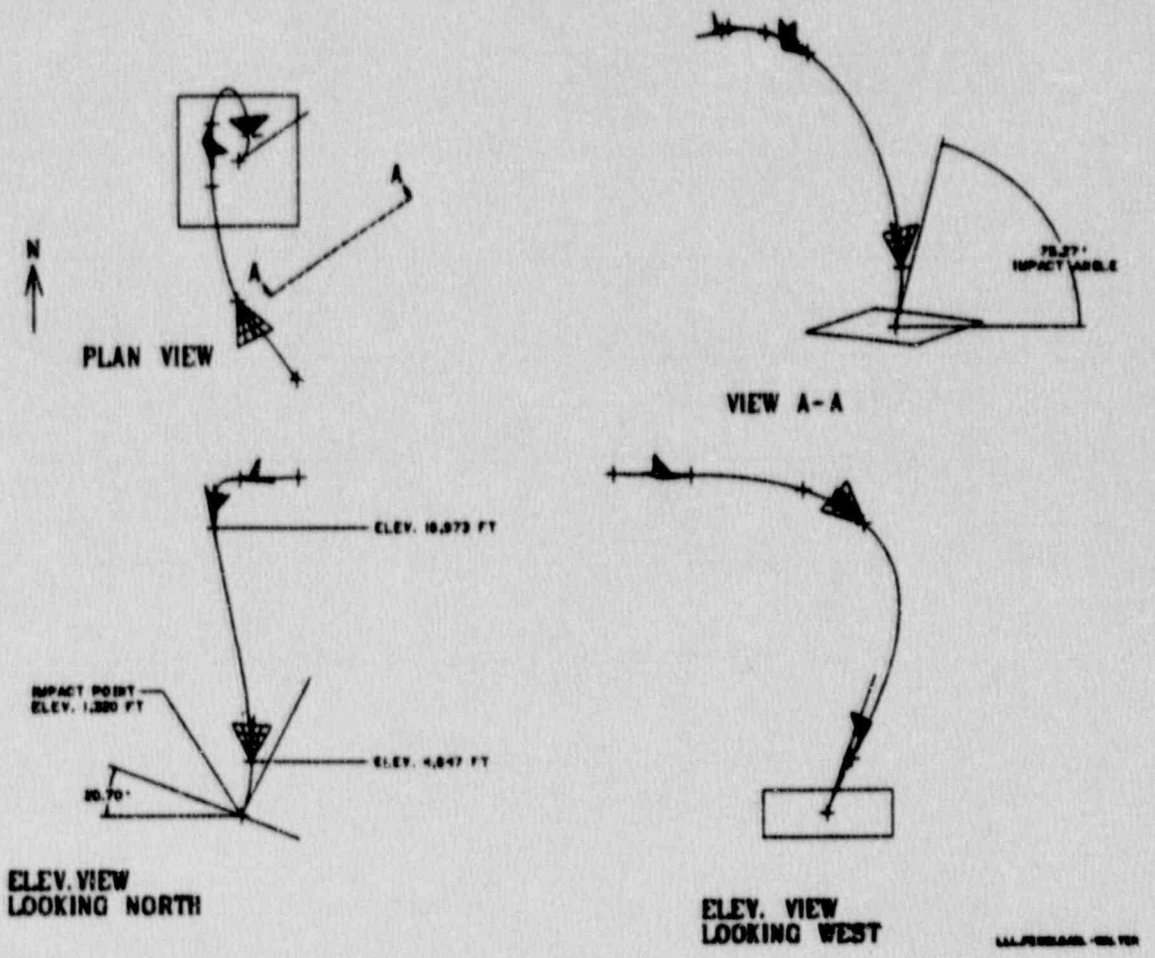

Fig. 3.3-1. Early attempt at estimating trajectory using 3-D curve-fitting technique. (The values shown are not our current best estimate.)

4. AIRCRAFT DEBRIS

We studied the aircraft debris from the PSA Flight 1771 crash in an attempt to better define the impact phenomena that occurred. The extensive fragmentation of the aircraft was not easily explainable. Indeed, the fragmentation was so great that we investigated whether an explosion might also have occurred. We conclude that this was not the case and offer a plausible but not a rigorous explanation for the extensive fragmentation which was observed.

4.1 Debris Size/Position

Examination of aerial photographs of the crash site taken by the San Luis Obispo County Sheriff's Office shortly after the crash of PSA Flight 1771 reveals a generally uniform distribution of debris in a relatively localized area. The photographs also show that the aircraft broke into a large number of very small pieces. None of the debris is recognizable by a casual observer as a section of fuselage or wing of an aircraft. Knowledgeable observers present at the site shortly after the crash were able to identify various components. Selected items of debris were identified and their locations plotted using laser survey equipment (Ref. 10). The resulting plot is reproduced in Fig. 4.1-1.

We calculated a horizontal distance of 15.0 m between the inboard engines after impact from their coordinates as given in the digital printout (Ref. 11) from the laser survey of the points shown in Fig. 4.1-1. We took inboard engines 2 and 3 to be points 4 and 10, respectively, in Fig. 4.1-1 on the basis of Refs. 10 and 12. The distance between the centerlines of the two inboard engines as installed on the BAe 146-200 is 8.4 m (Ref. 13). The difference between the installed and inferred impact location distance may be due to impact phenomena or incorrect interpretation of their location on Fig. 4.1-1.

As noted in Ref. 14, the engines were very badly damaged, and in general were missing a number of components. Therefore, many of the points within a radius of 60 m from the impact point in Fig.4.1-1 are identified as engine parts. The combustion turbine module (see Fig 4.1-2) represented the largest remaining assembly of each engine and was used by NTSB as the basis for engine identification and wing position. A qualitative sketch made in the field and reproduced in Fig. 4.1-3 shows the engine positions determined in this manner. According to Ref. 15, three engines were buried to a greater or lesser extent in the depression left by the impact. One engine came to rest on the hillside below the depression. Points 59, 60, 61, and 62 in Fig. 4.1-1 are described as left, back, right, and right edges of the crater, respectively. These data disagree with the visual recollection of the engines being "buried" in the "crater". In discussions with NTSB (Ref. 15) we learned that additional field notes which might be studied to clarify discrepancies between Figs. 4.1-1 and 4.1-3 were no longer available.

Considering the available data, we accept the qualitative disposition of the engines according to Ref. 15 (Fig. 4.1-3). We conclude that further quantitative analysis of the data provided in Ref. 10 is not possible within the scope of our investigation. We also note a discrepancy between the coordinates given in Ref. 10 for the "approximate center of the impact crater" and the coordinates of the impact point determined by our survey (see Ref. 4). We accept the latter. A comparison of Ref. 10 and our values is given in Table 4.1-1.

Table 4.1-1. Comparison of impact area coordinates and dimensions.

	NTSB (Ref. 10)	LLNL
Impact center coordinates[1]		
Latitude	35°31'12"	35°31'21"
Longitude	120°51'57"	120°51'22"
Impact "crater" dimensions (approx.)[2]		
Length	19.8	12
Width	12.2	6
Depth	3.7	3.5

1. This discrepancy in coordinates is substantial, representing a distance of 921 m. We choose our values as correct, since we know their basis.

2. The irregularity of the depression resulting from the aircraft impact, coupled with its location on the side of a hill, make simple dimensions ambiguous. Our values, also approximate, are based on measurement of geologic properties (see Ref. 4) after the depression had been excavated to some extent and filled (restored) to the original contour. There probably are no simple "correct" values.

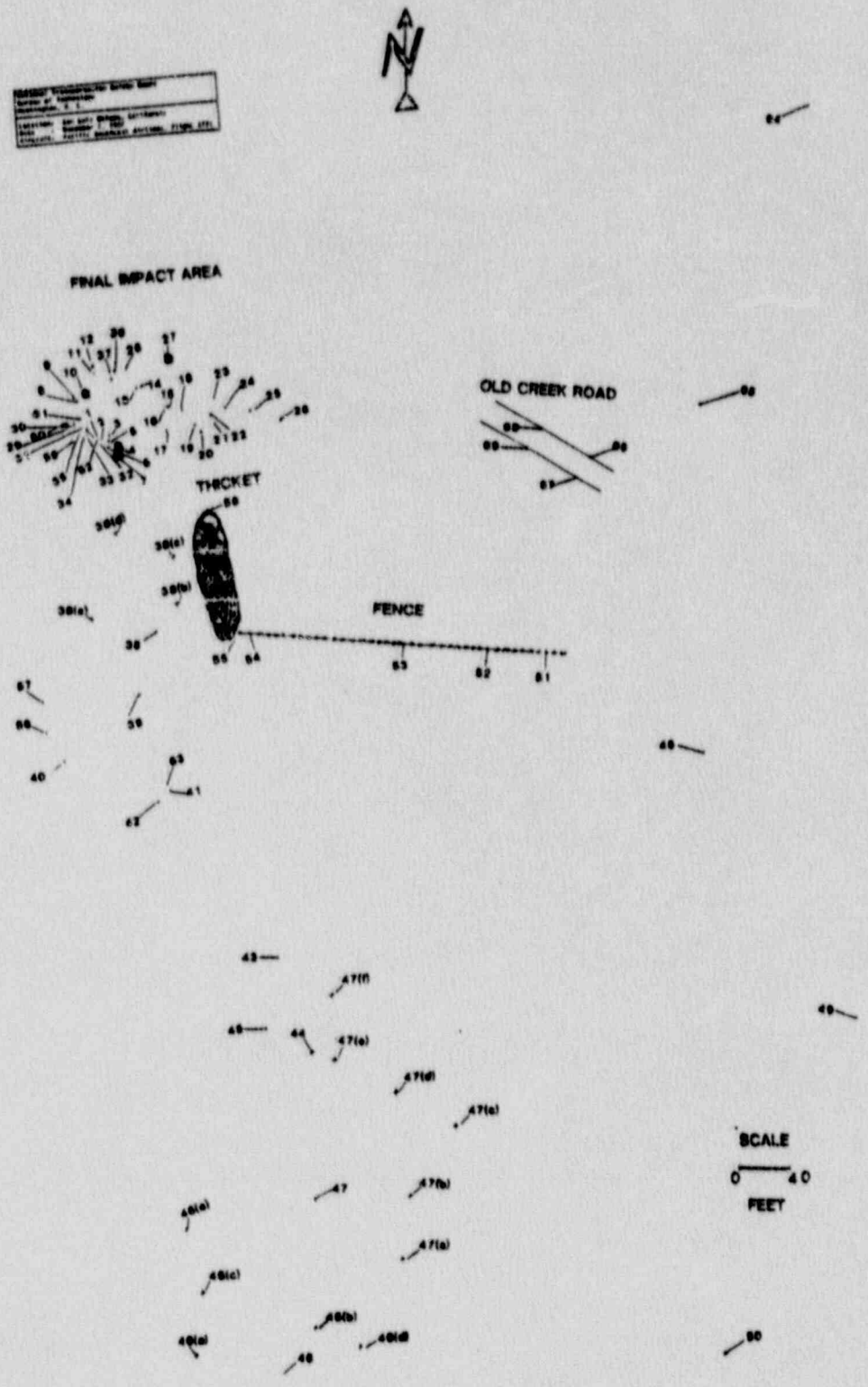

Fig. 4.1-1. Plot of identified debris items showing surveyed locations. Points 7, 4, 10, and 27 (identified by the filled-in squares) are believed to represent the main portions of engines 1, 2, 3, and 4, respectively.

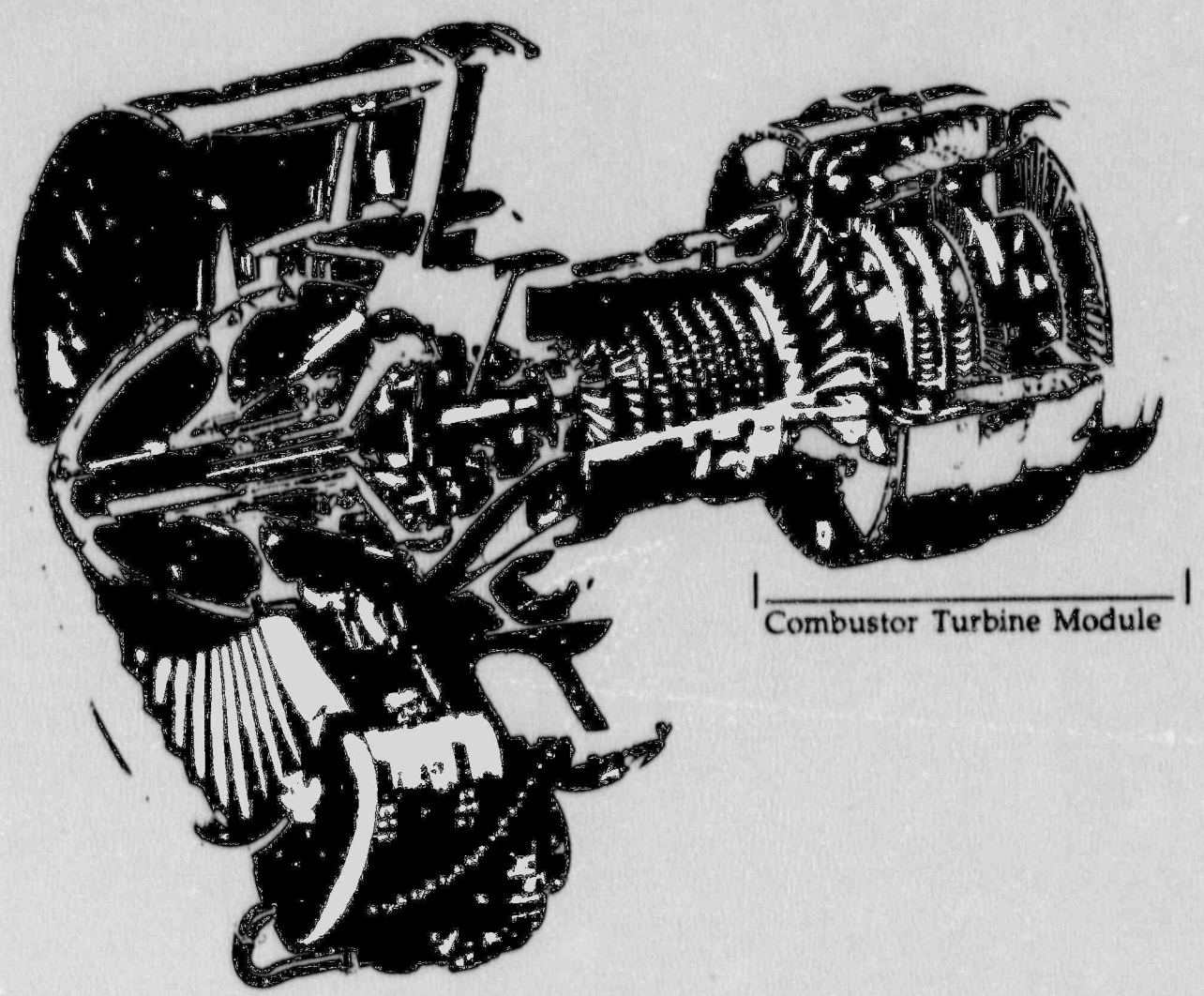

Fig. 4.1-2. Cutaway view of the ALF 502R engine used on the BAe 146-200.

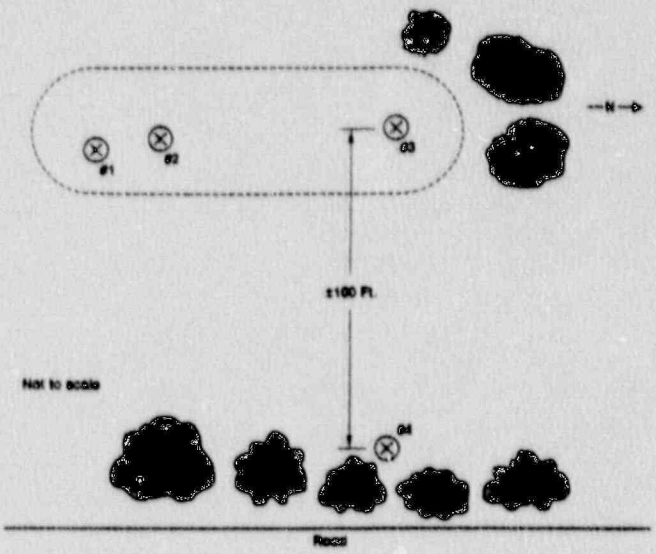

Fig. 4.1-3. Qualitative sketch of engine locations determined after crash.

4.2 Debris Distribution Analysis

To pursue the question of debris size and position distribution, a representative aerial photograph of the crash site was processed using a digital image enhancement technique. The objective of this investigation was to establish that the aircraft was intact until impact. The results and conclusions of this effort are reported in Ref. 16 and summarized below.

Histograms of debris size and distance from the impact point were obtained for a representative region of the debris field. As might be expected, the number of debris objects decreases as the size of the object increases as shown in Fig. 4.2-1. The final position of smaller sized pieces is relatively independent of distance from the impact point, while the larger sized pieces tend to be found closer to the impact point.

Because of the uncertainties in several factors affecting the observed debris area, application of the image processing technique did not allow a determination that all the debris could be observed. At best, 28% of the estimated outer surface area of the BAe 146-200 could be observed. Reference 16 provides a discussion of those factors. Crash witnesses generally reported that most of the aircraft debris was within view of the aerial photographs that we examined. We conclude therefore, although we could not corroborate, that essentially all of the aircraft is accounted for within the field of view of the photographs. A corollary to this conclusion is that the aircraft was intact until impact. As stated in Ref. 10, most of the debris was located within an angle of 42° fanning from the impact point to a radius of approximately 265 m southwest (in the direction of the aircraft heading just before impact). Some paper debris was found 800 m west of the impact point, and there are also reports of paper debris as far away as 2 km.

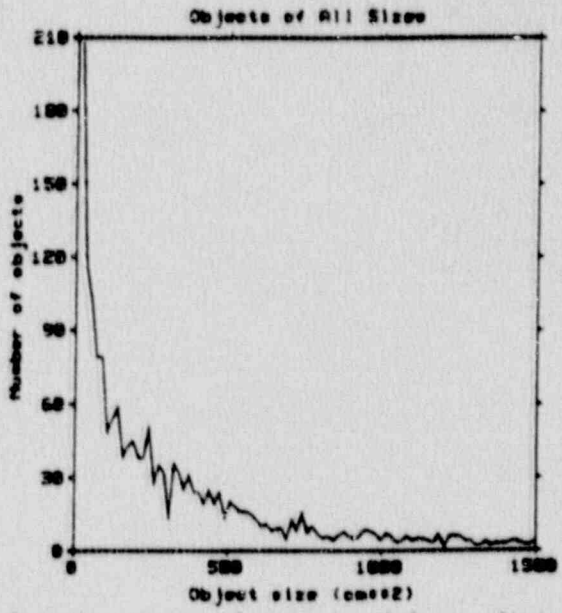

Fig. 4.2-1. Debris size distribution as determined from digital image enhancement techniques.

4.3 Fuselage Model Impact Tests

A short series of high-velocity impact tests was conducted on scale models of the fuselage. The objective of these exploratory high-impact tests was to discover the mechanism for aircraft fragmentation. A test consisted of firing a plastic projectile at the end of a lightly supported, thin-walled, 25-mm-diameter aluminum tube. The length-to-diameter ratio was chosen to match the fuselage ratio of the BAe 146-200. Although the thinnest commercially available tubing was used, the wall thickness was six to nine times thicker than required for proper scaling of the BAe 146-200. Projectile velocity was 290 m/s or higher in each test. The tests are described in Ref. 17, and the results and conclusions are briefly summarized below.

Five fragmentation mechanisms were considered to be candidates: 1) high strain rate, 2) high deformation rate, 3) air pressure buildup in fuselage at impact, 4) shrapnel from breakup of rigid/semi-rigid objects inside the fuselage, and 5) eruption of liquid present inside the fuselage. The tests established that "shattering" of the fuselage (and wing) which was observed at the crash of PSA Flight 1771 could be replicated to some extent in a laboratory environment. All five mechanisms were found to contribute to fragmentation of the scale fuselages. The presence of rigid, semi-rigid, and liquid mass inside the fuselage contributed most significantly to catastrophic fragmentation.

A sufficient number of tests were conducted to demonstrate the existence of several mechanisms which cause extensive fragmentation at high impact. Since an explosive energy source was not present in the tests, we conclude that the fragmentation observed at the PSA Flight 1771 crash site could have resulted without a chemical explosion. This is a significant conclusion that is discussed further in Section 5.

5. FIRE/EXPLOSION PHENOMENA

The extensive fragmentation which occurred on impact of PSA Flight 1771 raised the question of the possibility of an accompanying chemical explosion. Witness accounts of voluminous smoke at the time of the impact (Ref. 18) and the presence of fire fighters standing-by all night following the late afternoon crash to quench "spot fires" (Ref. 3) suggested that a large fire may have attended the crash. We conclude that there was no extensive fuel explosion, that there was a short-duration air-borne fire that rapidly self-extinguished, and that the consequences of fire were not significant in the overall damage assessment. The rationale for these conclusions is given below.

5.1 Fire Characterization

As reported in Ref. 3, the California Forestry Department fire fighters arrived at the site within half an hour of the crash of PSA Flight 1771. Nearby vegetation was wet from recent rains and did not burn, however numerous "spot" debris fires were extinguished on arrival of the Forestry Department. Reference 14 states there was no evidence of pre- or post-impact fire. Several witnesses (Ref. 18) described smoke rising from the impact point (but did not observe fire or smoke or objects coming from what appeared to be a complete aircraft before it crashed).

One of the witnesses (Ref. 18) was driving toward the crash site, did not see the aircraft crash, but did observe a "thick black dense smoke cloud rising quickly" over a ridge of hills. The "thick black dense smoke appeared to be oily and rolling upward". The cloud eventually peaked and drifted south. According to Ref. 3, wind was (from) N to NW at 3.6 m/s. This witness then continued toward the crash site arriving approximately 7 min later. The smoke at that time had a gray-white consistency. There were several spot fires and an object burning in a tree. The area was saturated with a strong smell of fuel. It was obvious that the fire had not burned on the ground as the trees, grass, and debris were not scorched (loose paper money was lying about).

Another witness driving home saw an aircraft diving toward the ground before it disappeared from view and he saw a "column of smoke". Recognizing that he had witnessed an aircraft crash, he called in the emergency and drove to the crash site. About a dozen people were already there. He noted smoke from an airplane engine near the road. (This would be engine number 4 shown in Fig. 4.1.3.)

Several witnesses provided similar accounts of what they had seen. Additional quotes from the interviewer of several witnesses to the crash (Ref. 18) are given below (words in brackets [ ] and emphasis are ours). Each indented paragraph below represents a separate witness.

> "The sky was blue and the sun was behind him ..... he closely viewed the aircraft and there was nothing missing ..... There was no smoke, no

fire, no breaks in the cabin and the aircraft appeared to be completely intact. ..... Moments after the crash, he observed a tall tower of black smoke which had a gray cast, but it was much like an oil fire. He observed no flame and no debris in that cloud. The column of smoke quickly turned to white, and a smoke ring then rose into the air. ..... [on arrival at the crash site] immediately began looking for the fuselage, but no recognizable pieces of aircraft were seen. There were several small isolated fires in the debris field and some of the fires were material hanging in the trees. They saw several of the aircraft engines." [According to Ref. 15, engines number 1, 2, and 3 were buried.]

"..... he then observed a black smoke cloud rising from behind an intervening hill. He did not see fire in the cloud or any objects, but the cloud rapidly ascended and then rapidly dispersed. ..... He walked up the hill toward the impact crater. There were several small fires approximately one foot in diameter which were burning at various places on the hillside."

"..... advised that the aircraft was intact and he saw no holes, no burn marks, no fire, no smoke, and no debris flying off of the aircraft. ..... driving past a very steep hill to the right so that they could not see the impact. He believes that 20 seconds or so after the crash a black cloud of smoke was seen rising from the area of the crash. The black smoke was rising rapidly and he did not see any debris or fire in the smoke. A smoke ring followed the original *detonation* cloud into the air. ..... arrived at the crash scene less than five minutes after the crash. ..... When ..... first entered the debris area, there were several small fires burning, and he stopped several of them by stamping them out with his shoe." [This witness referred to seeing a bullet casing two feet north of "the most intact aircraft engine" when he was in the impact crater. This implies that he saw more than one engine and that the ones he saw were not buried (fully) as implied by Ref. 15.]

"He recalled looking at his wristwatch as he made the turn from Highway 46 to Old Creek Road, [less than 2 km from the crash site] and at that time it was about 4:18 p.m. As he drove past the trees near the crash site he observed six vehicles parked at the scene. When he got out of his car ..... he observed the impact site with smoke coming from it and small fires all around it and also throughout the field, and even objects burning in the trees. ..... There was a strong odor of jet fuel in the area, and while in the trees he recalls seeing what he could best describe as heavy fabric material burning in the trees."

"She saw no flames, smoke, nor debris falling from this aircraft. Before disappearing behind the hill, the aircraft banked steeply, which was

unusual. A few minutes later she saw a black mist or black smoke generally in the area she believes the plane crashed."

We conclude from this information that the spot fires caused negligible damage. The spot fires resulted from combustible aircraft debris being ejected from the impact point and traveling through an airborne fuel fire. The fuel, also ejected from the impact point, mixed with air and was ignited by hot engine parts which were later found scattered over a large area (see Section 4.1). The odor of fuel, some of which was absorbed in the ground, was reported to be strong. During the engineering geologic investigation of the crash site that we conducted 16 months after the crash (March, April 1989) jet fuel stains were noted in core samples along a fracture at a depth of about 6 m (Ref. 4). An oily substance presumed to be jet fuel because of its odor was also present in the drilling fluid returns from drill hole number 1 used to obtain core samples (see Fig. 2.3-1).

Fire fighting equipment remained on standby at the site for several days in the event of subsequent ignitions. The next day, however, clean-up operations were suspended because of heavy rains. According to Ref. 3 "The area, *already very wet* from previous rains, became *very slippery*. The search was suspended due to dangerous conditions and to prevent destruction of items that may [sic] occur if items were stepped on and driven into the *soggy earth*."

We did not attempt to estimate the amount of fuel that burned as a result of the crash or to quantify the chemical energy expended in burning the fuel. We know that there was a noticeable quantity of unburned fuel in the ground as shown by our geotechnical investigations. It is interesting to note that the chemical energy in the fuel estimated to be onboard (see Section 2) at the time of the crash was two orders of magnitude (factor of 125) higher than the kinetic energy of the aircraft at impact.

We propose the following plausible scenario which explains what occurred: at impact, high hydrostatic pressure (above 30 MPa) was developed in the wings (fuel tanks), which together with other impact forces caused the wings to break open and flash high-pressure fuel in all directions. At the same time pieces from the hot engines and combustible debris from the fuselage were also being scattered in all directions. FDR data (see Section 7) indicates that the engines were operating essentially at full power immediately before the crash, assuring that hot turbine blades were present. The fuel became intimately mixed with air, aerosolized, and would have burned cleanly and completely when ignited if it were not for the very likely presence of "moist dust" and rocks which were also ejected from the impact "crater". The flame temperature achieved under these conditions has been shown (Ref. 19) to be very strongly affected by small amounts of dry soil. The effect is even more pronounced if the soil is wet as was the case at the PSA Flight 1771 crash site. Under these conditions, complete combustion is inhibited and the smoke produced is black, as was observed.

5.2 Complete Fuel Explosion Unlikely

Some of the witnesses quoted in Section 5.1 used the words "detonation" and "detonation cloud" to describe the smoke which they observed. One witness advised the interviewer that he had used dynamite extensively during his lifetime (age unknown). He went on to say that the crash site appeared to him as if a large dynamite charge had been detonated in the ground, as the explosion from such a charge can smoke for several hours.

We do not know whether the word "detonation" was intended as a means of describing an explosive process as distinguished from combustion. Since Ref. 18 reveals little, if any, information about the witnesses, we can not evaluate whether these witnesses used the word "detonation" in a precise sense. The dynamite expert's analogy of the crash scene to the smoke observed for hours from a dynamite explosion in the ground does not fit the observations of most of the other witnesses that the black smoke rose quickly, turned gray, and rapidly drifted away.

Since the aerosolized fuel contained moist ground material, a detonation wave, if initiated, was probably not sustained. This statement was reviewed with explosive experts at LLNL (Ref. 20), who find that the statement is reasonable but not conclusive. A partial aerosol gas explosion followed by a normal fuel fire seems likely.

6. FLIGHT SIMULATOR STUDY

Very early in our investigation of the PSA Flight 1771 crash, we determined that the Flight Data Recorder had been badly damaged. NTSB indicated (Ref. 21) that it would be difficult if not impossible to extract useful data from the broken tape. Accordingly, we decided to request British Aerospace to perform flight simulator analyses, and also to review and comment on the structural capability of the BAe 146-200 to remain intact prior to impact at airspeeds clearly in excess of design airspeed. A scope of work was prepared and BAe agreed to perform this work. The results of the aerodynamic analyses on the simulator are reported in Ref. 22. These results were reviewed for structural implications, and the review comments are given in Ref. 23. We have reproduced or paraphrased much of the information provided in Refs. 22 and 23 below.

6.1 Aerodynamic Analysis

The purpose of these analyses was to assess, as well as possible, the final velocity and dive angle before impact of PSA Flight 1771. It was judged that by varying key flight parameters the likely range of possible speeds and dive angles could be determined. The simulation was started from the known steady flight cruise condition at 22,000 ft and terminated at the known impact elevation of 1320 ft. The analyses were restricted to the pitch axis, i. e., the simulation was constrained in a vertical plane, although the radar data indicated that the trajectory had a "hooked" footprint as shown in Fig. 6.1-1. This limitation of the analyses should not alter the principal conclusion of the study. The strong increase in drag with increasing Mach number limits the maximum speed, and thus the impact speed, to an acceptably narrow range.

6.1.1 Design Speeds

The variations in design speeds with altitude for the BAe 146-200 are shown in Fig. 6.1-2. Some results of the simulator analyses are also indicated on this figure. The curves labeled V_C and M_C are limits on speed and Mach number for climb, cruise, and descent beyond which the aircraft should not be intentionally operated.

The curves labeled V_D and M_D are the corresponding limits for the design diving speed which could be reached as a consequence of an upset maneuver in cloud or severe turbulence, or due to atmospheric gusts, windshear, or emergency avoidance maneuvers. Demonstration of specified handling characteristics at speeds up to V_D/M_D are necessary for certification purposes. BAe plans to increase the BAe 146-200 design Mach number M_C/M_D to 0.73/0.80 in the near future as shown in Fig. 6.1-2. During development and certification testing the aircraft has been flown up to M=0.80.

Point	Time, s	Lat. (35°+)	Long. (120°+)	Coordinates** E-W ft	Coordinates** N-S ft
0	0	29' 13"	50' 38"	0	0
1	12	29' 58"	51' 23"	3,710 W	4,636 N
2	24	31' 6"	51' 42"	1,565 W	7,001 N
3	36	31' 43"	51' 42"	0	3,809 N
4	48	31' 36"	51' 14"	2,306 E	722 S
5	50*	31' 21"	51' 22"	659 W	1,542 S

Point	Altitude ft	Δh, ft	Linear Horiz. Dist. ft	Est. Slant Dist. ft	Est. Speed ft/s
0	22,000	- - -	- - -	- - -	- - -
1	21,900	100	5,935	5,935	495
2	21,000	900	7,172	7,228	602
3	12,000*	9,000	3,809	9,773	814
4	2,000*	10,000	2,418	10,288	857
5	1,320	680	1,680	1,812	906
		TOTAL	21,014		

* Assumed

** Coordinates are measured from the preceding point.
- - Linear horizontal distance between coordinates.
— Probable curved horizontal between coordinates.

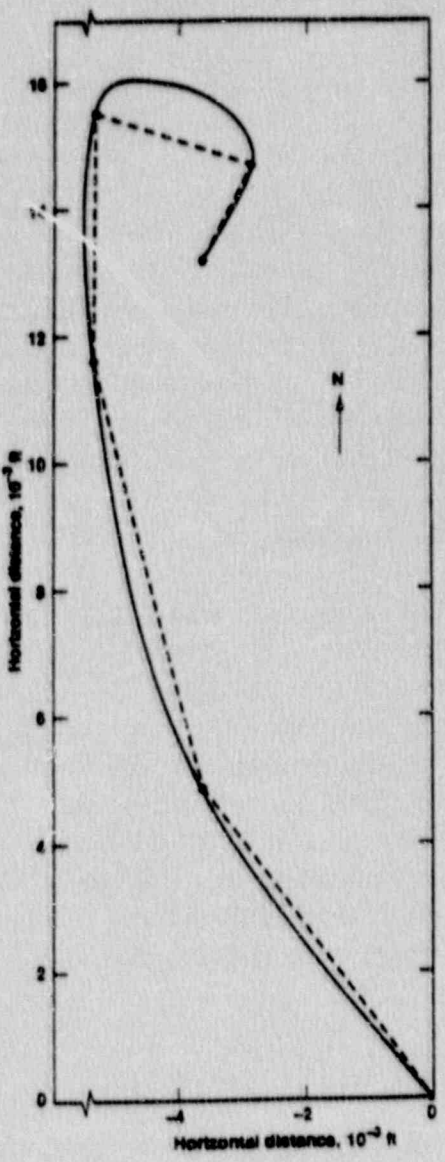

Fig. 6.1-1. Horizontal representation of the terminal flight coordinates based on radar data and our topological survey. Approximate aircraft speed between adjacent points is estimated on the basis of slant distance.

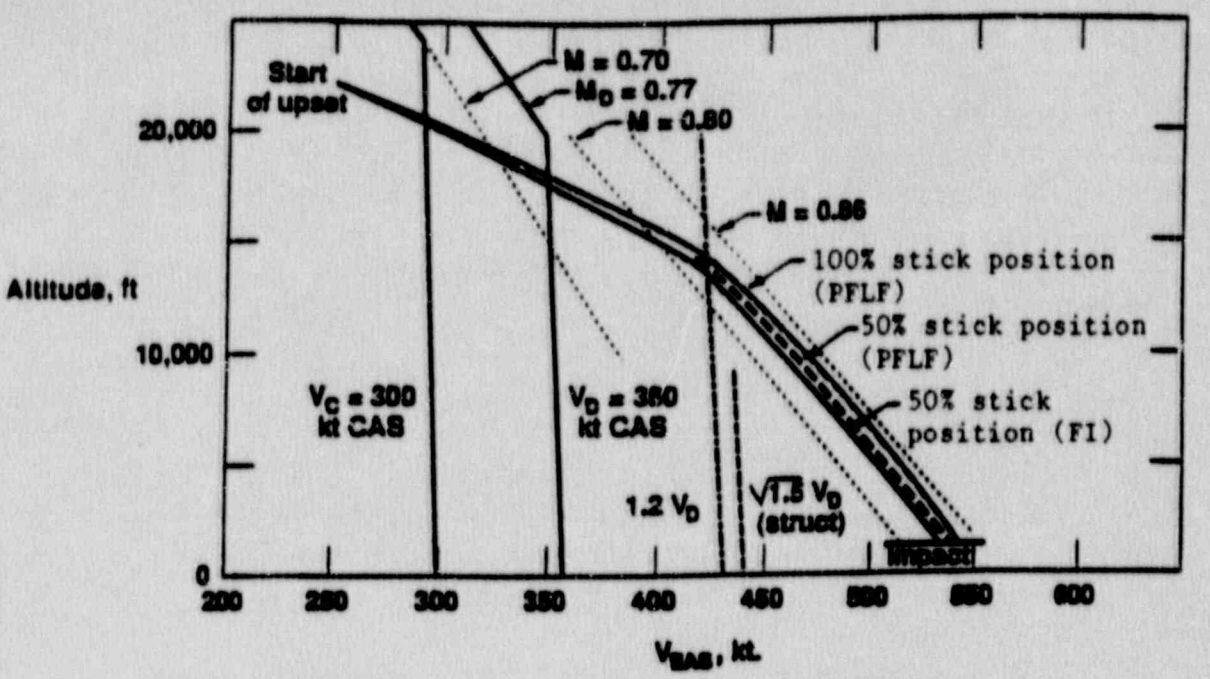

Fig. 6.1-2. Design speeds of the BAe 146-200 with simulation results superimposed.

The 1.2 V_D boundary is also shown on Fig. 6.1-2. Freedom from flutter is demonstrated up to V_D by flight testing; between V_D and 1.2 V_D flutter clearance is determined by theoretical methods supported empirically by static ground vibration tests and flight tests at the lower speeds. Despite the certification work performed it is difficult to predict, for a specified aircraft loading, the minimum altitude/speed conditions where flutter will occur. BAe engineers state that their mathematical aeroelastic model indicates that the elevator torsional mode becomes unstable at speeds of about 450 to 500 kt EAS, and there is an engine mode with low damping that could result in flutter above 520 kt EAS. However, the prediction of some form of flutter in these cases is dependent on an accurate knowledge of unsteady aerodynamic forces at high Mach number and structural damping. Without such data, estimates of flutter speeds can be considerably in error.

6.1.2 Simulator Design

The BAe simulation facility (at Hatfield, England) is a moving base simulator with a visual display designed primarily for pilot-in-the-loop investigations but also capable of unpiloted analyses. The simulator has six degrees of freedom, the mathematical modeling being done on a digital computer system. The mathematical model of the aircraft is based on aerodynamics derived from both flight test measurements and high- and low-speed wind tunnel tests. Good correlation between the aircraft and the design simulator characteristics has been proved. At Mach numbers above 0.78 the aerodynamic data are based on high-speed wind tunnel tests which extend up to 0.83.

One of the most important aerodynamic parameters in this analysis is the aircraft drag. At a typical cruise condition the total drag, C_D, is 0.032. The variation of one of its components, the compressibility drag coefficient C_{DM}, with C_L and Mach number is shown in Fig. 6.1-3. At the typical cruise condition at M=0.7, C_{DM} is 0.002 as indicated on the figure. At about the same value of C_L, the total drag at M=0.83 would be 0.085, almost 3 times greater. This illustrates the very large increase in drag as the aircraft accelerates from the design cruise speed through the dive limit envelope, M_D = 0.77.

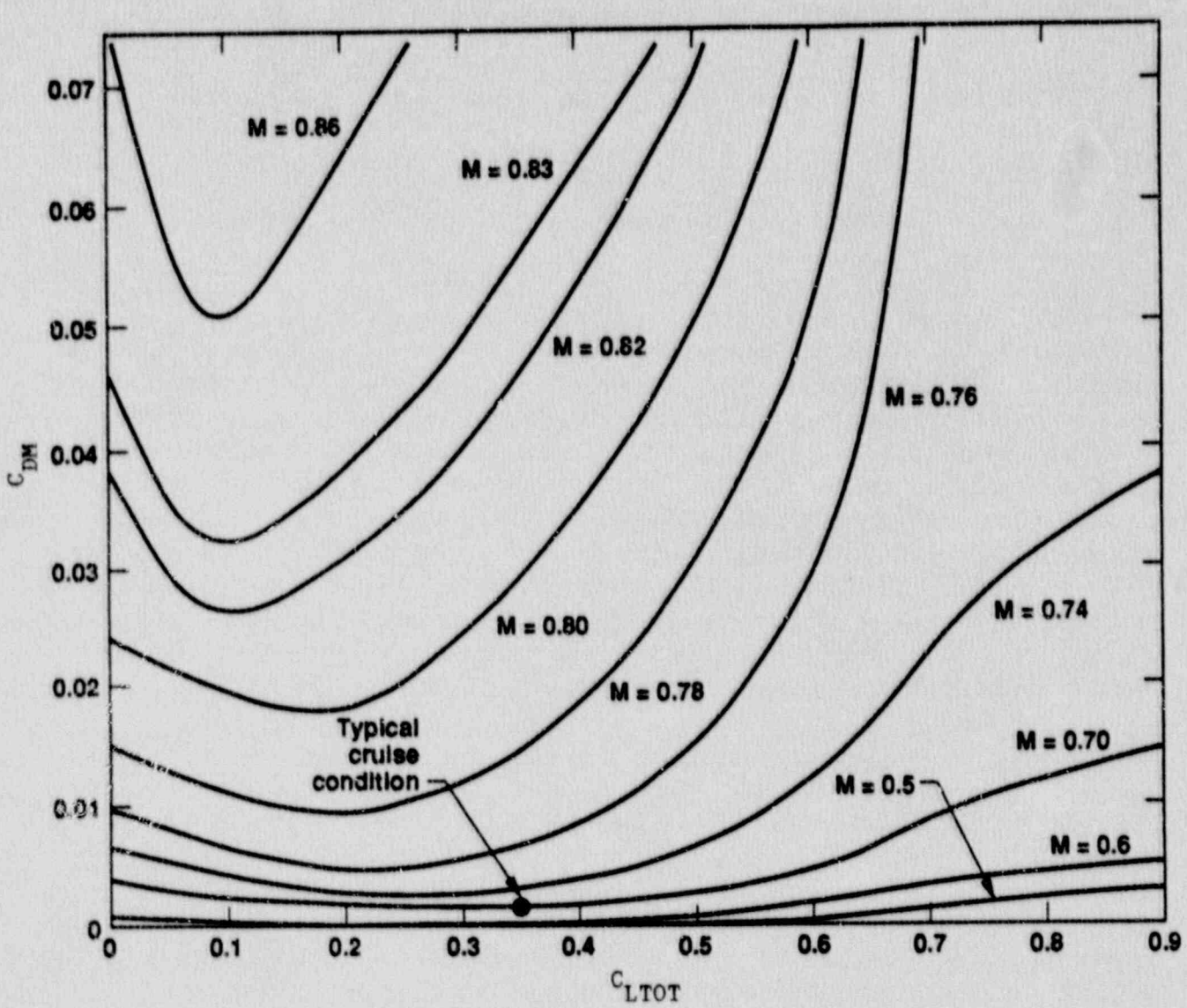

Fig. 6.1-3. Drag coefficient increment due to Mach number.

The curve for M = 0.86 shown in Fig. 6.1-3 was extrapolated. It had been intended to examine the sensitivity of the results to the extrapolated aerodynamic characteristics in a region where the accuracy was suspect by repeating the tests with a tolerance on the data at Mach numbers in excess of 0.83. However, this was found not to be necessary because the ultimate Mach number in the simulations did not exceed 0.855 in any case examined. It is considered that any likely error in the simulation model between 0.83 and 0.855 would have a negligible effect on the terminal velocity.

The total drag on the aircraft depends on the drag coefficient as well as the square of the equivalent airspeed (see Table 6.1-1 or 6.1-2). Thus, the total drag on the aircraft just prior to impact in the simulations was about nine times greater than the cruise condition.

6.1.3 Parameters Investigated

A number of simulation runs were made to establish the aircraft trajectory starting from the steady level flight cruise speed of 250 kt EAS at 22,000 ft with the following conditions:

- Fixed-angle dives of -60°, -70°, -80°, and -90° following a push-over maneuver. The lateral and pitch movements were inhibited. The effect of engine thrust on speed was investigated.

- Fixed-stick-position push-overs using successively 25%, 50%, 75% and 100% of total forward stick travel. All lateral movements were inhibited. Engine thrust effects were assessed.

- Fixed-stick-position push-overs but with lateral motion introduced in an attempt to set up a steep dive in a roll/push-over maneuver.

The aircraft weight and C.G. location were estimated on the basis of the crew and passenger manifest and the fuel load at the time of the incident. The estimated weight was 64,500 lb (29,300 kg) and the C.G. was located at 0.35 smc. Engine thrust was set up for constant speed in level flight at the initial cruise condition and the throttle position was assumed not to change throughout the dive except in those cases where flight-idle thrust was selected at the start of the push-over maneuver. With a fixed throttle position, thrust increases as altitude is reduced as defined in the engine specification. The autopilot was inoperative in all the runs.

Since the control input was not known there was no way of estimating the flight trajectory accurately. A witness report that the aircraft entered a vertical or near

vertical dive was considered relevant and guided the organization of the study.* The purpose of the fixed-angle dives was to determine, if possible, the likely terminal velocity if it was reached before impact. It was considered that this velocity might be largely independent of the sequence of events, particularly the pitch control inputs in the transitional period between cruise and dive. The horizontal distance covered by the aircraft is an important parameter as it is clearly a function of dive angle.

The push-over runs with a fixed stick position were a trial and error attempt to reproduce a steep dive prior to impact by simulating the aircraft response over a range of pitch control inputs. Initially the runs were limited to the pitch axis only because data on asymmetric control inputs through the ailerons or rudder during the crash episode could never be determined. It was appreciated that large stick movements of the order of 50% full travel or more might be unrealistic at these speeds in that very high stick forces were implied and that control or structural stressing limits could be exceeded. The runs were done to determine if and in what circumstances a near vertical dive could be achieved and how the terminal velocity varied with dive angle.

6.1.4 Results

Simulator output plots are provided for each run. Each plot records the following parameters on a time base:

Mach number
Equivalent airspeed (kt EAS)
True airspeed (ft/s TAS)
Altitude, ft
Horizontal distance, ft
Normal acceleration, gee
Stickforce, lb
Elevator angle, deg
Pitch angle, deg

In addition, a cross plot of altitude versus Mach number is provided. All the plots obtained are included in Ref. 15. The significant results are summarized in Tables 6.1-1 and 6.2-2 where the various dive maneuvers that were studied may be compared.

It is apparent that the terminal Mach number and the impact velocity are practically independent of dive angle or engine thrust. This at first seems a surprising result, but after examining the nature of the Mach number drag rise and the relative contribution of engine thrust and aircraft weight components to the accelerating force, the conclusions are understood and accepted.

* Witness accounts (Ref. 18) of the dive angle tended to agree qualitatively as steep. But quantitatively, their perceptions of the angles varied from -45° to -100° (10° past vertical) from the horizontal.

The fixed-angle dives are all initiated at 300 kt EAS at 20,000 ft being preceded by a push-over maneuver of 9 s duration from the steady cruise speed of 250 kt EAS (corresponding to the inertial speed of 349 kt as determined from radar data, see Section 3.1). The tabular data (Table 6.1-1) refers to the horizontal distance and time to impact inclusive of the push-over maneuver. The terminal Mach number which is reached before impact is 0.858 and the impact velocity is 935 ft/s TAS or 545 kt EAS. These speeds do not vary significantly with thrust or dive angle. The horizontal distance which is measured from the initial upset varies considerably with dive angle, of course, as shown in Table 6.1-1.

Table 6.1-1. Fixed-angle dives.

RUN	1	2	3	4	5	6
Pitch angle, deg*	60	60	70	80	80	90
Engine thrust	PFLF	FI	PFLF	PFLF	FI	PFLF
Terminal Mach number	0.857	0.843	0.858	0.858	0.846	0.858
Impact speed, kt EAS	540	534	543	545	537	543
Impact speed, ft/s TAS	930	920	935	938	925	935
Horizontal distance to impact, ft	15,200	15,400	11,300	7,800	7,900	4,500
Time to impact, s	33.2	33.7	31.4	30.4	30.7	30.2

* Dive angle (flight path) = Pitch Angle + Incidence (~2° at impact)

Table 6.1-2. Fixed-stick-position push-overs.

RUN	7	8	9	10	11	12	13
Stick position (% fwd)	25	50	50	50	75	75	100
Engine thrust	PFLF	PFLF	FI	PFLF	PFLF	FI	PFLF
C.G. (smc)	0.35	0.35	0.35	0.42	0.35	0.35	0.35
Max. pitch angle	29°	55°	54°	63°	75°	75°	90°
Stick force (lb)							
- initial	45	90	90	90	140	140	220
- final	83	250	250	250	380	380	500
Terminal Mach No.	---	0.846	0.843	0.846	0.852	0.849	0.855
Impact speed, kt EAS	---	540	537	540	543	540	543
Impact speed, ft/s TAS	---	930	925	930	935	930	935
Horizontal distance to impact, ft	---	21,500	21,500	18,000	13,500	13,500	9,000
Time, to impact, s	---	39.0	38.8	36.0	32.8	32.9	30.8

The fixed-stick-position push-overs (Table 6.1-2) are considered to be more relevant with respect to time and distance. A stick position 25% of full forward travel is not considered to be representative of the event since a maximum pitch angle of 29° is achieved followed by recovery at about 10,000 ft. The case with stick fully forward (100%) although showing a final pitch angle of -90° is unrealistic because of the very high stick forces required at these speeds and because of the relatively short distance to impact of 9,000 ft. It is important to note in the consideration of stick forces that it is assumed that the aircraft is trimmed for the level flight cruise and that subsequently the trim wheel has not been moved; this may not be true.

A fixed stick position between 25% and 50% of available travel would be expected to give results that are closest to the observed data but with moderately large stick forces. For a fixed stick position of 50%, the pitch angle reaches a maximum of -55° at impact at a horizontal distance of 22,000 ft after 39 s. The stick force, initially 90 lb, builds up progressively to 250 lb at high speed. A 75% stick position results in a -75° pitch angle with stick forces of 140 to 380 lb and a distance of 13,500 ft at 33 s. Plots representing the results of the simulations for fixed stick positions of 25% (Case 7) and 50% (Case 8) of available travel are reproduced in Appendix 2.

From these results it appears unlikely that the flight path angle was vertical or near vertical. Within the limitations and assumptions imposed in this investigation it is conceivable that the final dive angle was between -55° and -65° and that the crash occurred between 36 and 38 s after the initial upset at a horizontal distance of the order of 17,000 to 22,000 ft.

Table 6.1-2 indicates that the effect of engine thrust and aircraft C.G. position on speed are relatively small although C.G. does affect dive angle and distance to impact. The most significant parameter affecting maximum speed is the Mach number drag rise which is based on wind tunnel measurements on a 1/15th scale model.

Figure 6.1-2 shows the variation of speed with altitude for some of the fixed-stick-position push-overs superimposed on the design speed envelope. Estimated speeds below 10,000 ft altitude are seen to be well in excess of the certificated flutter-free (1.2 V_D) boundary. BAe calculations indicate unstable elevator and engine modes in this region and therefore flutter might be expected, but not certain, to occur.

Attempts to put the aircraft into a 90° dive by doing a roll/push-over maneuver with the "pilot" flying the simulator from the cockpit were unsuccessful. It was concluded that the introduction of the roll-off maneuver does not make the task of putting the aircraft into a steep dive noticeably easier or quicker.

6.1.5 Comparison with Radar Data and Conclusions

As shown in Fig. 6.1-1 the horizontal distance from start of upset (assumed to be coincident with the time for the last radar data at 22,000 ft altitude) to the impact site (from surveyed location of crater) is approximately 21,000 ft; the corresponding elapsed time is estimated to be 50 s. The results obtained on the simulator can be compared with the radar and crash site survey data given in Fig. 6.1-1, by "unwinding the turn". This should not incur a significant error in the comparison. The comparison is made with respect to both horizontal distance and time. It is important to note that the assumptions about intermediate points, where there is no measured altitude, are very significant in the assessment of speed and Mach number. While the estimation of horizontal distance and time using this radar-based analytical approach is credible, the derivation of speed and Mach number, in this manner, is of doubtful accuracy because of their dependence on the assumed altitude-time history. Both horizontal distance and time estimates would be lower if the *dive* period is assumed to commence later.

Figure 6.1-4 shows the time and horizontal distance from the initiation of pushover to impact plotted against the fixed stick position as determined from the simulator results. The maximum pitch angle achieved in the simulation runs is also plotted. The radar-based estimates of time, 50 s, and distance, 21,000 ft, from Fig. 6.1-1 are superimposed (broken lines). Figure 6.1-4 indicates that in order to best approximate both these time and distance estimates a fixed stick position of 40% of forward travel is required. Lower time and distance estimates would require a greater fixed-stick position to approximate the simulation results.

Figures 6.1-5 and 6.1-6 illustrate the variation of altitude with horizontal distance and time respectively for fixed stick positions of 50% and 75% of forward travel. The radar and survey data are also shown for comparison. The comparison between the flight trajectory estimated from the simulator runs and that based on the radar and survey data is not close. Again the comparison is better at the lower value of stick position.

Because of the characteristics of the Mach number drag rise it is found that the terminal Mach number and impact speed are not particularly dependent on the final flight path angle or the assumptions concerning engine thrust; they are strongly dependent on the accuracy of the aircraft drag at "off-design" conditions (low C_L and high Mach number) derived from high-speed wind tunnel tests.

The belief of crash witnesses that the flight path was near vertical prior to the crash is not substantiated for an aircraft trimmed for level flight as assumed. The effect of a nose-down-pitch trim input on the stick force necessary to achieve a -90° dive was investigated subsequent to a preliminary review of the flight simulator results. This showed conclusively that the trim control was sufficiently powerful to put the aircraft into a -90° dive even with zero stick force. Thus, the issue of impact angle

would have been subject to dispute if the FDR data had not become available (see Section 7).

To summarize, on the basis of the aerodynamic analysis results from the simulator, radar data used to determine location and speed at the time of the upset, and a survey of the impact site, it is estimated that the ultimate dive speed was 930 ft/s TAS, 540 kt (911 ft/s) EAS and the Mach number was 0.835, which is considerably in excess of the aircraft design airspeed. It is also greater than the certificated flutter-free speed and it must be considered a strong possibility that flutter could have occurred in the later stages of the dive. However, there is not adequate data on unsteady aerodynamic forces and structural damping to be certain.

Unless the pitch trim was changed from the steady cruise setting it is unlikely that the dive angle exceeded -65°. Considering transition from the steady cruise at 250 kt EAS to a final -65° dive, the estimated time and location of impact are not inconsistent with recorded radar and survey data.

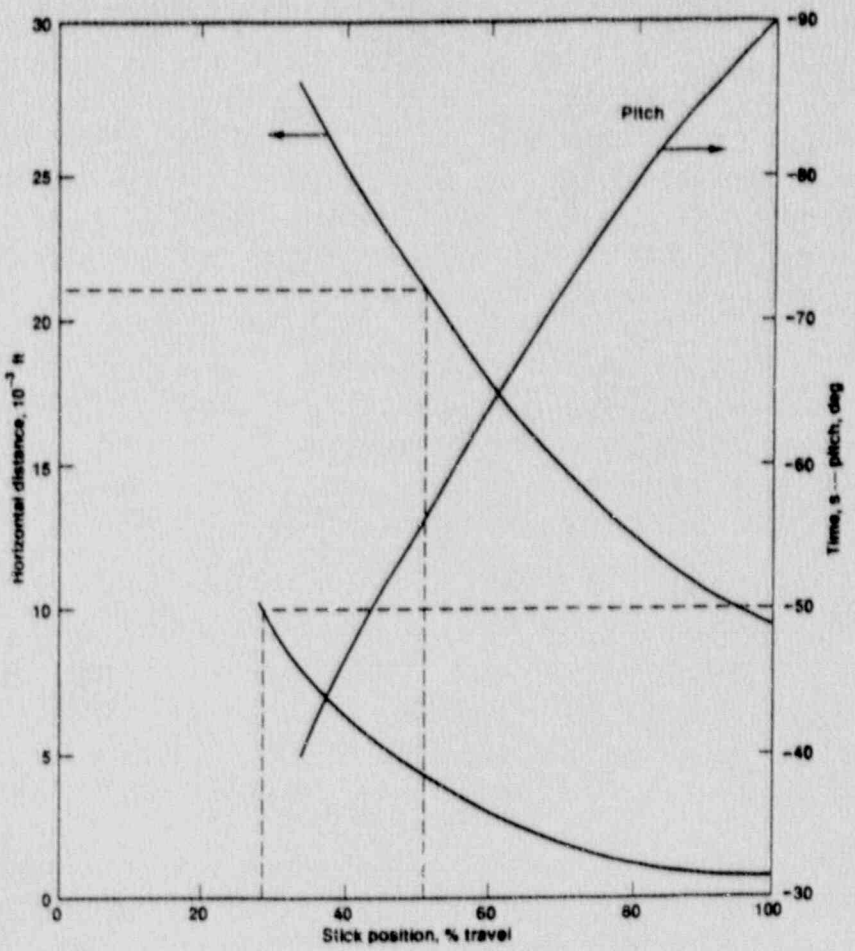

Fig. 6.1-4. Solid curves represent the results from fixed-stick simulations (PFLF). Dashed lines are estimates of horizontal distance and time from initial upset to impact based on radar data (Fig. 6.1-1).

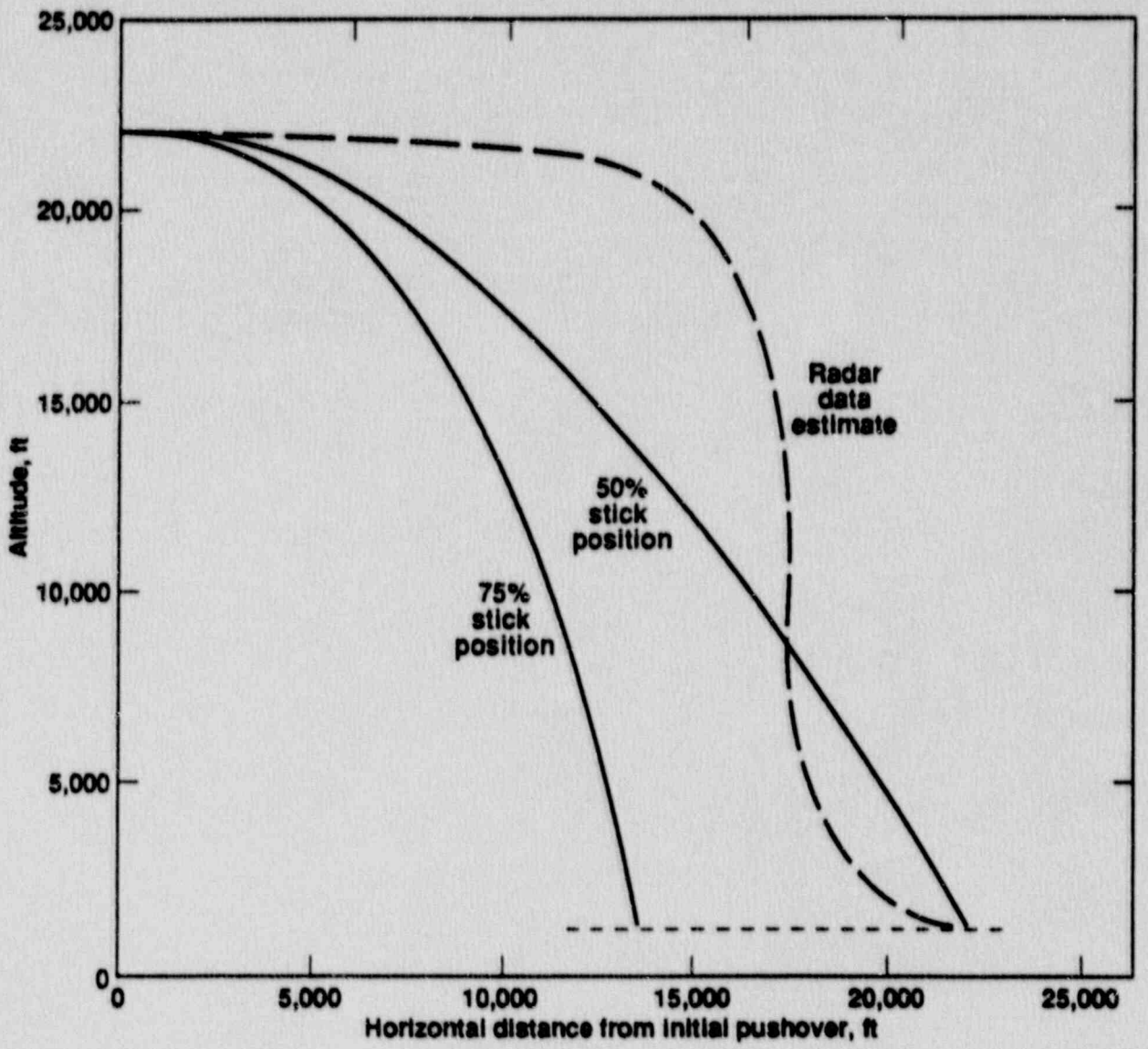

Fig. 6.1-5. Predicted trajectories (PFLF) in fixed-stick-position push-overs compared with radar/survey data (and altitude, time assumptions).

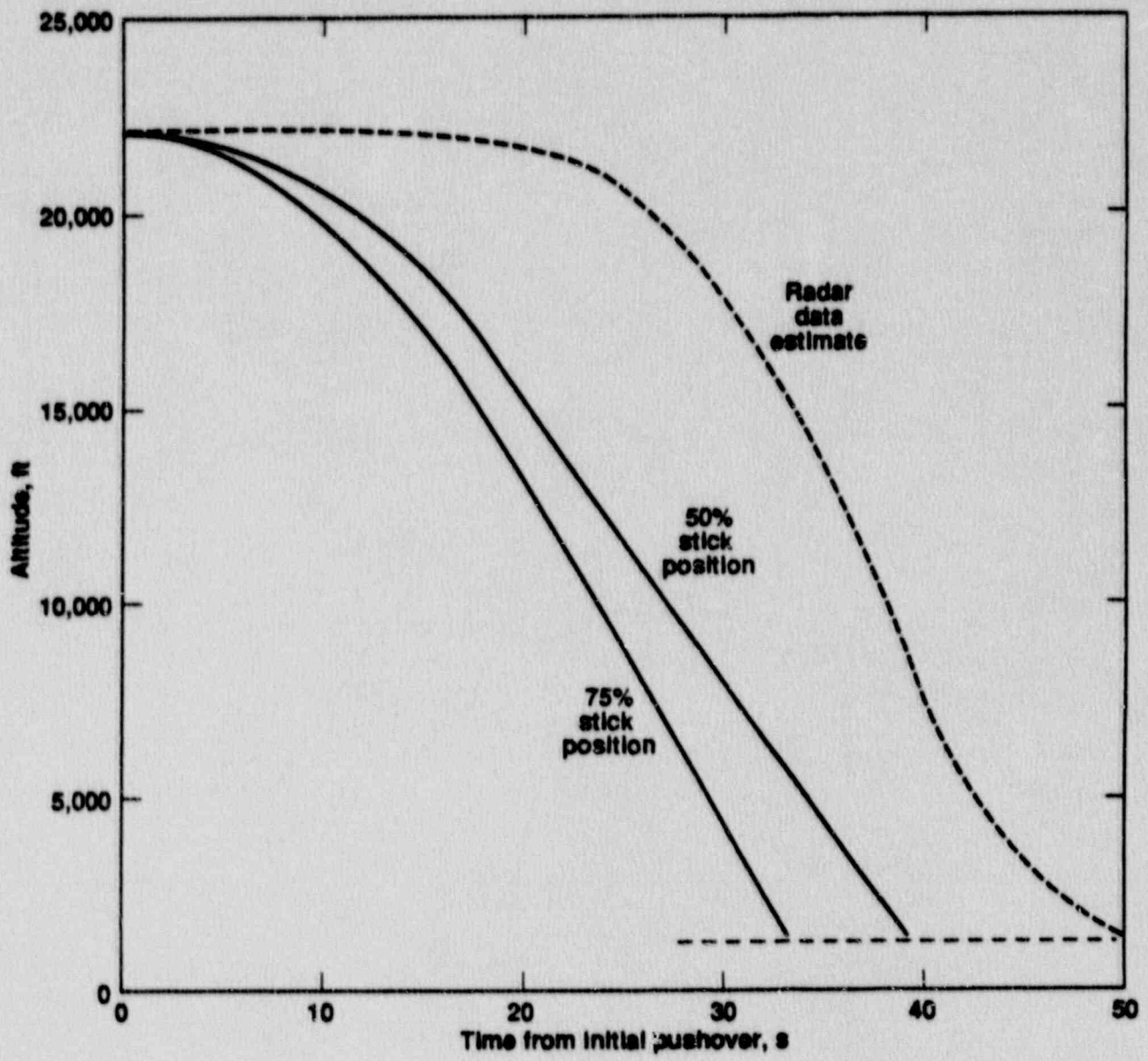

Fig. 6.1-6. Variation of altitude with time during fixed-stick-position push-overs (PFLF) compared with radar/survey data (and altitude, time assumptions). Note that, initially, altitude changes more quickly in the simulation.

6.2 Structural Considerations

BAe reviewed the structural implications of flying the BAe 146-200 aircraft in the most likely manner indicated by the simulator study. They concluded (Ref. 23):

> "It is not surprising that the structure remained intact until impact with the Aerodynamic Department's most likely predicted speeds, accelerations and manoeuvres, although these are outside the design envelope and therefore precise conditions and data are not available."

The BAe 146-200 structure has been designed for all the design speeds up to V_D (see Fig. 6.1-2) combined with lateral or vertical gust or maneuver loads, vertical loads due to elevators, lateral loads due to rudder, or roll loads due to ailerons. Both FAR and JAR requirements dictate a safety factor of 1.5 under these load combinations.

The primary structural considerations are loads normal to the flight path both vertically and laterally. Loads parallel to the flight path are of less significance. The only other consideration relative to fairings, fillets and shroud is aerodynamic suction, which is a function of dynamic pressure. This consideration assumes that unknown Mach number effects are negligible between 0.80 and 0.85.

The vertical-maneuver design loads for the aircraft's primary structure are shown in Fig. 6.2-1. The most likely simulator runs stay within this envelope without invoking the additional 1.5 factor for actual strengths. The loads are further reduced in the specific case analyzed, as the actual weight of 64,500 lb is significantly less than the maximum design weight of 89,500 lb.

Using the product of velocity-squared times elevator angle as the criterion, the imposed loads on the elevator are comparable with design ultimate loads. However, the elevator has significant strength margins under ultimate design loads, so it is considered unlikely to fail.

The fairings and fillets were designed at an early stage of aircraft design for V_D = 390 kt EAS. The effect of aerodynamic suctions on these secondary structures, together with the design transverse gusts or maneuvers but ignoring additional higher Mach number effects, could cause these structures to fail at a speed of 390 x 1.5 or 478 kt EAS. In addition, assuming the aircraft stays reasonably straight without pitch and yaw once in the dive then the suctions would be further reduced and hence it is not surprising that seemingly all parts were in place at impact at about 540 kt EAS.

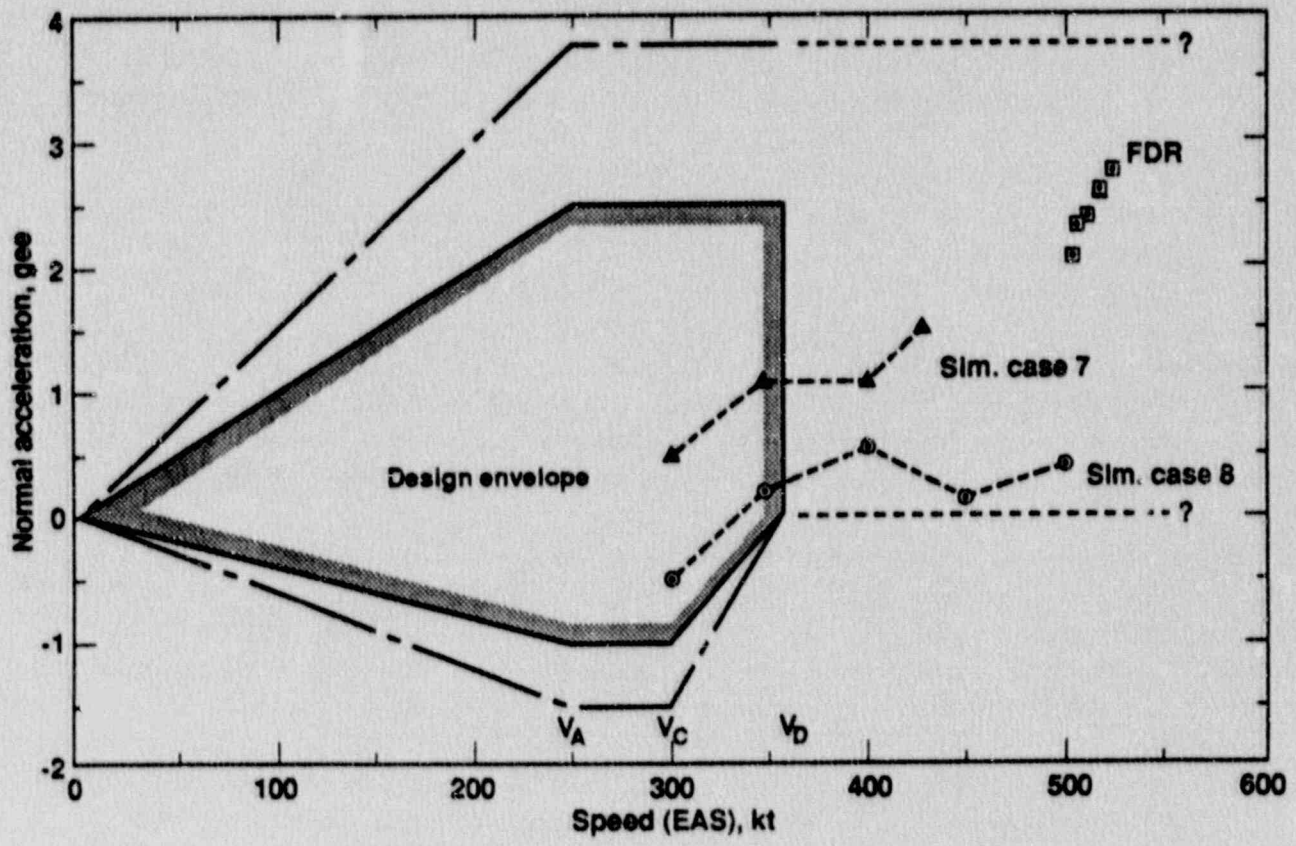

Fig. 6.2-1. Approximate vertical-maneuver design load envelope showing structural safety factor, normal acceleration derived from simulator Cases 7 and 8, and data from vertical accelerometer recorded on the FDR.

7. FLIGHT DATA RECORDER ANALYSIS

Both the FDR and CVR units used on PSA Flight 1771 sustained extensive damage under impact loads estimated (Ref. 24) to be higher than 5000 gee. The FDR, Lockheed Model 209F, was the more severely damaged of the two recorders, but nevertheless provided definitive terminal flight data.

7.1 FDR Design and Extent of Damage

Photographs of the FDR and its tape reel assembly, with a similar undamaged unit alongside for comparison, are shown in Figs. 7.1-1 and 7.1-2.

A drawing of the coaxial tape reel assembly in the FDR is shown in Fig. 7.1-3. The recording tape, stored on two coaxial reels, provides for 25 h of data which are recorded on 6 adjacent tracks. The direction of tape travel thus reverses approximately every 4.25 h when end-of-tape is sensed. The tape is pulled across a recording head by the capstan.

Tape stored on the reels was fractured due to compression and distortion of the reels. The tape within the tape transport region was broken into many pieces which had ends too badly damaged to allow reconstruction. At the time the FDR was recovered, the terminal tape segment was trapped against the capstan and was assumed to have the most recent data. The ends of this segment apparently broke at the location of the recording head and the capstan.

Pieces of the tape are shown in Fig. 7.1-4. Only the piece at the top of the photograph was analyzed. Approximately 80 mm long, this piece of tape contained recorded flight data for the final 7 s of flight. The last altitude measurement that could be read was 179 m above the impact elevation. Thus, only a small amount of extrapolation was required to determine impact conditions.

7.2 Data Extraction Method

On receipt of the tape, NTSB determined that the synchronization bits necessary to break down the multiplexed data words were missing. NTSB considered it to be a long and possibly unsuccessful process to attempt the data extraction. Since NTSB was otherwise occupied and the crash of PSA Flight 1771 was not a safety incident, they did not attempt to extract the data.

In response to our questioning, NTSB suggested (Ref. 12) that Lockheed Aircraft Service Company (designer of the FDR) might be able to extract the data from the terminal tape segment. Accordingly we negotiated a contract with Lockheed to attempt the data recovery. Their results are contained in a letter report, Ref. 25.

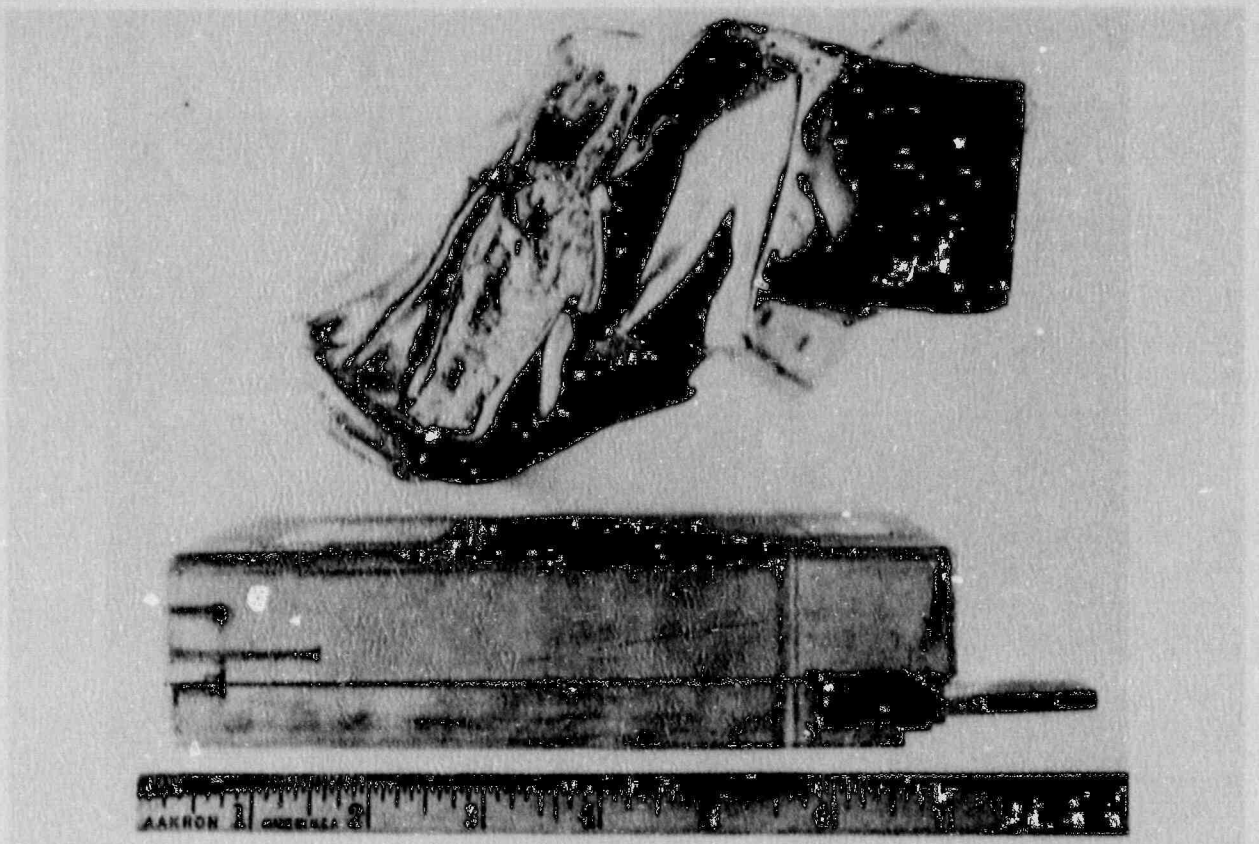

Fig. 7.1-1. Photograph of the PSA Flight 1771 FDR with a similar undamaged unit.

Fig. 7.1-2. Photograph of the tape reel assembly recovered from the PSA Flight 1771 FDR with a similar undamaged unit.

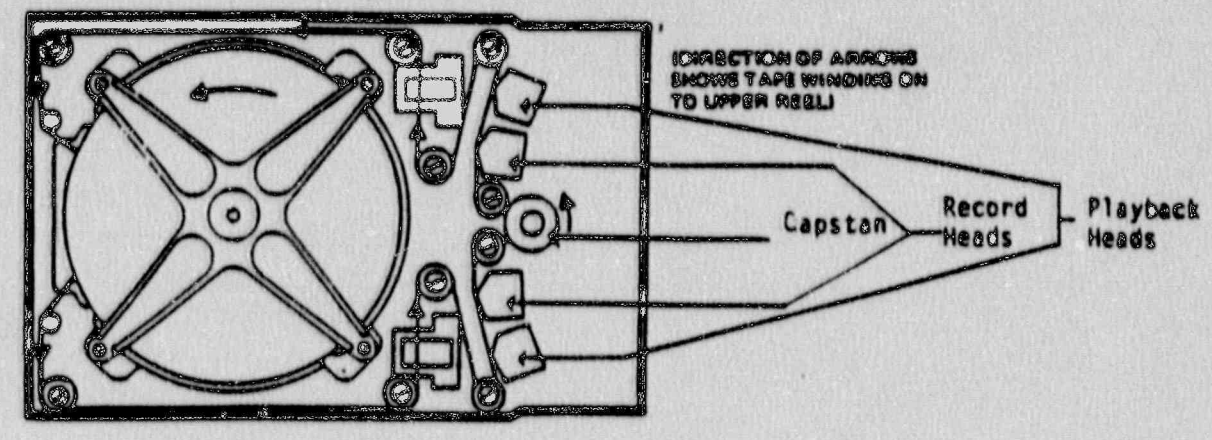

Fig. 7.1-3. Drawing showing the tape transport path in the FDR.

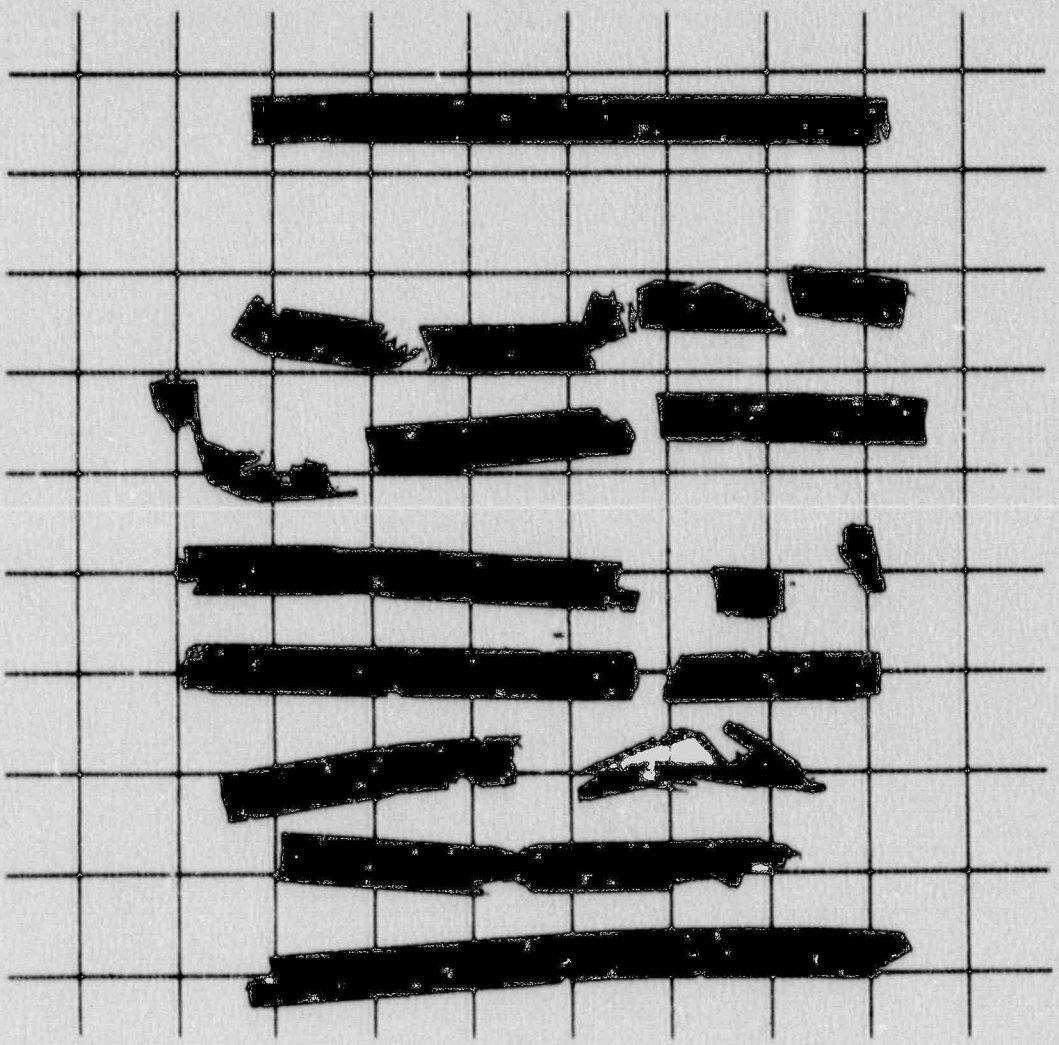

Fig. 7.1-4. Photograph of tape fragments removed from the PSA Flight 1771 FDR (approximately full scale).

Most of the data of interest on the terminal tape segment were successfully recovered.* The tape segment was stretched and damaged at both ends. The data immediately prior to impact were either not on the tape segment or were unobtainable because of the end condition of the tape.

Two methods of data reduction were used to recover flight parameter data of primary interest:

- Automatic data playback station. Lockheed's data playback station automatically reads out data utilizing a "Super Sync" feature. This method permits nearly instantaneous data synchronization, but can (and did) result in the output of erroneous data. The erroneous data are readily identifiable.

- Manual waveform interpretation. Special techniques were also used to recover data by recording the Harvard bi-phase data signal on a paper strip chart. The recorded signal was reviewed to identify the "ones" and "zeros". The decoded data stream was then examined to find synchronization words and, by counting data bits, the desired parameters were identified. It is also possible to use a constant or slowly varying parameter within a subframe as a pseudo synchronization word. For example, the elevator trim position, word 43, was used to locate airspeed and altitude, words 31 and 32.

A partial listing of the reduced data (Ref. 25) is shown in Table 7.2-1. A data subframe consists of 64 twelve-bit words recorded each second. A data frame consists of four subframes. The data given in Table 7.2-1 are referenced to their subframe and word. Additional data are reproduced in Appendix 3.

7.3 Data Analysis

Our primary interest in the reduced data from the FDR was directed toward establishment of the impact speed and angle. These values were obtained according to the procedure described below using the fine altitude, pitch angle, and calibrated speed data.

* Other data could be obtained from the tape segment that has been returned to NTSB.

Table 7.2-1. Partial listing of reduced data obtained from the FDR on PSA Flight 1771.

	Fine Altitude ft	Radio Altitude ft	Airspeed (CAS) kt	Magnetic Heading deg	Engine Speed N1, %	Outside Air Temp. °C
Data Word	32	16	31	17	63	33
Subframe						
2.2	6426	---	498	193.6	#2 86	---
2.3	5562	---	507	193.6	#3 93	42.4
2.4	4741	---	512	194.0	#4 94	---
3.1	4203	---	516	193.2	#1 95	---
3.2	3369	---	521	194.0	#2 79	---
3.3	2669	---	524	194.5	#3 90	---
3.4	1909	1880	526	194.9	#4 84	---

	1 Pitch deg	2 Pitch deg	3 Pitch deg	4 Pitch deg	1 Roll deg	2 Roll deg
Data Word	5	21	37	53	14	46
Subframe						
2.2	-62.3	-61.5	-60.6	-59.2	18.4	18.8
2.3	-59.7	-58.3	-57.0	-56.1	20.6	21.1
2.4	-55.2	-54.8	-53.9	-53.0	16.3	18.4
3.1	-52.0	-51.3	-50.4	-49.5	18.4	17.2
3.2	-48.2	-47.3	-46.1	-45.2	16.0	16.0
3.3	-44.1	-43.5	-42.2	-41.4	15.1	13.4
3.4	-40.3	-39.4	-38.3	-37.5	11.0	8.9

	1 Vert. Accel. gee	2 Vert. Accel. gee	3 Vert. Accel. gee	4 Vert. Accel. gee	5 Vert. Accel. gee	6 Vert. Accel. gee	7 Vert. Accel. gee	8 Vert. Accel. gee
Data Word	2	10	18	26	34	42	50	58
Subframe								
2.2	2.10	2.09	2.08	2.03	2.00	2.13	2.34	2.28
2.3	2.21	2.10	2.06	2.02	1.96	2.17	2.52	2.58
2.4	2.56	2.52	2.50	2.39	2.28	2.21	2.28	2.48
3.1	2.53	2.60	2.58	---	---	---	---	---
3.2	2.57	2.53	2.58	2.52	2.44	2.49	2.37	2.38
3.3							2.6	2.7
3.4	2.56	2.61	2.57	---	2.74	2.75	2.63	2.63

Note: Underlined data values extracted using manual methods.

7.3.1 Altitude, Pitch, and Speed

The fine altitude data (reduced from word 32) for seven subframes (7 s) is quite linear with time as shown in Fig. 7.3-1. Manually extracted data, not shown in Table 7.2-1 but included in Appendix 2, were also plotted and considered in establishing the linear relationships of altitude, h (ft), and arbitrary time, t (s). The correlations are:

3 auto, 4 man data values:	$h_1 = 7084 - 739.607\ t$	
	avg. dev.	1.14%
	max. dev.	2.61%
	$h_1 = 1320$ ft @ $t = 7.79$ s	
7 manual data values:	$h_2 = 7239 - 765.786\ t$	
	avg. dev.	1.17%
	max. dev.	2.01%
	$h_2 = 1320$ ft @ $t = 7.73$ s	
last 4 manual data values:	$h_3 = 7207.6 - 758.2\ t$	
	avg. dev.	0.74%
	max. dev.	1.41%
	$h_3 = 1320$ ft @ $t = 7.77$ s	

All three correlations represent the terminal altitude data quite well. We adopt the h_3 correlation since it represents the data of most interest, it was reduced in a consistent manner, and the time to the surveyed impact elevation lies between the values given by the h_1 and h_2 correlations. The impact time is thus established as being 0.77 s after the last reduced fine altitude value. The h_3 correlation for altitude with impact time, t_i, referenced to zero at impact, can therefore be rewritten as:

$$h = 1320 - 758.2\ t_i \qquad \text{for: } -4 < t_i < 0$$

Other parameter values were correlated in time depending on their word position in the subframe relative to the fine altitude data (word 32) in the time frame of reference, t_i. The last pitch value that was reduced (word 53 in subframe 3.4 as given in Table 7.2-1) is thus plotted at $t_i = -0.44$ s with earlier pitch data at appropriately earlier times as shown in Fig. 7.3-2. The last 16 pitch values only were plotted and used to establish the correlation. It is seen that these data are also quite linear and are well represented by the correlation:

$$p = -35.639 + 3.955\ t_i \qquad \text{for: } -4.5 < t_i < 0$$

where p is the pitch angle (deg) of the fuselage datum axis and t_i is the time referenced to impact as before. The average deviation of the correlation is 0.26% and the maximum deviation is 0.51%.

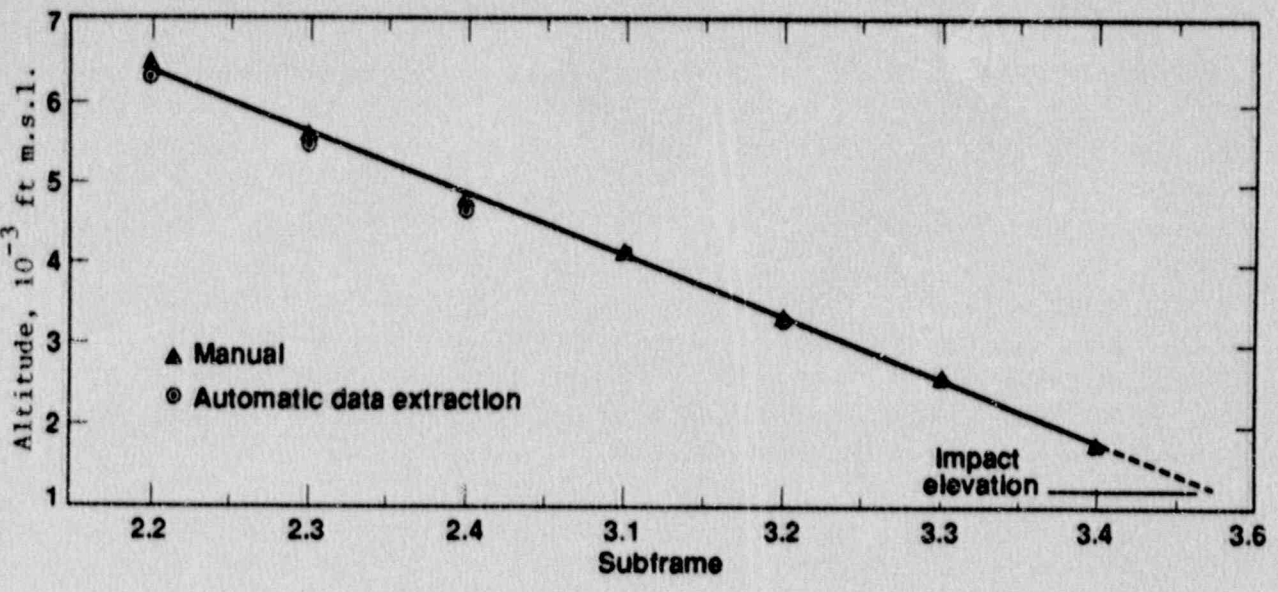

Fig. 7.3-1. Plot of fine altitude data as reduced from the FDR and extrapolated to impact.

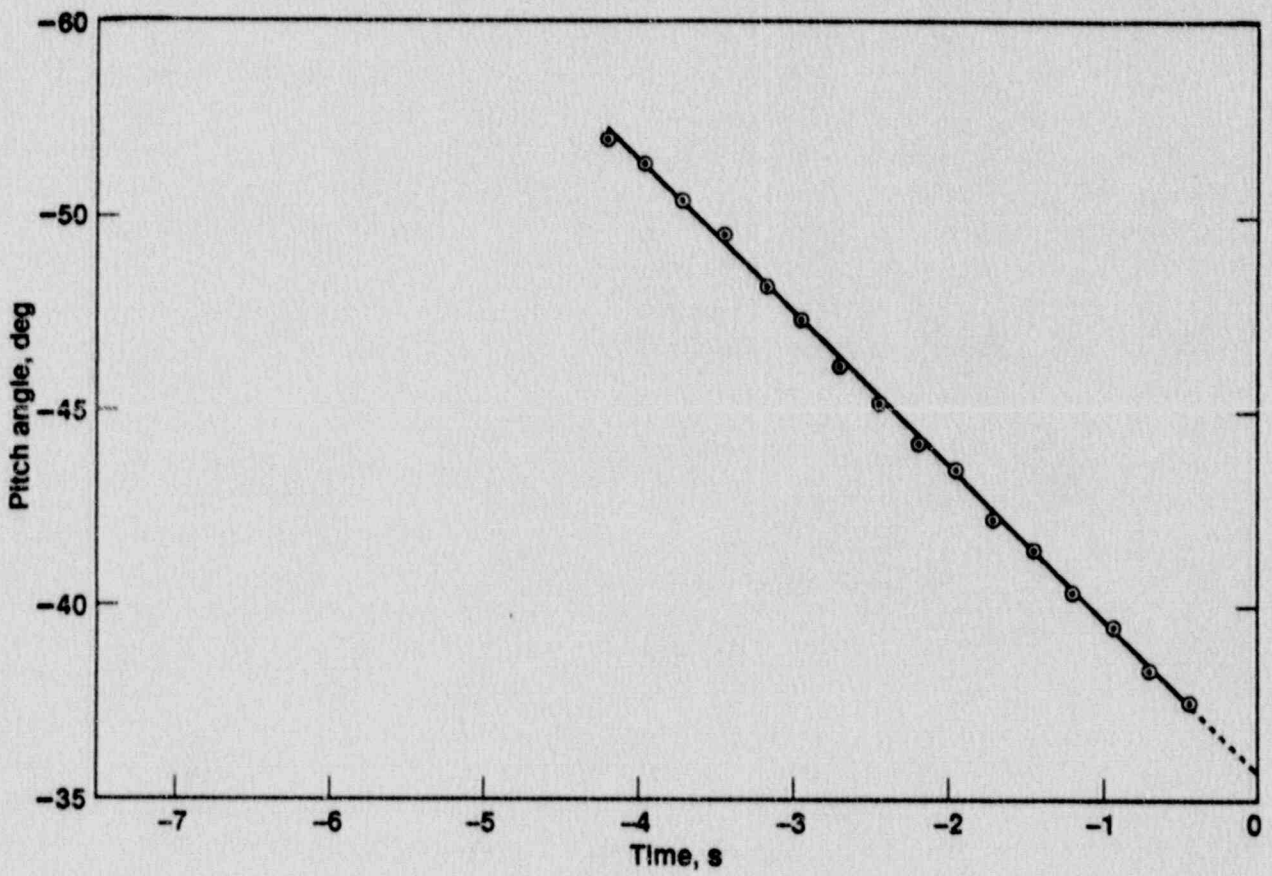

Fig. 7.3-2. Plot of pitch angle data correlated with impact time derived from FDR fine altitude data and surveyed impact elevation.

The calibrated airspeed data obtained from the FDR can not be used without modification for the purpose of determining inertial impact speed Three effects must be considered, giving rise to two corrections. The combined position error and compressibility correction, provided by Ref. 26, was applied to the calibrated airspeed reduced from the FDR to yield the equivalent airspeed. The equivalent airspeed must then be corrected for air density to yield the true airspeed. We assume the true airspeed to be the aircraft inertial (ground) speed since winds were reported to be light. Wind conditions were reported to be north to northwest at 7 kt in Ref. 3, but the location of the anemometer and the time of the measurement were not given. Since the reported wind speed is a low value and relevance of the measurement is undetermined, our assumption seems valid.

The calibrated airspeed reduced from the FDR data (as given in Table 7.2-1), the equivalent airspeed from Ref. 26, and the true airspeed are plotted versus t_i in Fig. 7.3-3. Although the calibrated and equivalent airspeeds are increasing with decreasing time to impact, there is a perceptible non-linear decreasing trend in the terminal true airspeed. We developed a correlation for the true airspeed, V_t (kt), based on the last four FDR-derived data values modified as discussed above. The correlation is:

$$V_t = 548.5 - 6.8\, t_i - t_i^2 \qquad \text{for: } -4 < t_i < 0$$

which correlates the calculated true airspeed values with an average deviation of 0.07% and a maximum deviation of 0.10%. The aircraft true airspeed at t_i=0, measured along the fuselage datum axis, is therefore 548 kt. It is noted that the true airspeed measurement is not affected in most cases (Ref. 27) by angles of incidence to the flow direction less than about 15°. The angle of incidence of the aircraft with the flight trajectory was well within this value (see below).

The altitude calculated from the true airspeed and pitch angle correlations is lower than the altitude calculated from the altitude correlation at the same value of t_i. This is to be expected since the fuselage datum axis is most likely at a small angle of incidence (slightly less steep) with respect to the aircraft inertial trajectory. We attempted to reconcile this discrepancy by postulating a constant angle of incidence, which brings the two calculations into close agreement. We found however that an unreasonably large incidence angle (about 10°) was required. BAe estimated (Ref. 28) that the angle of incidence at the time of impact was about 3° and that any greater difference must be due to errors in the recorded pitch, altitude, and speed.

To resolve this issue, we calculate the average terminal trajectory angle from the altitude and velocity correlations as given above. We consider this value, -53.8°, to be an upper bound on the aircraft trajectory angle. A lower bound is provided by the pitch angle at impact, -35.6°, as given by the pitch angle correlation also given above. The average of these bounding values is -44.7°. For convenience, we round the latter value to -44°, which when combined with the impact surface slope, 16° (see Table 2.1-1), results in a total impact angle of 60°.

We accept the BAe estimate of 3° as the incidence angle of the fuselage at impact (i.e. a pitch angle of -41°). Its precise value, for angles less than 15 to 20°, does not significantly affect the impact load on the aircraft or its contents. Because of this insensitivity to incidence angle, we did not attempt to reconcile the discrepancies between altitude, pitch, and velocity correlations as derived from the FDR.

On the basis of the information available to us, our analyses, and the work of BAe, we conclude that the best estimates are: impact speed was 282 m/s (925 ft/s, 548 kt), flight trajectory angle was -44°, and aircraft pitch angle was -41°.

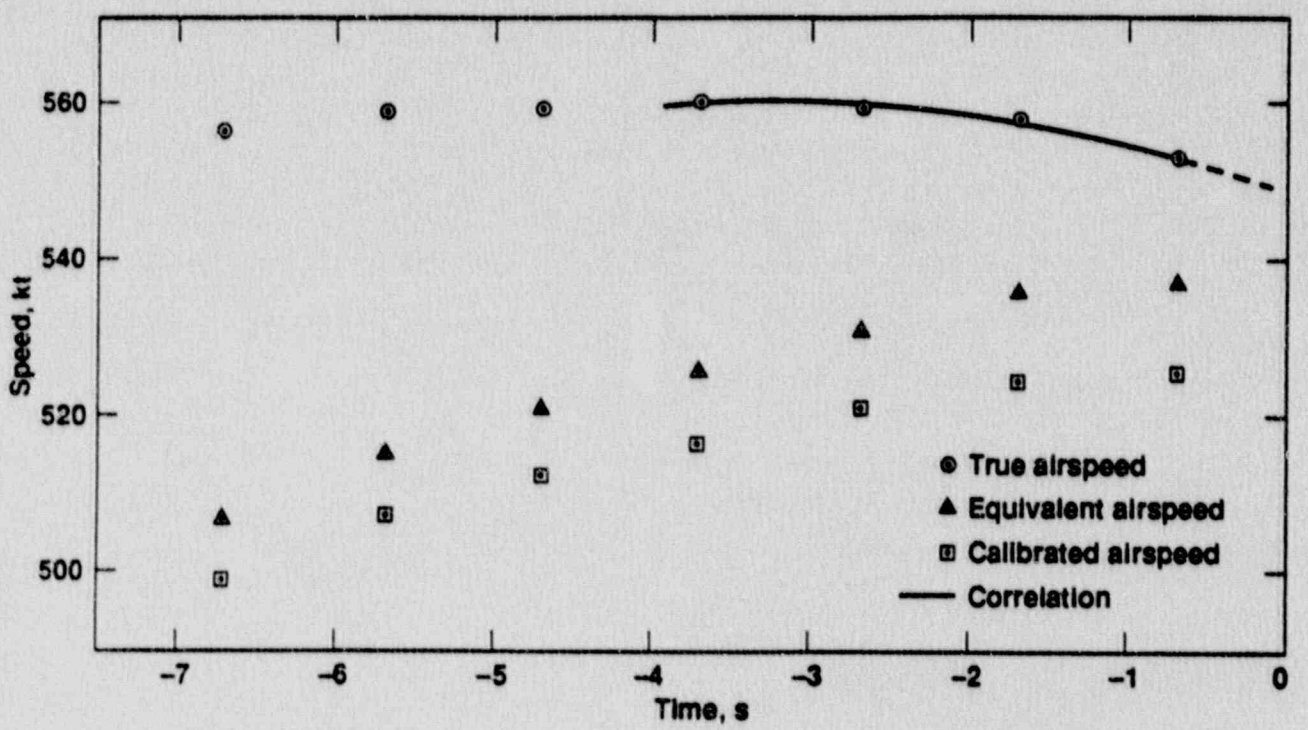

Fig. 7.3-3. Plot of calibrated airspeed reduced from FDR, equivalent airspeed with position and compressibility corrections applied, and true airspeed.

7.3.2 Outside Air Temperature

An interesting check on the validity of the true airspeed is provided by the single recorded (stagnation) temperature value of 42.4°C at an altitude slightly lower than 5562 ft as given in Table 7.2-1. The standard atmosphere temperature at this altitude is 4°C or 277 K. Since the surface temperature was reported (Ref. 3) to be about 2°C below the standard atmosphere temperature, we assume that at the altitude of interest the temperature was likewise lower, or 275 K. At 275 K, sonic velocity in air is 332.4 m/s. From Fig. 7.3-3 the true airspeed at the time of interest is about 559 kt (287.6 m/s). Thus the Mach number is found to be 0.865, which compares well with the higher terminal Mach numbers determined by BAe in the simulator study (see

Tables 6.1-1 and 6.1-2). At Mach number 0.865 the stagnation temperature (measured by the temperature probe) is calculated to be 316.2 K or 43.0°C. The agreement with the FDR value is excellent.

7.3.3 Vertical Acceleration

The vertical acceleration measurements exhibit a gradually increasing trend with a superimposed oscillation at a frequency of about 1 Hz. The average vertical acceleration, a_v, during this period is well correlated by the relation:

$$a_v = 2.63 + (7.21 \times 10^{-5})\, t_i - 0.11\, t_i^2.$$

These data are shown in Fig. 7.3-4, and representative values are also plotted against equivalent airspeed in Fig. 6.2-1. BAe found (Ref. 26) that the average acceleration compared well with the simulator when the stick is fixed in the position necessary to match the recorded acceleration at subframe 2.2. However, it was not possible to simulate a fixed-stick pushover from the start of the upset which would match the recorded acceleration. A successful trajectory simulation was only achieved with the elevator angle set at a much lower value than that recorded by the FDR and with unrealistically high stick force.

While the recorded vertical acceleration values were high, they remained within the design safety margin as seen in Fig. 6.2-1.

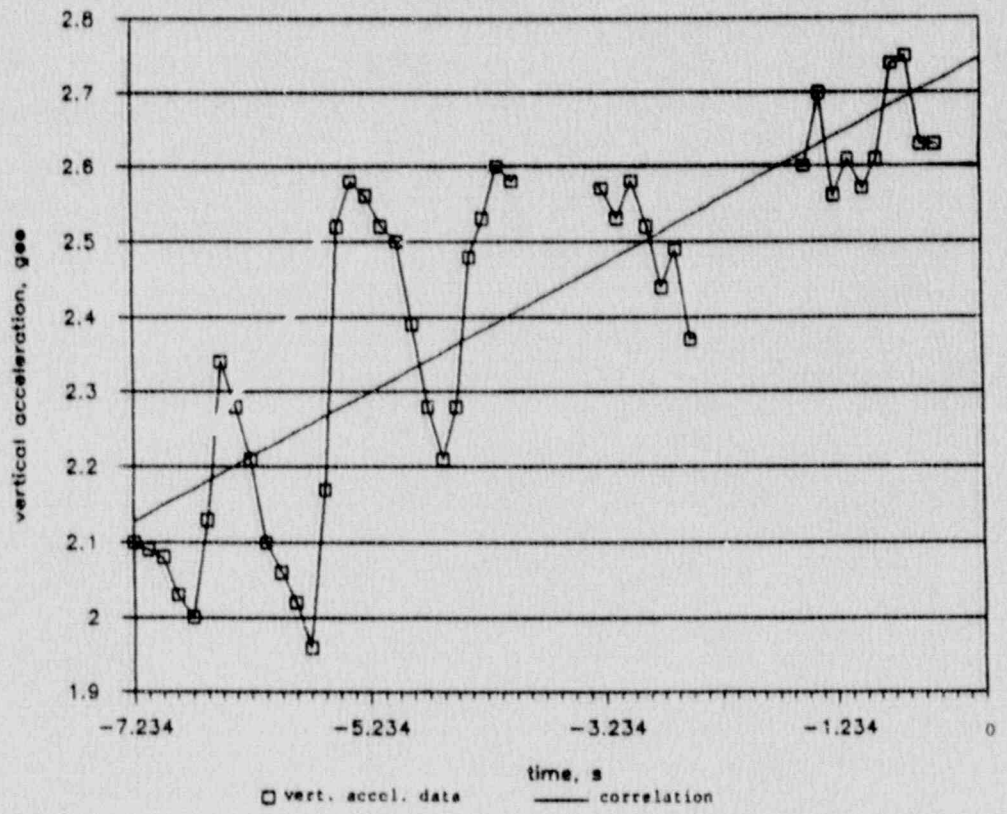

Fig. 7.3-4. Plot of vertical acceleration recorded on the FDR.

7.3.4 General Discussion of FDR Data

After the simulation analyses were completed, we asked BAe to review the FDR data which had then became available. BAe concluded (Ref. 26) that there was no fixed stick position starting from the initial upset which would correlate well with the FDR data for the last 7 s. We infer from this conclusion and from consideration of other possibilities that there may have been some manipulation of flight controls during the upset.

BAe advanced a possible explanation for the inability of the simulator to reproduce all of the recorded terminal flight conditions. They postulate that the longitudinal control characteristics on the simulator may not be entirely representative of the aircraft at these flight conditions for the following reasons:

- The combination of high equivalent airspeed and Mach number are in an area of uncertainty with respect to flexibility effects on the rear aircraft structure and on the elevator and tabs.

- The hinge moment and aerodynamic characteristics of the elevator and the tabs can be significantly altered by the formation of shocks at high Mach number. The hinge moments will in turn affect the control angles assumed. Experimental data on these characteristics at high Mach number are not available.

Nevertheless, conditions were found under which the simulator correlates well with the FDR data, especially with respect to aircraft speed and trajectory.

We were unable to explain the single unsaturated FDR radio altimeter value. By taking into account aircraft pitch and roll angles together with data from our topographical survey data for the terrain beneath the aircraft, we calculate that the radio altimeter reading should have been about half that which was recorded. Earlier saturated radio altimeter data points (included in Ref. 25) are explainable on the basis of the altimeter design (Ref. 28) and would be expected to be saturated for the corresponding flight/terrain conditions.

An anomaly in the data obtained was the airbrake position, which is recorded (Ref. 25) as being fully open at 62° during the terminal flight period. This value is not possible at high speed. At the airspeed in the simulation, if full airbrake had been selected in the cockpit, the maximum angle would have been 17° (Ref. 26). The recorded reading would be maximum if the airbrake position transducer failed or lost power. It is surmised that this may have occurred, as the CVR recording head (also located in the rear of the plane) appears to have been subjected to considerable vibration and loss of continuous tape contact. The simulation showed that the effect of the airbrake being applied (over the last 7 s) would be to reduce impact speed by 3 kt and increase vertical acceleration by 0.2 gee.

We conclude that all four engines were operating nominally at cruise thrust. In the meager data available (see Table 7.2-1) we note a down-trend in engine speed. As determined from the simulation study (see Tables 6.1-1 and 6.1-2), impact speed was insensitive to engine thrust over the range of FI to PFLF.

The values of rudder angle and asymmetric aileron angles (Ref. 25) were consistent with the lateral accelerations recorded. These control surface deflections appear to have resulted in a stabilized bank angle on the aircraft.

The recorded (magnetic) heading of the aircraft (see Table 7.2-1) may be compared with the radar based footprint shown in Fig. 6.1-1. The magnetic declination in the impact area is 15.5°. There is excellent agreement.

The aircraft appeared to be straightening from a roll in its terminal flight period, as seen in Table 7.2-1. The final recorded value was under 9°, and further extrapolation of the decreasing roll angle trend yields a roll angle at impact of less than 8°. It is clear therefore that the aircraft nose impacted before the wing made contact with the ground.

8. COCKPIT VOICE RECORDER ANALYSIS

The CVR unit used on PSA Flight 1771, Fairchild Model A100A, was severely damaged, but survived the crash in considerably better fashion than the FDR. The FBI assumed custody of the tape at the crash site, and the tape was not analyzed by NTSB. For the FBI to utilize the tape, however, it was necessary to reattach the broken tape in several places and this was done by NTSB at the request of the FBI. With considerable effort, we were able to obtain a copy of the tape and the FBI transcript of the tape (Refs. 29 and 30). We also obtained a video tape of a TV broadcast (Ref. 31) which was a dramatic representation of the CVR transcript aired by a San Francisco Bay Area TV station, Channel 2 KTVU.

Our early interest in the information available in the CVR was motivated by reports that the aircraft speed was supersonic (it was not), and that this could be inferred from a sound change in the cockpit. We were also hopeful that we could establish the time of impact to aid in interpretation of the radar data. Both issues were eventually resolved in other ways. Nevertheless, our analysis of the CVR tape provides some insight into the final moments of the flight and is consistent with all other conclusions.

8.1 CVR Tape Format and Inputs

At the nominal CVR tape speed of 47.6 mm/s (1-7/8 in./s) the length of tape recorded is about 7 m for the time of interest (under 150 s). Since we did not have access to the original tape, we are unable to evaluate the effect of splices on timing. These splices were carefully made, however, and NTSB believes (Ref. 32) that timing between events is not significantly distorted. The CVR is powered by a 400-Hz power supply. Leakage currents from the power supply can be detected on the tape and used to correct for off-nominal tape speed. The tape does not record an absolute time reference.

Normally, four tracks are recorded, and the FBI information (Ref. 30) indicates that this was the case for PSA Flight 1771. One channel, referred to as CAM, records an open microphone in the cockpit area. The other channels record sound of radio transmissions at frequencies tuned at the pilot, co-pilot, and occasional crew sets. These might all receive the same input depending on the communication frequency selected by the pilot, etc. Our copy of the tape had only two channels, which were quite similar, and we were unable to distinguish which ones they were. This is probably not important.

8.2 Method of Data Reduction and Analysis

The procedure used for the data reduction and analysis was as follows (Ref. 33). First, a high quality VHS format magnetic tape was generated in our sound studio using several bandpass equalizing filters. This accomplished two objectives: 1) enhancement of the voices and events region of the sound spectrum while

diminishing the background (hiss) noise; and 2) creation of a tape in a format more suitable to our digitization and processing techniques. Next, various frequency domains, filters, and voltage settings were explored in order to establish the best set of parameters from which to base the analysis. The third step in the procedure was to digitize the time domain data and to download the results to a computer for post-processing. The fourth step involved correcting the time base to account for changes in the CVR tape recording speed. Figure 8.2-1 shows a recorded spike generated by the 400 Hz power supply at approximately 402 Hz (the signal wanders from 401.75 to 402.25) in the frequency domain. As a result, all time values needed to be corrected by a factor of 402/400.

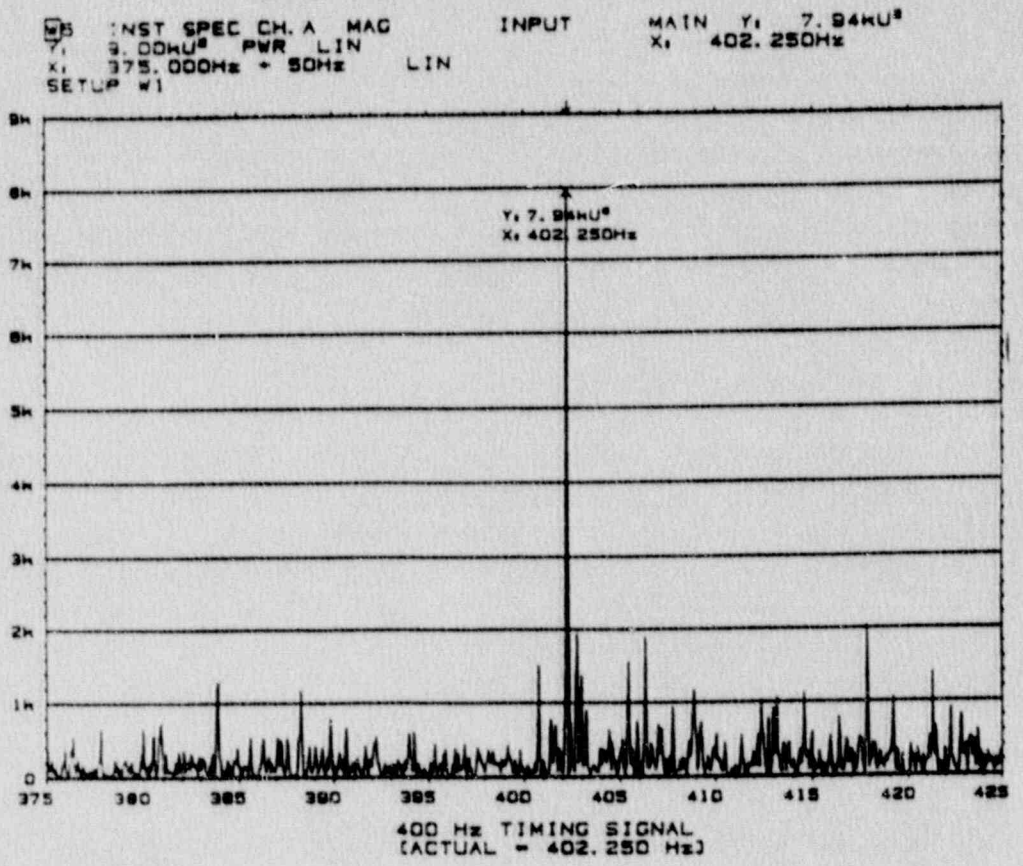

Fig. 8.2-1. Typical frequency domain plot showing offset of the 400 Hz power supply signal as recorded.

Finally, the corrected time values were plotted and various events annotated. These results are shown in Figs. 8.2-2a through 8.2-2e. These consecutive 30-s time history plots represent the last seconds of PSA Flight 1771 beginning with the end of *pre-upset* operation and extending through the *trouble-awareness* and *dive* periods (see Section 3.1). The plots are annotated with abbreviated monologs and relative times of occurrence of some events. Zero time for these plots was arbitrarily chosen to correspond to the leading edge of the tape-on voltage spike. Other events are noted relative to this datum. The last audible noise occurs at approximately 127.2 s.

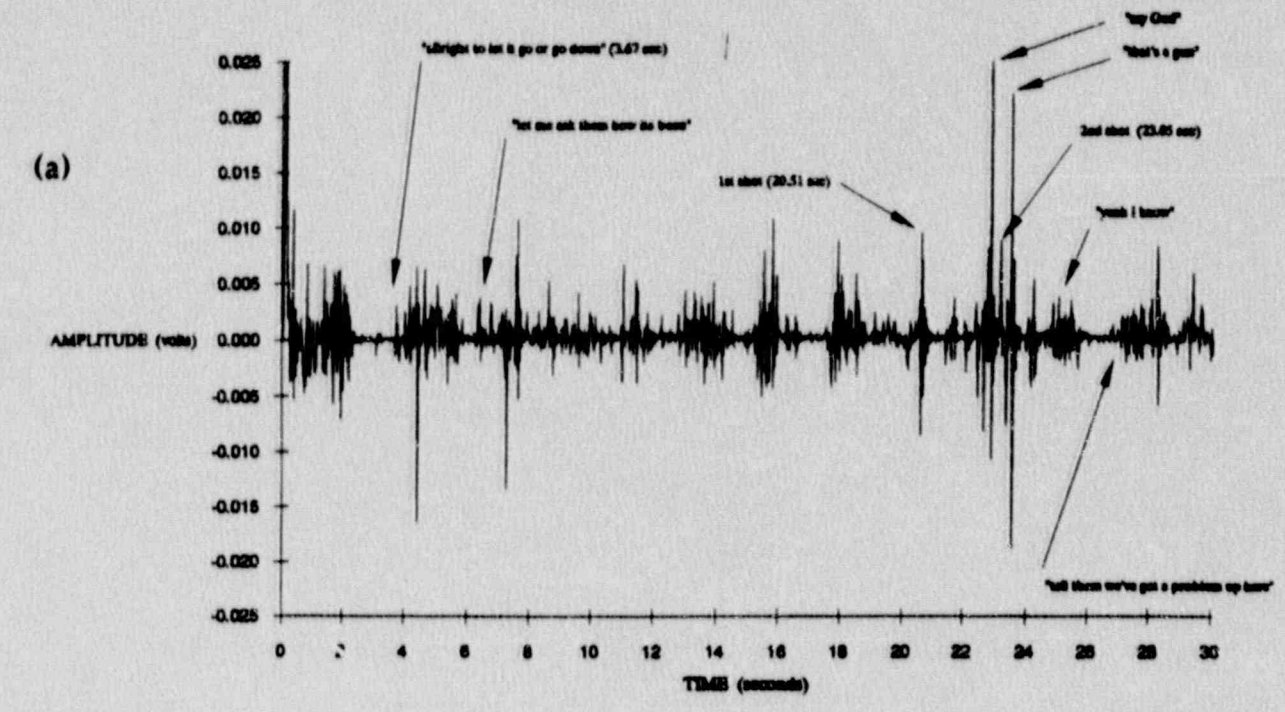

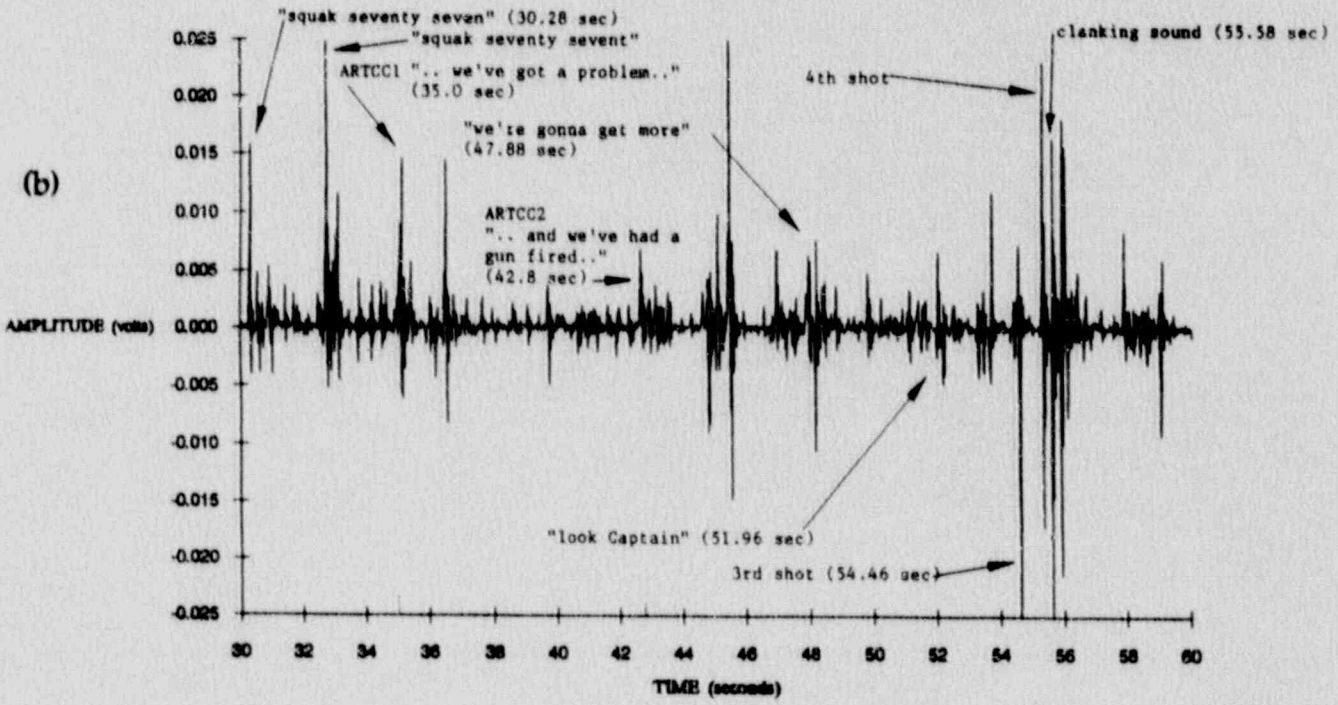

Fig. 8.2-2. Consecutive time histories, (a) 0-30 s, (b) 30-60 s, (c) 60-90 s, (d) 90-120 s, and (e) 120-150 s, of cockpit sounds based on our analysis of the CVR tape.

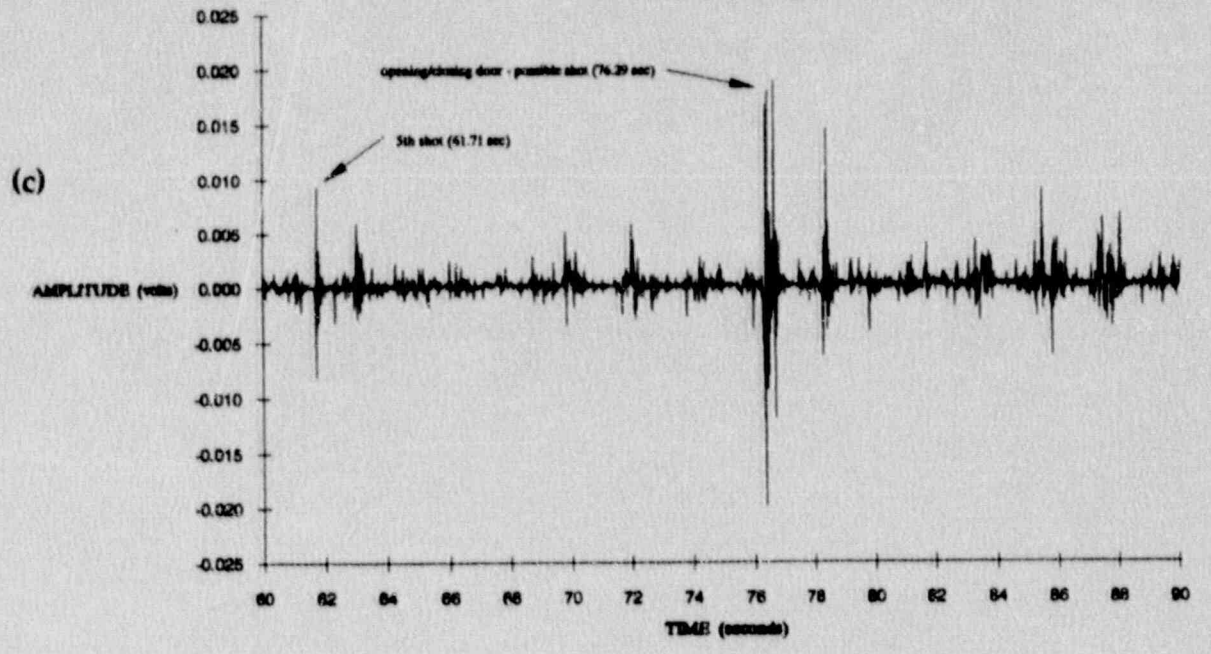

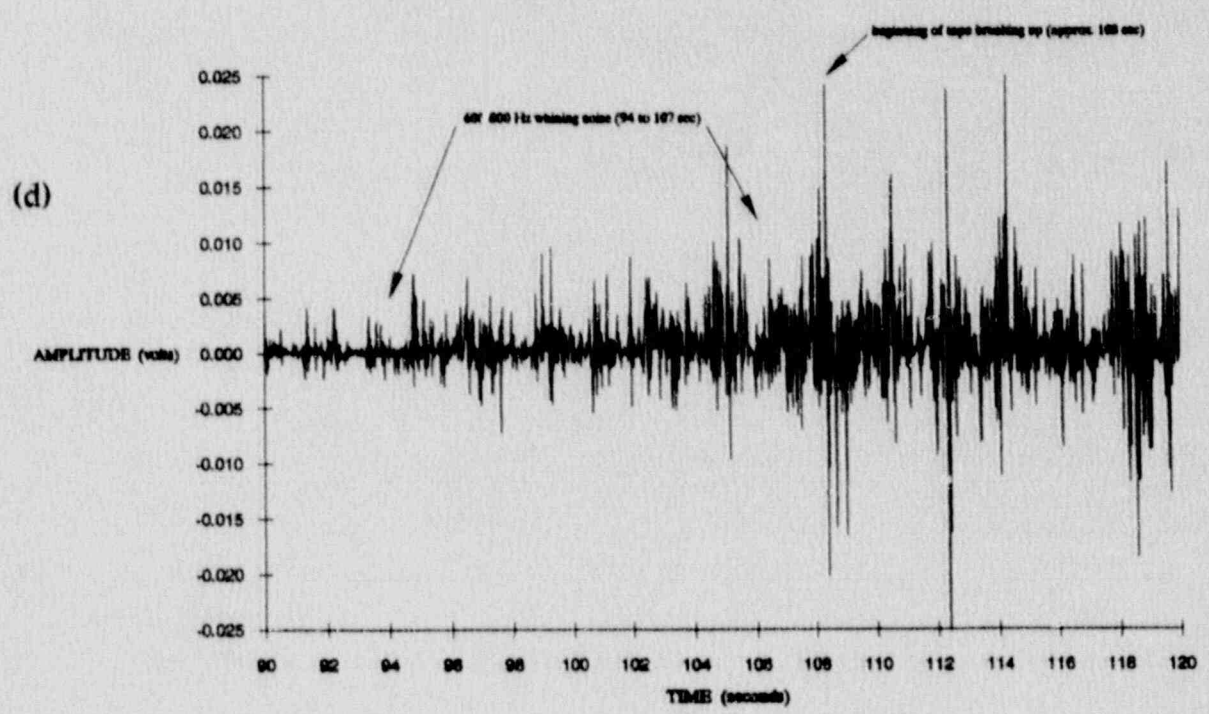

Fig. 8.2-2 - continued

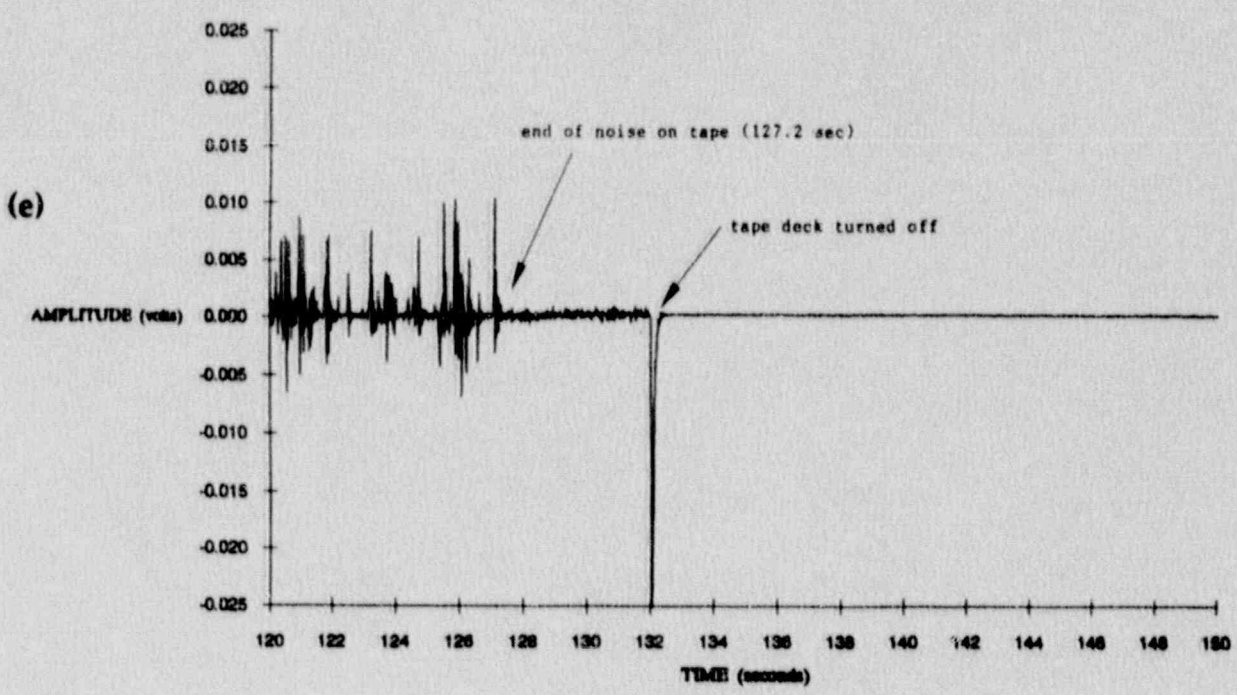

Fig. 8.2-2 - continued

8.3 Discussion of CVR Data

The end of recording on the CVR is clearly defined (see Fig. 8.2-2e). This discrete point in time could have resulted from: 1) interruption of power or audio signal to the CVR due to excessive shaking on the aircraft in flight, or 2) aircraft destruction on impact with the ground. We believe the latter assumption is reasonable. With this assumption our analysis indicates that duration of the flight between the first shot and inferred impact is 106.7 s. Table 8.3-1 lists selected events that are noted in Fig. 8.2-2 with zero time referenced to the first shot. Elapsed times from the first shot derived from the FBI transcript (Ref. 30) are also listed in Table 8.3-1 for comparison. There is generally good agreement. Two exceptions are noted: 1) the time of the sixth shot according to Ref. 30 is 31 s later than the value we derived, and 2) the elapsed time between the two radio communications from the aircraft to the Oakland ARTCC is 10 s according to Ref. 30 while our value is ~8 s.

There are only three events listed in Table 8.3-1 which can be cross-referenced to an absolute time scale: 1) the first aircraft-to-ARTCC communication, 2) the second aircraft-to-ARTCC communication, and 3) assumed impact. From the elapsed times given in Table 8.3-1, we may infer several values of absolute impact time. In each case we assume that impact is coincident with the end of recording. The reference absolute times are: 1) first radio transmission, designated ARTCC1 at 00:13:03 UTC as reported in Ref. 3; 2) second radio transmission, designated ARTCC 2 at 00:13:11

UTC as reported in Ref. 3; and 3) seismic signal (see Section 9) sensed at 00:14:36 UTC as reported in Ref. 34. Inferred impact times based on these reference times and consideration of seismic signal delay (see Section 9) are listed in Table 8.3-2.

Table 8.3-1. Elapsed time(s) for key events during the terminal flight period.

Basis	Fig. 8.2-2	Ref. 30
EVENT		
First shot	0	0
Second shot	2.5	2
First radio comm. (ARTCC 1)	14.3	11
Second radio comm. (ARTCC 2)	22.3	21
Third shot	34.0	33
Fourth shot	35.0	34
Fifth shot	41.2	40
Door open/close	55.8	55
Sixth shot (uncertain in Fig. 8.2-2)	55.8	87
Begin whistle	73.0	
Recorder vibration	87.0	
End of recording (assumed impact)	106.7	105

Table 8.3-2 Inferred absolute time of impact (UTC, December 8, 1987).

Basis	Fig. 8.3-2 data	Ref. 30
ARTCC 1	00:14:35	00:14:37
ARTCC 2	00:14:35	00:14:35
Seismic	----------00:14:35----------	

On the basis of our analysis of the CVR tape data and data from Ref. 30, we conclude that the best estimate of absolute time of impact is 00:14:35 UTC on December 8, 1987. This estimate is in exact agreement with the estimate based on seismic detection of the impact.

A corollary of this conclusion is that the Oakland ARTCC timing signal for radio communications could have been fast by 2 s in one case and that their timing signal for radar data was fast by 4 s. The latter part of this corollary is necessary since the last radar position was stated to be recorded at 00:14:36 UTC, which is after the seismic-derived impact time and therefore not possible. The correlations for altitude, pitch, and true airspeed derived from analysis of the FDR data (Section

7.3.1), as well as the horizontal distance between the last radar coordinates and the impact point coordinates (Fig. 6.6.1), are best satisfied for t_i = -2.7 s. Therefore the correct absolute time for the last radar data should be 00:14:32 UTC instead of 00:14:36 UTC on December 8, 1987.

The indicated possible errors in ARTCC timing are not surprising. Much greater discrepancies have been observed in other incidents investigated by NTSB (Ref. 35). We note that a shorter time difference between radio communications, 8 s versus 10 s, allows consistent estimates of absolute impact time from both radio communications if applied to Ref. 30 data. If the shorter time difference is obtained by delaying the first radio communication by 2 s, then the estimates of absolute impact time derived from Ref. 30 are not only internally consistent, but also consistent with the estimate derived from seismic signal detection.

One can speculate about various scenarios during the final 100 s. One such scenario based on our analysis of the CVR tape follows. The first two shots were undoubtedly fired in rapid succession in the passenger cabin perhaps at only one person, the gunman's primary target. There may have been three crew members in the cockpit and apparently three more shots were fired within a period of 6 s in the cockpit. (Reference 31 states that an off-duty crew person was in the third "occasional" crew seat.) Just before the sixth shot (our analysis is ambiguous about this sound being a shot) there is the sound of the (cockpit) door opening and closing. We conclude that a passenger (or flight attendant) entered the cockpit and was shot by the gunman; it seems reasonable that someone aboard would attempt to subdue the gunman. The gunman may have been in the process of pushing the stick forward and possibly also changing the elevator trim position to reduce the force required to hold the stick in a forward position.* As a result, the aircraft pitched to a nose-down attitude and the airspeed increased. It would have been difficult, if not impossible, for a person to walk to the rear of the aircraft if the pitch angle was steeper than about -30°. Even steeper angles were encountered later. We presume that the gunman remained in the cockpit.

According to Ref. 30, the sound of the sixth shot, like the first and second, is characteristic of sound occurring outside the cockpit. This is not obvious from our analysis. On the contrary if amplitude is a measure, the amplitude of the fifth shot (see Fig. 8.2-2) matches the amplitudes of the first and second shots. If the sixth shot occurred in the passenger cabin 31 s later than our analysis seems to indicate, how did the gunman walk up the aisle with the aircraft in a pitch-down attitude? While we did not pursue a resolution of this discrepancy, at issue could be who, if anyone, was alive in the cockpit just before impact.

---

* The FBI files include a list of items found in the trunk of the alleged gunman's automobile after it was recovered from a Los Angeles airport parking lot. Among the items was a "Student Pilot Flight Manual". We do not have information that indicates the extent of the gunman's flying knowledge.

9. SEISMIC SIGNATURE OF IMPACT

In May 1989, we inquired of the University of California Seismographic Station, Richmond, California, and the U.S. Geological Survey, Menlo Park, California, whether any seismic activity had been recorded about the time of the crash on December 7, 1987. The responses were negative. We then made a similar inquiry to Pacific Gas and Electric Company which operates the Diablo Canyon nuclear electric power plant, located about 32 km from the crash site. PG&E operates a multi-station network around the plant to monitor seismic activity. One of their stations, called BLV, is located at 35°32.03' north, 120°54.40' west, 457 m m.s.l. which is 4.75 km from the crash site. Normally, an electronic record is automatically obtained when the seismic level at three stations exceeds a certain threshold. The impact of PSA Flight 1771, although below threshold, was detected at BLV. Although there was no electronic record, a "paper and ink" drum recording of the event was obtained since a maintenance check of the system was coincidentally being conducted at the time of the crash. The recording, included in Ref. 34, is reproduced in Fig. 9-1.

The BLV seismic station is a high-gain, vertical-component, 1-Hz, telemetered station recorded in the PG&E offices in San Francisco. An accurate time signal based on NIST absolute time is used to correlate the signals from each station in the network. PG&E also provided us with commentary on Fig. 9-1. Note that a small but impulsive seismic event was recorded at 00:14:36 UTC on December 8, 1987 (i.e. 16:14:36 PST on December 7, 1987). The time marks on each trace represent one minute from the leading edge of one mark to the leading edge of the next one. Although the first motion is very difficult to see due to the high frequency of the event, it is concluded (Ref. 34) that the motion is from the ground up, which is consistent with the first motion expected for a surface explosion or impact. There does not appear to be a clear S-wave. The duration of the event (time from first arrival to end of the coda) is about 11 s, which corresponds to a magnitude of near 1.0. For comparison, there happens to be another small seismic event on this record near the bottom of Fig. 9-1 that is of similar duration and amplitude, but has a visible S-wave and looks like a small micro-earthquake.

Shock waves produced by the impact reach a surface sensor much more quickly by following a curved path deep into the earth than might be inferred from our measurements of surface compression wave velocity (see Table 2.3-1). PG&E also provided (Ref. 36) an estimate of travel time of about 1 s from the crash site to station BLV. Using this estimate of signal arrival time, we establish the absolute impact time of PSA Flight 1771 as 00:14:35 UTC on December 8, 1987.

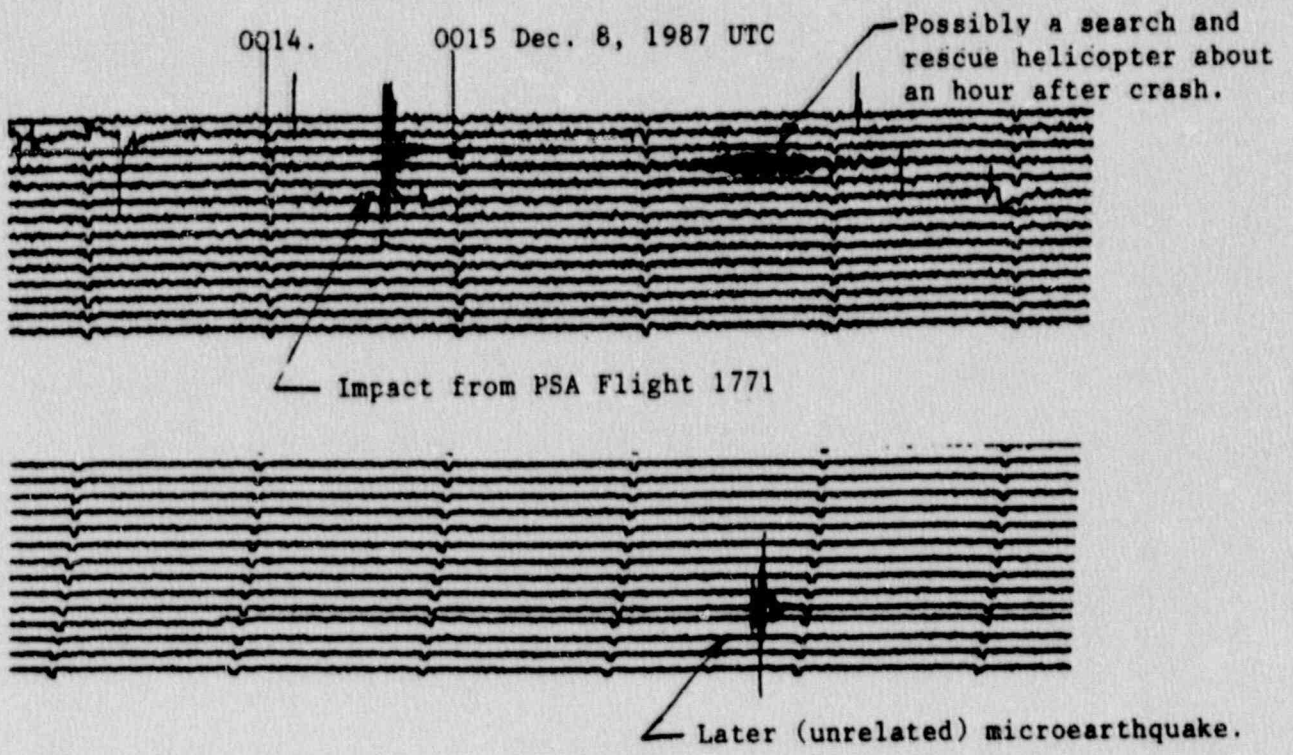

Fig. 9-1. Seismic signals detected at PG&Es seismic station BLV.

10. REFERENCES

1. Agreement between the United States Nuclear Regulatory Commission and the Power Reactor and Nuclear Fuel Development Corporation on the Testing and Administrative Program for certifying Plutonium Air Transport Packages - Phase One: Draft Criteria Development, December 16, 1988.

2. Nuclear Regulatory Commission, Selection of a Worst Actual Aircraft Accident for Murkowski Amendment Implementation (Public Law 100-203), NRC Memo SECY-88-344, December 15, 1988.

3. E. C. Williams, "Crash of Pacific Southwest Airlines Flight 1771", San Luis Obispo County Sheriff-Coroner Office After-Action Report, January 1988.

4. D. W. Carpenter, J. C. Chen, and G. S. Holman, "An Engineering Geologic Evaluation of the PSA Flight 1771 Crash Site Near Paso Robles, California", LLNL Interim Report PATC-IR 89-04, October 1, 1989.

5. S. C. Blair, J. C. Chen, W. R. Ralph, and D. V. Ruddle, "Mechanical Properties of Rocks from PSA 1771 Crash Site", LLNL Interim Report PATC-IR 89-05, November 1, 1989.

6. C. Y. Chang, J. A. Egan (Geomatrix Consultants, Inc.), and J. C. Chen, "Constitutive Models and Dynamic Behavior of Soils Under Impact Loading Conditions", LLNL Interim Report PATC-IR 89-06, August 1989.

7. G. D. Taylor, FAA Oakland ARTCC, computer printouts to C. E. Walter, April 6, 1989.

8. R. L. Webb, FAA Los Angeles ARTCC, letter to C. E. Walter, May 4, 1989.

9. V. Williamson, personal communication to C. E. Walter, March 1989.

10. B. Dickens (NTSB, Air Safety Investigator), memorandum to K. C. Ensslin (NTSB, Investigator-in-Charge, PSA Flight 1771), March 1, 1988.

11. T. D. Weaver-Berry (NTSB Accident Investigator), letter to C. E. Walter, May 26, 1987.

12. D. R. Grossi (FDR expert, NTSB), personal communication to C. E. Walter, May 16, 1989.

13. British Aerospace Document HC.000.H.00.12, Vol. 1, April 1983.

14. P. Baker, Power Plant Group Chairman Factual Report, NTSB Number DCA-88-M-A008, June 15, 1988.

14. P. Baker, Power Plant Group Chairman Factual Report, NTSB Number DCA-88-M-A008, June 15, 1988.

15. P. Baker (NTSB power plant group chairman), personal communication to C. E. Walter, May 16, 1989.

16. R. J. Sherwood, "Debris Scattering from a Jet Transport Aircraft Accident", LLNL Interim Report PATC-IR 89-02, September 19, 1989.

17. B. W. Davis, C. K. Chou, C. E. Walter, "Fuselage Model Crash Tests", LLNL Interim Report PATC-IR 89-03, August 14, 1989.

18. Federal Bureau of Investigation, Files 149A-2178-A4, A6, A10, A12, A13, A-14, A-15, A-16, A-17 pertaining to investigation of destruction of aircraft, PSA Flight 1771, December 7, 1987.

19. B. W. Davis, personal communication to C. E. Walter, December 27, 1989.

20. E. L. Lee, personal communication to C. E. Walter, February 20, 1990.

21. D. R. Grossi (FDR expert, NTSB), personal communication to C. E. Walter, January 11, 1989.

22. R. E. Wells, "Investigation of BAe 146 PSA Flight 1771 Crash in California on 7th Dec. '87 for Lawrence Livermore National Laboratory", British Aerospace Commercial Aircraft Ltd Report HAD.R.462.FD1780, June 6, 1989.

23. J. C. Geering, "Investigation of BAe 146 PSA Flight 1771 Crash in California on 7th Dec. '87 for Lawrence Livermore National Laboratory", British Aerospace Commercial Aircraft Ltd Report HSO.R.462.00.2009, June 6, 1989.

24. H. F. Napfel (Sr. Staff. Engr., Fairchild Western Systems, Inc.), personal communication to M. C. Witte, January 4, 1989.

25. R. W. Nance, Lockheed Aircraft Service Company, letter to C. E. Walter, June 13, 1989.

26. L. G. Burgess, "Analysis of PSA Flight 1771 for LLNL - Evaluation of Data Retrieved from Flight Data Recorder", British Aerospace Commercial Aircraft Ltd Report HAD.R.462.FD.1849, October 12, 1989.

27. R. P. Benedict, "Fundamentals of Temperature, Pressure, and Flow Measurements", 2nd ed., John Wiley and Sons, 1977.

28. W. G. Jackson, BAe, letter to C. E. Walter, LLNL, dated August 3, 1989.

29. J. M. Moody, FBI-Los Angeles, California, letter to K. F. Graham, June 23, 1989.

30. Federal Bureau of Investigation, File Number 149-2178-D3.

31. Channel 2 KTVU, Oakland, California, videotape of PSA Flight 1771 news story, January 30, 1989.

32. J. R. Cash (CVR expert, NTSB), personal communication to C. E. Walter, November 29, 1989.

33. R. B. Burdick, internal memorandum to C. E. Walter, November 10, 1989.

34. W. U. Savage (Senior Seismologist, PG&E), memorandum to C. E. Walter, May 24, 1989.

35. W. M. O'Rourke (radar expert, NTSB), personal communication to C. E. Walter, May 16, 1989.

36. W. U. Savage (Senior Seismologist, PG&E), personal communication to C. E. Walter, December 1, 1989.

APPENDIX 1
REPRINT OF SECTION 5062 OF PUBLIC LAW 100-203

SEC. 5062. TRANSPORTATION OF PLUTONIUM BY AIRCRAFT THROUGH UNITED STATES AIR SPACE. 42 USC 2241 note.

(a) IN GENERAL.—Notwithstanding any other provision of law, no form of plutonium may be transported by aircraft through the air space of the United States from a foreign nation to a foreign nation unless the Nuclear Regulatory Commission has certified to Congress that the container in which such plutonium is transported is safe, as determined in accordance with subsection (b), the second undesignated paragraph under section 201 of Public Law 94-79 (89 Stat. 413; 42 U.S.C. 5841 note), and all other applicable laws.

(b) RESPONSIBILITIES OF THE NUCLEAR REGULATORY COMMISSION.—

(1) DETERMINATION OF SAFETY.—The Nuclear Regulatory Commission shall determine whether the container referred to in subsection (a) is safe for use in the transportation of plutonium by aircraft and transmit to Congress a certification for the purposes of such subsection in the case of each container determined to be safe.

(2) TESTING.—In order to make a determination with respect to a container under paragraph (1), the Nuclear Regulatory Commission shall—

(A) require an actual drop test from maximum cruising altitude of a full-scale sample of such container loaded with test materials; and

(B) require an actual crash test of a cargo aircraft fully " loaded with full-scale samples of such container loaded with test material unless the Commission determines, after consultation with an independent scientific review panel, that the stresses on the container produced by other tests used in developing the container exceed the stresses which would occur during a worst case plutonium air shipment accident.

(3) LIMITATION.—The Nuclear Regulatory Commission may not certify under this section that a container is safe for use in the transportation of plutonium by aircraft if the container ruptured or released its contents during testing conducted in accordance with paragraph (2).

(4) EVALUATION.—The Nuclear Regulatory Commission shall evaluate the container certification required by title II of the Energy Reorganization Act of 1974 (42 U.S.C. 5841 et seq.) and subsection (a) in accordance with the National Environmental Policy Act of 1969 (83 Stat. 852; 42 U.S.C. 4321 et seq.) and all other applicable law.

(c) CONTENT OF CERTIFICATION.—A certification referred to in subsection (a) with respect to a container shall include—

(1) the determination of the Nuclear Regulatory Commission as to the safety of such container;

(2) a statement that the requirements of subsection (b)(2) were satisfied in the testing of such container; and

(3) a statement that the container did not rupture or release its contents into the environment during testing.

(d) DESIGN OF TESTING PROCEDURES.—The tests required by subsection (b) shall be designed by the Nuclear Regulatory Commission to replicate actual worst case transportation conditions to the maximum extent practicable. In designing such tests, the Commission shall provide for public notice of the proposed test procedures, provide a reasonable opportunity for public comment on such procedures, and consider such comments, if any.

(e) TESTING RESULTS; REPORTS AND PUBLIC DISCLOSURE.—The Nuclear Regulatory Commission shall transmit to Congress a report on the results of each test conducted under this section and shall make such results available to the public.

" Copy reads "full".

President of U.S.

(f) ALTERNATIVE ROUTES AND MEANS OF TRANSPORTATION.—With respect to any shipments of plutonium from a foreign nation to a foreign nation which are subject to United States consent rights contained in an Agreement for Peaceful Nuclear Cooperation, the President is authorized to make every effort to pursue and conclude arrangements for alternative routes and means of transportation, including sea shipment. All such arrangements shall be subject to stringent physical security conditions, and other conditions designed to protect the public health and safety, and provisions of this section, and all other applicable laws.

(g) INAPPLICABILITY TO MEDICAL DEVICES.—Subsections (a) through (e) shall not apply with respect to plutonium in any form contained in a medical device designed for individual human application.

(h) INAPPLICABILITY TO MILITARY USES.—Subsections (a) through (e) shall not apply to plutonium in the form of nuclear weapons nor to other shipments of plutonium determined by the Department of Energy to be directly connected with the United States national security or defense programs.

(i) INAPPLICABILITY TO PREVIOUSLY CERTIFIED CONTAINERS.—This section shall not apply to any containers for the shipment of plutonium previously certified as safe by the Nuclear Regulatory Commission under Public Law 94-79 (89 Stat. 413; 42 U.S.C. 5841 note).

(j) PAYMENT OF COSTS.—All costs incurred by the Nuclear Regulatory Commission associated with the testing program required by this section, and administrative costs related thereto, shall be reimbursed to the Nuclear Regulatory Commission by any foreign country receiving plutonium shipped through United States airspace in containers specified by the Commission.

APPENDIX 2
SELECTED FLIGHT SIMULATION RESULTS

Representative plots obtained by BAe from the flight simulation study of the PSA Flight 1771 December 7, 1987, crash are shown in Figs. A2-1 through A2-6.

Figures A2-1 through A2-3 pertain to Case 7 in which the stick position is at 25% of available travel. This condition results in a minimum obtained altitude of 10,000 ft and does not result in the observed crash at an elevation of 1320 ft.

Figures A2-4 through A2-6 pertain to Case 8 in which the stick position is at 50% of available travel. This condition results in impact at an elevation of 1320 ft.

Reference

R. E. Wells, "Investigation of BAe 146 PSA Flight 1771 Crash in California on 7th Dec. -87 for Lawrence Livermore National Laboratory," British Aerospace Commercial Aircraft Ltd. Report HAD.R.462.FD1780, June 6, 1989.

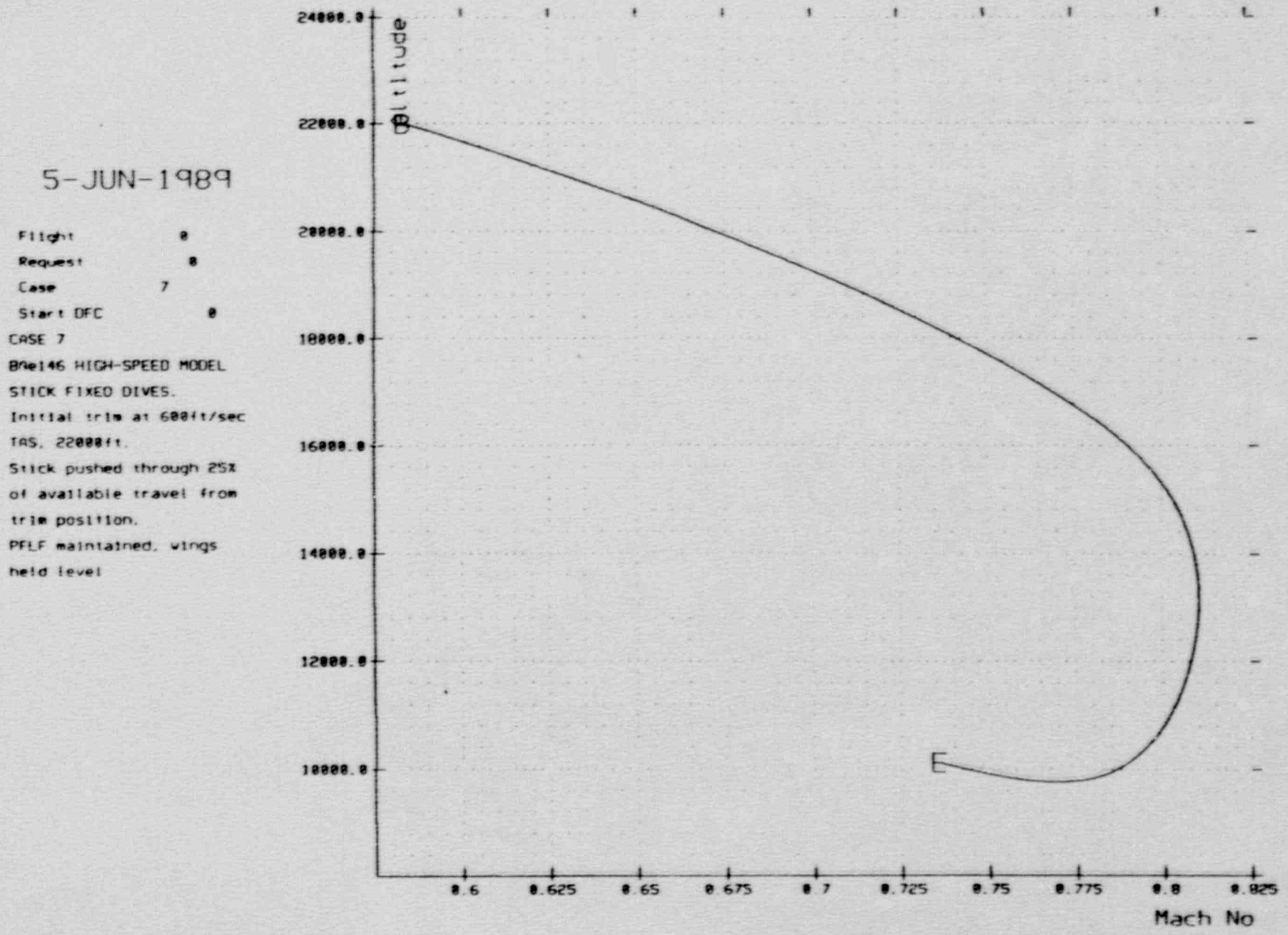

Fig. A2-1. Case 7 plot obtained by BAe from the flight simulation study of the PSA Flight 1771, December 7, 1987 crash.

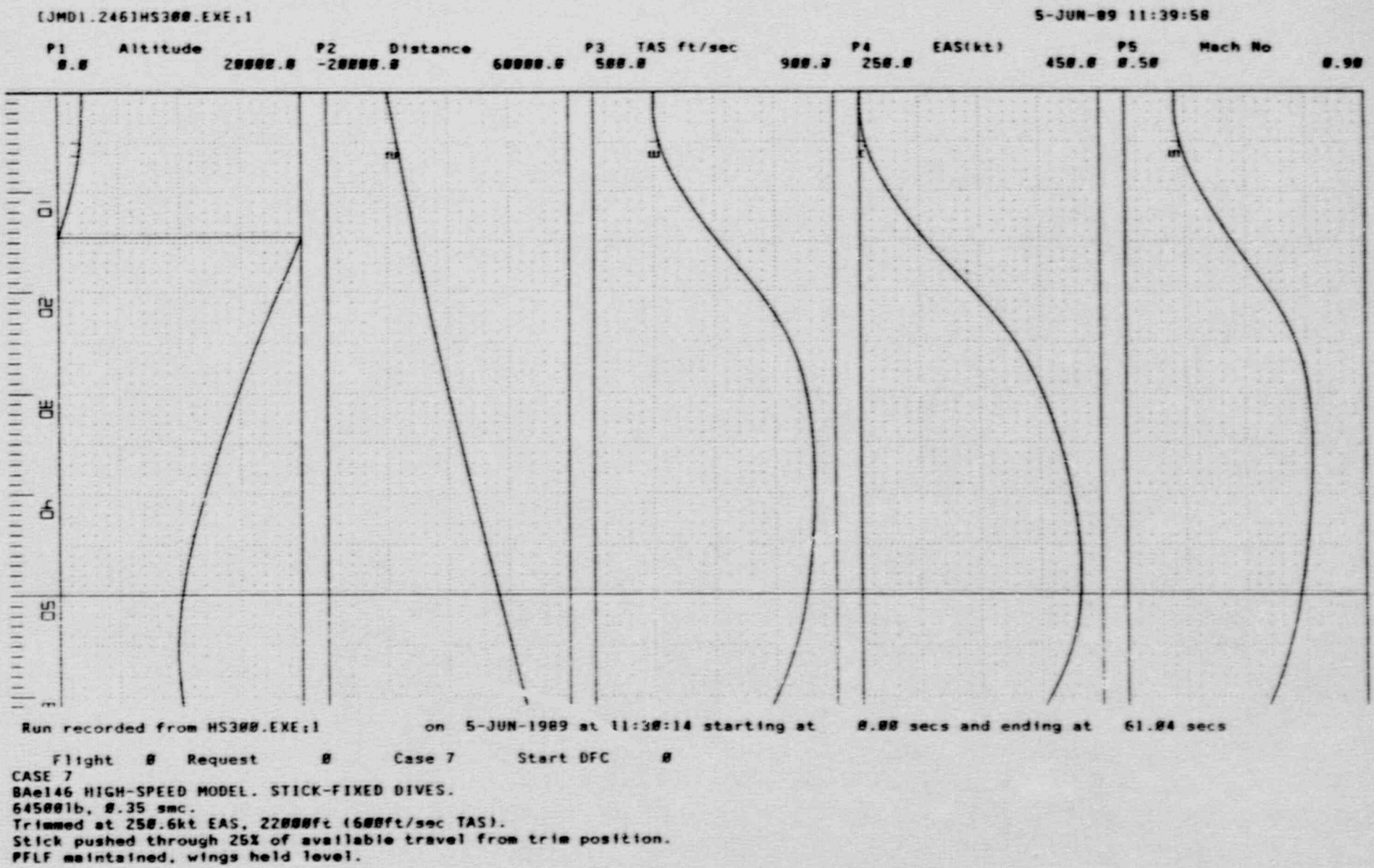

Fig. A2-2. Case 7 plot obtained by BAe from the flight simulation study of the PSA Flight 1771, December 7, 1987 crash.

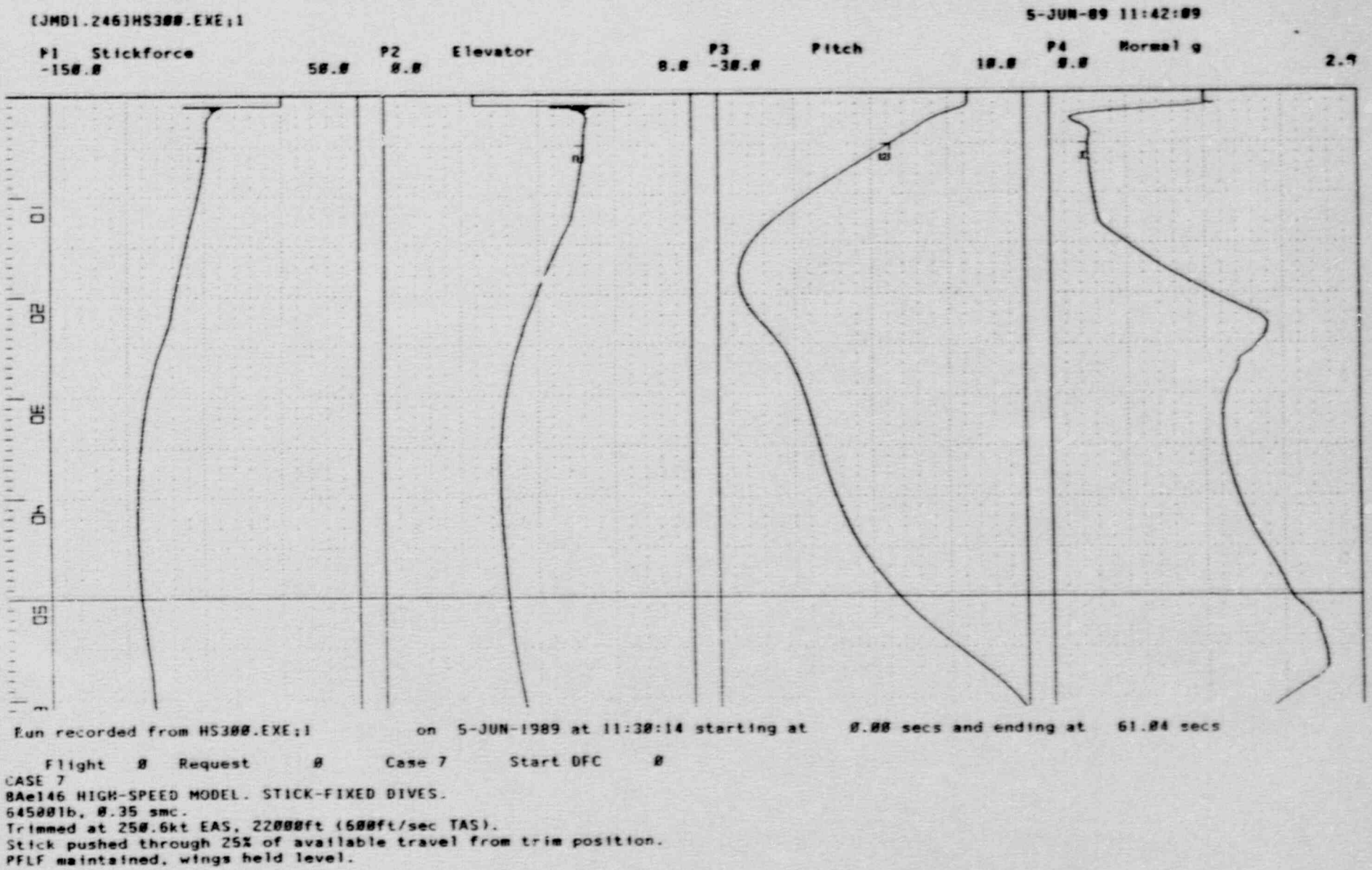

Fig. A2-3. Case 7 plot obtained by BAe from the flight simulation study of the PSA Flight 1771, December 7, 1987 crash.

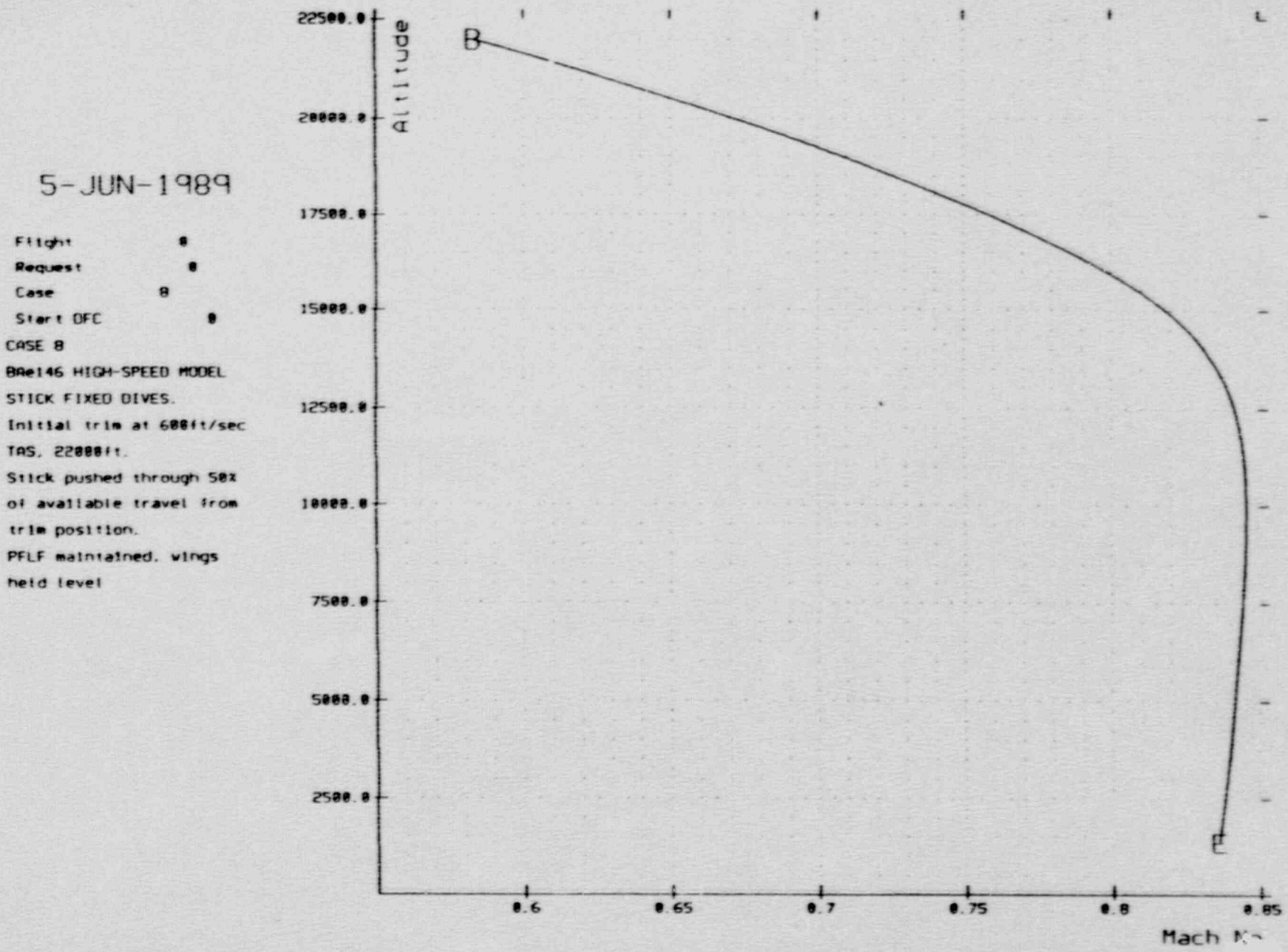

Fig. A2-4. Case 8 plot obtained by BAe from the flight simulation study of the PSA Flight 1771, December 7, [illegible] crash.

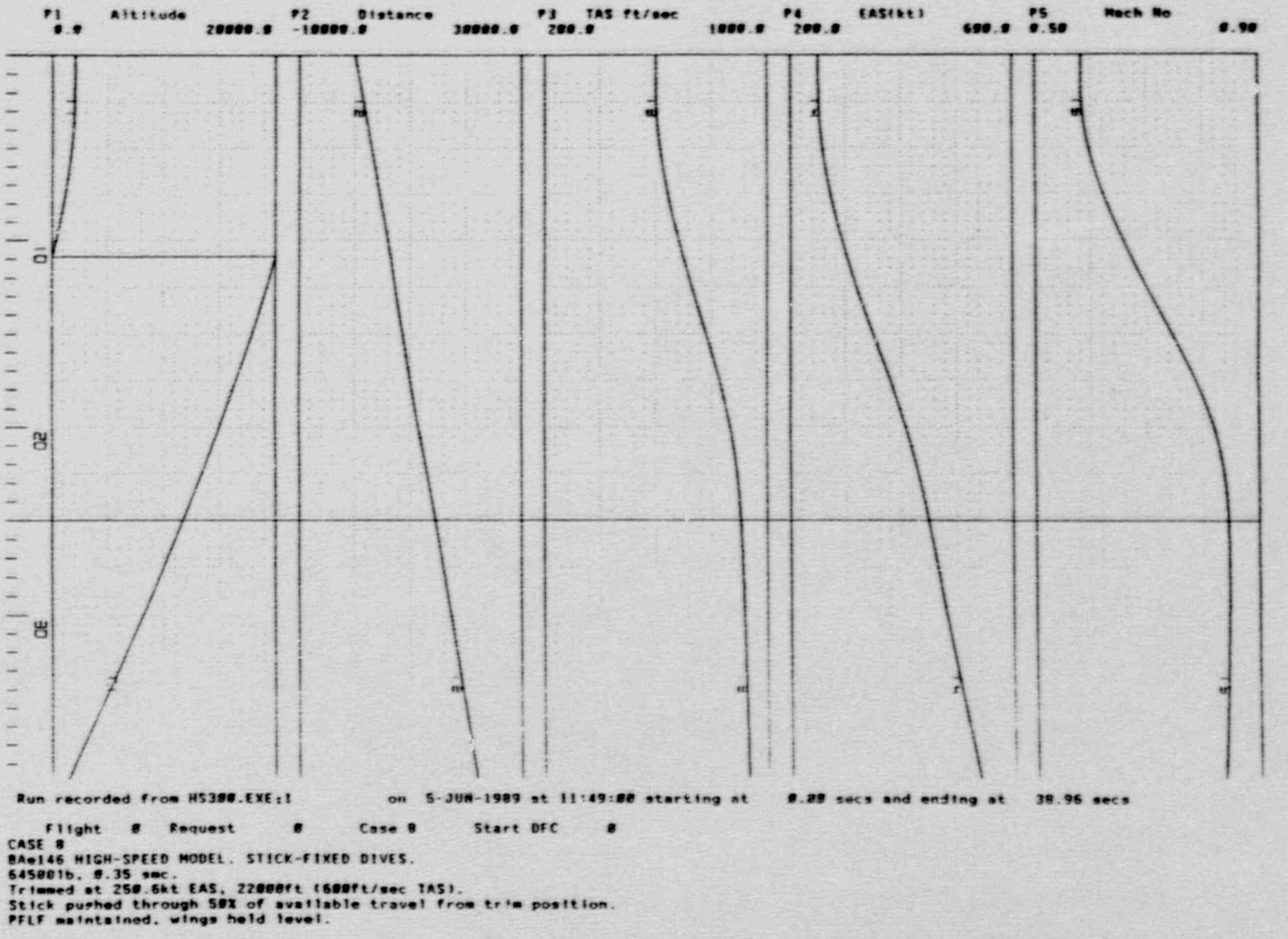

Fig. A2-5. Case 8 plot obtained by BAe from the flight simulation study of the PSA Flight 1771, December 7, 1987 crash.

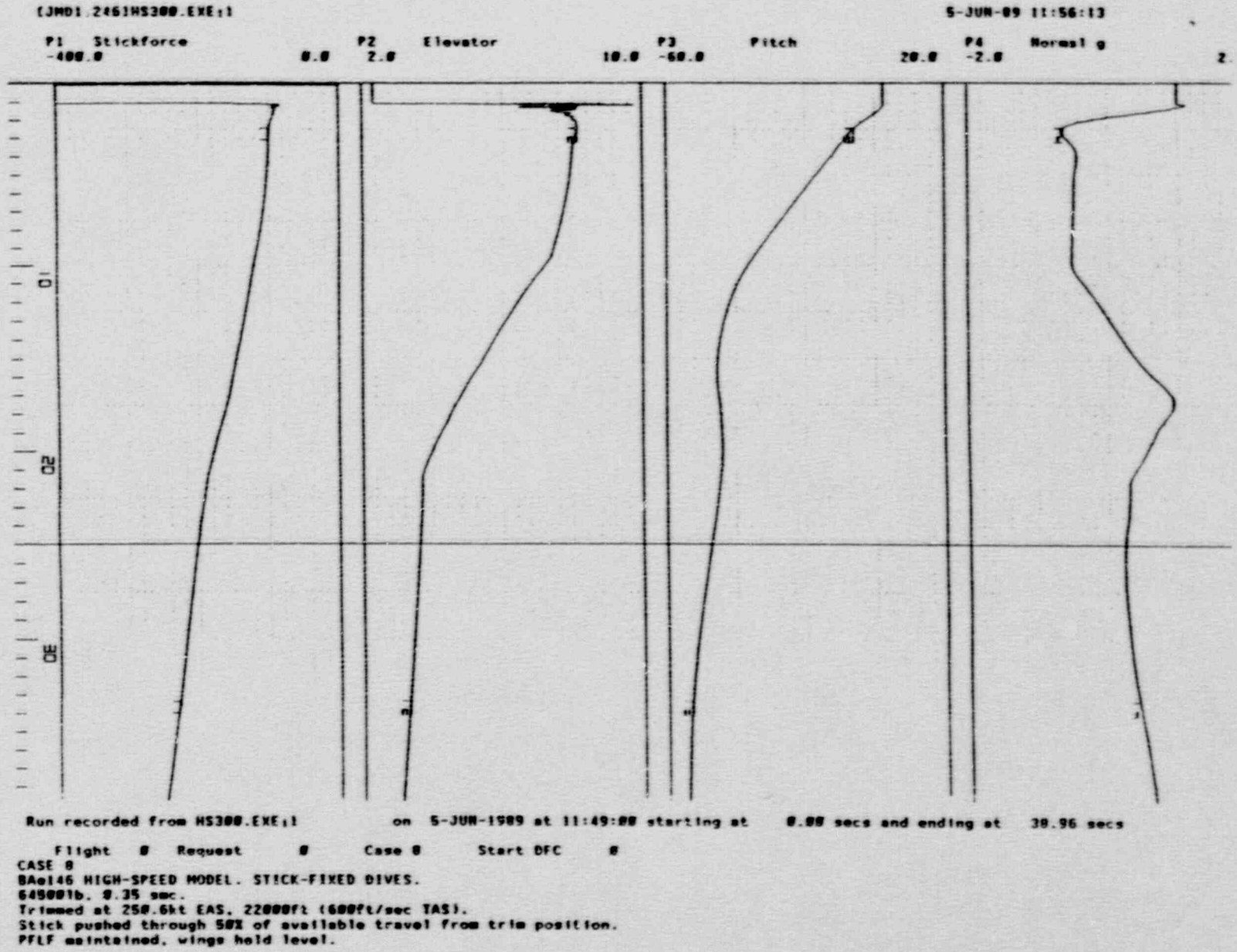

Fig. A2-6. Case 8 plot obtained by BAe from the flight simulation study of the PSA Flight 1771, December 7, 1987 crash.

APPENDIX 3
REDUCED DATA FROM THE PSA FLIGHT 1771 FDR

All of the data reduced from the damaged FDR on PSA Flight 1771 are reproduced on the following pages. A listing of the parameters with their word addresses and sampling rate is also provided in Table A3-1.

Table A3-2 contains the results from manual reduction of data for some of the parameters analyzed. These results are compared with automatic data reduction through the ground station (see Table A3-3) where available.

Table A3-3 is a reproduction of the computer listing of the results from automatic data reduction through the Lockheed playback ground station. Some of the values obtained in this manner are erroneous.

Reference

R. W. Nance, Lockheed Aircraft Service Company, letter to C. E. Walter, June 13, 1989.

Table A3-1. BAe 146, parameter listing, flight data recorder.

PARAMETER	WORD	SF	SAMPLES PER SF	BIT
Fine Altitude	32	1234	1	
Coarse Altitude	49	0204	1	
Airspeed	31	1234	1	
Heading	17	1234	1	
Flap Angle	15, 47	1234	2	
Vertical Acceleration	2	1234	8	
Roll Angle	14	1234	2	
Radio Altitude	16	1234	1	
Rudder Pos.	6	1234	4	
Pitch Attitude	5, 21, 37, 53	1234	4	
L. H. Aileron	12	1234	4	
R. H. Aileron	13	1234	4	
Longitudinal Acceleration	30	1234	1	
Lateral Acceleration	4	1234	4	
Radio Altitude	16	1234	1	
R. H. Roll Spoiler	7	1234	2	
N1 Engine #1	63	1000	1	
N1 Engine #2	63	0200	1	
N1 Engine #3	63	0030	1	
N1 Engine #4	63	0004	1	
Localizer #2	48	1234	1	
Glideslope #2	62	1234	1	
Airbrake Pos.	27, 59	1234	2	
Gear Up	63	1234	1	2
Gear Down	63	1234	1	1
Outside Air Temp.	33	1030	1	
L. H. Elevator	3	1234	4	
R. H. Elevator	9	1234	4	
Elevator Trim	11, 43	1234	2	
Auto Pilot Engaged	14	1234	2	2
EVENT, FDEP	49	1030	1	1
DDI, FDEP	49	1030	1	2

Table A3-1 - continued.

PARAMETER	WORD	SF	SAMPLES PER SF	BIT
DATA, FDEP	49	1030	1	
VHF Keys	14	1234	2	1
LH Roll Spoiler	8, 40	1234	2	
Low Oil Press # 1 & 2	2	1234	4	1,2
Low Oil Press # 3 & 4	6	1234	4	1,2
Pylon o/Heat # 2 & 3	32	1234	1	1,2
Pylon o/Heat # 1	11	1234	2	2
Pylon o/Heat # 4	64	1030	1	1
Fire Eng # 1 & 2	16	1234	1	1,2
Fire Eng # 3 & 4	30	1234	1	1,2
Fire APU	11	1234	2	1
YAW Damper # 1 & 2	17	1234	1	1,2
ALT ACQ ARM	5	1234	4	2
Synch Mode Engaged	5	1234	4	1
Localizer Capture	15	1234	2	1
Glideslope Capture	15	1234	2	2
Essential AC	33	0204	1	1

Table A3-2. Results from manual data reduction (compared with automatic data ground station values where available).

ALTITUDE (FINE) FEET

(WORD 32)

-1250 TO 14,000 ft., ALT = 14.9x - 1250

FRAME, SUBFRAME	BITS(10)*	HEX	DEC.	ALT	GROUND STATION ALT VALUES
2.2	10 0000 1100	20C	524	6558	6426
2.3	01 1101 0001	1D1	465	5679	5562
2.4	01 1001 1001	199	409	4844	4741
3.1	01 0110 1110	16E	366	4203	(1431)
3.2	01 0011 0110	136	310	3369	3291
3.3	01 0000 0111	103	263	2669	x
3.4	00 1101 0100	0D4	212	1909	x

*10 Most significant bits used

NOTES:
1) Data in parenthesis is erroneous
2) "x" indicates no data recovered
3) Altitude (Coarse) not used below 15,000 ft.

INDICATED AIRSPEED (Knots)

(WORD 31)

IAS = 0.635x + 15 knots

Manual Extraction from Strip Chart

FRAME, SUBFRAME	BITS(10)	HEX	DEC.	CALCULATED IAS	GROUND STATION IAS VALUES
2.2	10 1111 1001	2F9	761	498.2	498
2.3	11 0000 0111	307	775	507.1	507
2.4	11 0000 1110	30E	782	511.6	512
3.1	11 0001 0101	315	789	516.0	(265)
3.2	11 0001 1100	31C	796	520.5	521
3.3	11 0010 0010	322	802	524.0	x
3.4	11 0010 0101	325	805	526.0	x

NOTES:
1) Data in parenthesis is erroneous
2) "x" indicates no data recovered

Table A3-2 - continued.

HEADING

(WORD 17)

FOR COUNT = 512-649

$$\text{HEADING} = 180 + \text{TAN}^{-1}\left(\frac{x - 512}{128}\right) - 240$$

FRAME, SUBFRAME	BITS(10)*	HEX	DEC. x	HEADING	GROUND STATION VALUES
2,2	10 0001 1111	21F	543	193.6	193.6
2,3	10 0001 1111	21F	543	193.6	193.6
2,4	10 0010 0000	220	544	194.0	194.0
3,1	10 0001 1110	21E	542	193.2	193.2
3,2	10 0010 0000	220	544	194.0	194.0
3,3	10 0010 0001	221	545	194.5	X
3,4	10 0010 0010	222	546	194.9	X

*10 Most significant bits used

VERTICAL ACCELERATION
(MANUAL DATA EXTRACTION)

$$\text{VERT. ACCEL.} = (9.16)10^{-3}(x) - 3.375$$

FRAME, SUBFRAME	BITS	DEC. (x)	VERT ACCEL (gees)
3,3 7 VERT G	10 1000 1111	655	2.63
8 VERT G	10 1001 0011	659	2.66
3,4 1 VERT G	10 1000 1000	648	2.56
2 VERT G	10 1000 1101	653	2.61
3 VERT G	10 1000 1100	652	2.57
4 VERT G	(No data)		
5 VERT G	10 1001 1011	667	2.74
6 VERT G	10 1001 1101	669	2.75
7 VERT G	10 1001 0000	656	2.63
8 VERT G	10 1000 1111	655	2.63

Table A3-2 - continued.

ROLL
(MANUAL DATA EXTRACTION)

$$\text{ROLL ANGLE} = (180 + \cot^{-1}(\frac{x - 768}{-128})) - 240$$

FRAME. SUBFRAME		BITS	DEC. (x)	ROLL ANGLE (Deg.)
2.2	1 Roll	10 1110 0110	742	18.4
	2 Roll	10 1110 0111	743	18.8
2.3	1 Roll	10 1110 1011	747	20.6
	2 Roll	10 1110 1100	748	21.1
2.4	1 Roll	10 1110 0001	737	16.3
	2 Roll	10 1110 0110	742	18.4
3.1	1 Roll	10 1110 0110	742	18.4
	2 Roll	10 1110 0011	739	17.2
3.2	1 Roll	10 1110 0000	736	16.0
	2 Roll	10 1110 0000	736	16.0
3.3	1 Roll	10 1101 1110	734	15.1
	2 Roll	10 1101 1010	730	13.4
3.4	1 Roll	10 1101 0100	724	11.0
	2 Roll	10 1100 1111	719	8.9

RADIO ALTITUDE (Feet)

(WORD 16)

$h(ft) = 183.96\ e^{x} - 20$
where x = DEC. X 0.00313

FRAME. SUBFRAME	BITS(10)*	HEX	DEC.	x = DEC. X 0.00313	CALCULATED RADIO ALTITUDE $183.96\ e^{x} - 20$
2.2	11 1001 0100	394	916	2.86708	3215
2.3	11 1001 0100	394	916	2.86708	3215
2.4	11 1001 0100	394	916	2.86708	3215
3.1	11 1001 0100	394	916	2.86708	3215
3.2	11 1001 0100	394	916	2.86708	3215
3.3	11 1001 0100	394	916	2.86708	3215
3.4	10 1110 1010	2EA	746	2.33498	1880.2

*10 Most significant bits used

COMMENTS:

As can be seen above, the Radio altitude reading remained constant until the last reading which may be reasonably valid since it is similar to the fine altitude reading. However, due to the pitch attitude, the airframe manufacturer and instrument manufacturer should be consulted to verify validity.

Table A3-2 - continued.

PITCH
(MANUAL DATA EXTRACTION)

$$\text{PITCH ANGLE} = (180 + \text{TAN}^{-1}\left(\frac{x - 512}{-128}\right)) - 240$$

FRAME. SUBFRAME		BITS	DEC. (x)	PITCH ANGLE (Deg.)
3.1	1 PITCH	10 0001 0010	530	-52.0
	2 PITCH	10 0001 0100	532	-51.3
	3 PITCH	10 0001 0110	534	-50.4
	4 PITCH	10 0001 1000	536	-49.5
3.3	2 PITCH	10 0010 0110	550	-43.5
	3 PITCH	10 0010 1001	553	-42.2
	4 PITCH	10 0010 1011	555	-41.4
3.4	1 PITCH	10 0010 1110	558	-40.3
	2 PITCH	10 0011 0000	560	-39.4
	3 PITCH	10 0011 0011	563	-38.3
	4 PITCH	10 0011 0101	565	-37.5

N1%
ENGINES 1, 2, 3, & 4

(WORD 63)

Manual Extraction from Strip Chart

FRAME. SUBFRAME	BITS(10)*	HEX VALUE	x DEC. VALUE	Nn = .129x%	GROUND STATION VALUES
2.2	10 1001 1100	29C	668	2N1 = 86.2	86.1
2.3	10 1101 0000	2D0	720	3N1 = 92.9	92.8
2.4	10 1101 0110	2D6	726	4N1 = 93.6	93.6
3.1	10 1110 0011	2E3	739	1N1 = 95.3	(47.1)
3.2	10 0110 0010	262	610	2N1 = 78.7	(7.2)
3.3	10 1011 1011	2BB	699	3N1 = 90.2	x
3.4	10 1000 0111	287	647	4N1 = 83.5	x

*10 Most significant bits used

NOTES:
1) Data in parenthesis is erroneous
2) "x" indicates no data recovered

Table A3-3. Reproduced computer listing of automatic data reduction results obtained on the Lockheed playback ground station.

E.S.	PRALT FEET	CAS KTS	ALTF FEET	ALTC FEET	HEADING DEG	1PITCH DEG	2PITCH DEG	3PITCH DEG	4PITCH DEG
2.2	6426.	498.	6426.	7150.	193.6	-62.3	-61.5	-60.6	-59.2
2.3	5562.	507.	5562.		193.6	-59.7	-58.3	-57.0	-56.1
2.4	4741.	512.	4741.	5230.	194.0	-55.2	-54.8	-53.9	-53.0
3.1	1431.	265.	1431.		193.2	-51.7	-50.8	35.0	35.5
3.2	3291.	521.	3291.	3970.	194.0	-48.2	-47.3	-46.1	-45.2
3.3	LOSS OF SYNC								
3.4	LOSS OF SYNC								

E.S.	PRALT FEET	CAS KTS	1LAT G'S	2LAT G'S	3LAT G'S	4LAT G'S	LONG G'S	1RUDDR DEG	2RUDDR DEG	3RUDDR DEG	4RUDDR DEG
2.2	6426.	498.	0.33	0.28	0.24	0.39	-0.84	2.3	2.4	2.4	
2.3	5562.	507.	0.50	0.36	0.04	0.11	-0.86	2.5	2.4	2.3	
2.4	4741.	512.	0.32	0.51	0.52	0.20	-0.92	2.4	2.6	2.7	
3.1	1431.	265.	0.25	0.38	0.68	0.62	-0.95	2.4	2.3	22.6	
3.2	3291.	521.	0.25	0.29	0.27	0.28	-0.81	2.4	2.5	2.5	
3.3	LOSS OF SYNC										
3.4	LOSS OF SYNC										

E.S.	PRALT FEET	CAS KTS	1AILL DEG	2AILL DEG	3AILL DEG	4AILL DEG	1AILR DEG	2AILR DEG	3AILR DEG	4AILR DEG
2.2	6426.	498.	1.1	0.2	0.3	2.2	18.3	11.5	19.2	17.2
2.3	5562.	507.	0.1	1.7	1.4	1.0	16.9	19.2	12.4	13.6
2.4	4741.	512.	1.4	0.9	0.1	7.8	16.1	18.8	14.1	14.0
3.1	1431.	265.	3.0	21.9	23.7	23.4	14.8	27.4	-15.0	-13.7
3.2	3291.	521.	9.4	7.2	6.0	7.9	10.6	14.3	11.0	12.9
3.3	LOSS OF SYNC									
3.4	LOSS OF SYNC									

Table A3-3 - continued.

E.S.	PRALT FEET	CAS KTS	1ELEVT DEG	2ELEVT DEG	1ELEVL DEG	2ELEVL DEG	3ELEVL DEG	4ELEVL DEG	1ELEVR DEG	2ELEVR DEG	3ELEVR DEG
2.2	6426.	498.	2.9	2.9	41.9	-0.4	-0.3	-0.5	-1.0	-0.9	
2.3	5562.	507.	2.9	2.9	-0.3	-0.4	0.0	0.1	-0.9	-0.6	
2.4	4741.	512.	2.9	2.9	0.0	0.1	0.1	0.1	-0.5	-0.2	
3.1	1431.	265.	2.9	19.2	0.2	0.3	-21.0	-21.1	-0.4	-0.3	
3.2	3291.	521.	2.9	3.1	0.2	0.2	0.2	0.2	-0.2	-0.2	
3.3	LOSS OF SYNC										
3.4	LOSS OF SYNC										

E.S.	PRALT FEET	CAS KTS	1VERT DEG	2VERT DEG	3VERT DEG	4VERT DEG	5VERT DEG	6VERT DEG	7VERT DEG	8VERT DEG
2.2	6426.	498.	2.10	2.09	2.08	2.03	2.00	2.13	2.34	2.28
2.3	5562.	507.	2.21	2.10	2.06	2.02	1.96	2.17	2.52	2.58
2.4	4741.	512.	2.56	2.52	2.50	2.39	2.28	2.21	2.28	2.48
3.1	1431.	265.	2.53	2.60	2.58	4.91	4.19	-0.56	4.21	-0.49
3.2	3291.	521.	2.57	2.53	2.58	2.52	2.44	2.49	2.37	2.33
3.3	LOSS OF SYNC									
3.4	LOSS OF SYNC									

E.S.	PRALT FEET	CAS KTS	1ROLL DEG	2ROLL DEG	1FLAP DEG	2FLAP DEG	1AIRBK DEG	2AIRBK DEG	N11234 %RPM	OAT DEG
2.2	6426.	498.	18.5	18.9	1.	1.	62.	62.	86.1	
2.3	5562.	507.	20.7	21.1	1.	1.	62.	62.	92.8	42.4
2.4	4741.	512.	16.4	18.5	1.	1.	62.	62.	93.6	
3.1	1431.	265.	16.5	71.4/7.2	1.	15.	85.	85.	47.1	98.0
3.2	3291.	521.	16.0	16.0	1.	1.	62.	62.	7.2	
3.3	LOSS OF SYNC									
3.4	LOSS OF SYNC									